

Instituto Universitario de Ciencia de  
Materiales Nicolás Cabrera  
**XXIV YOUNG RESEARCHERS MEETING**



17 de Diciembre de 2021  
Residencia La Cristalera, UAM  
Miraflores de la Sierra, Madrid  
<http://www.inc.es>

## PROGRAM

### 9:30 – 9:45 Welcoming session

### 9:45 – 10:15 Session I (Chair A. de Andres)

9:45 *Invited speaker*: Gloria Platero, “Simulation of topological phases in quantum dot arrays”, ICM – CSIC

### “Chema Gómez-Rodríguez” awards to the best paper

10:15 Eva Cortés-del Río et al, “Observation of Yu-Shiba-Rusinov States in Superconducting Graphene” *Adv. Mater.* 2021, 33, 2008113.

10:40 Elisa Ortiz-Rivero, “Laser Refrigeration by an Ytterbium-Doped NaYF<sub>4</sub> Microspinner”, *Small* 2021, 21003122.

### 11:10 – 11:30 Coffee Break

### 11:30 – 13:00 Session II (Chair A. Gutiérrez)

### INC & Programa de Doctorado en Materiales Avanzados y Nanotecnología

11:30 Nuria Jiménez Arévalo “BCN coatings on TiO<sub>2</sub>/TiS<sub>3</sub> heterostructures for electrolytic water splitting”, M-4

11:50 Alejandro José Uría Álvarez “Deep learning for disordered topological insulators through entanglement spectrum”, M-3

12:10 Carlos Sebastián Vicente “Light and Thermally Induced Charge Transfer and Ejection of Micro/Nanoparticles from Ferroelectric Crystal Surfaces”, M-5

12:30 Daniel Arribas “On-Surface Dehydrogenation and Cyclisation of n-Octane (C<sub>8</sub>H<sub>18</sub>) on Pt(111)”, M-12

### 13:00 – 14:30 Poster Session

### 14:30 – 15:45 Lunch

### 15:45 – 17:30 Session III (Chair J. J. de Miguel)

### INC & Programa de Doctorado Interuniversitario en Física de la Materia Condensada, Nanociencia y Biofísica

15:45 Antonio Tiene “The two-dimensional Fermi polaron problem”, M-5

16:05 Aitor Zambudio Sepúlveda “Fine Defect Engineering of Graphene Friction”, Universidad de Murcia

16:25 Gonzalo Álvarez Pérez “Refraction and lensing of nano-light in an anisotropic two-dimensional material”, Universidad de Oviedo

16:45 Sergio Puebla “In-plane anisotropic optical and mechanical properties of two-dimensional MoO<sub>3</sub>”, ICM – CSIC

17:05 César González-Ruano “Boosting Room Temperature Tunnel Magnetoresistance in Hybrid Magnetic Tunnel Junctions Under Electric Bias”, M-3

### 17:25 – 17:45 Wrap up and closing session

## Session I - Chair of the session: A. de Andres

**Invited speaker:**

---

9:45 "Simulation of topological phases in quantum dot arrays"

**Gloria Platero**

ICMM – CSIC

---

### Simulation of topological phases in quantum dot arrays

Gloria Platero

Instituto de Ciencia de Materiales de Madrid (CSIC), Cantoblanco, 28049, Madrid.

Recent experiments demonstrate a controllable 12-semiconductor quantum-dot (QD) device[1]. The fabrication and control of long semiconductor quantum dot arrays open the possibility to use these systems for transferring quantum information between distant sites. Interestingly, it also opens the possibility of simulating complex hamiltonians as for instance one-dimensional topological insulators. An example is the Su-Schrieffer-Hegger (SSH) model, a chain of dimers. This system presents chiral symmetry and bond ordering of nearest-neighbor couplings and displays two topological phases. In a finite chain, the presence of protected edge states, allows to transfer electrons between edges, and therefore their implementation is promising for quantum information transfer. However, the SSH model does not account for long range hopping effects which should occur in real systems and which can destroy the topological properties and the edge states formation [2].

In this presentation I will first introduce the state of the art of pristine semiconductor QD arrays. Then, I will discuss how to use QD arrays with long-range hopping amplitudes as quantum simulators of new 1D chiral topological phases. I will show that, by applying a periodic driving protocol, all hopping amplitudes can be modified at will, imprinting bond-order and effectively producing structures such as dimers chains. Importantly, our protocol allows for the simultaneous suppression of all the undesired long-range hopping processes, enhancement of the necessary ones, and the appearance of new topological phases with increasing number of edge states. I will discuss the dynamics of two interacting electrons in a 12-QD array when configurations with different number of edge states are considered. The correlated dynamics, which can be experimentally detected with QDs charge detectors, allows to discriminate between different topological phases and importantly, it opens a new avenue for quantum state transfer protocols [3].

- [1] D.M. Zajac et al., Phys. Rev. App., 6 (2016), 054013
- [2] B. Pérez-González et al., Phys Rev. B, 99 (2019), 035146
- [3] B. Pérez-González et al., Phys. Rev. Lett., 123 (2019), 126401

## Chema Gómez-Rodríguez awards to the best paper

10:15 "Observation of Yu-Shiba-Rusinov States in Superconducting Graphene"

Eva Cortés-del Río

Física de la Materia Condensada

# Observation of Yu-Shiba-Rusinov states in superconducting graphene

E. Cortés-del Río<sup>1</sup>, J. L. Lado<sup>2</sup>, V. Cherkez<sup>3</sup>, P. Mallet<sup>3</sup>, J-Y. Veuillen<sup>3</sup>, J.C. Cuevas<sup>1</sup>, J. M. Gómez-Rodríguez<sup>1</sup>, J. Fernández-Rossier<sup>4</sup> and I. Brihuega<sup>1</sup>

<sup>1</sup>Universidad Autónoma de Madrid, Madrid, Spain.

<sup>2</sup>Aalto University, Espoo, Finland

<sup>3</sup>Université Grenoble Alpes, Institut NEEL, F-38042 Grenoble, France

<sup>4</sup>QuantaLab, International Iberian Nanotechnology Laboratory (INL), Braga, Portugal

Email: eva.cortes@uam.es

Nowadays, the properties of pristine graphene are well known. This means that we are now in a position of going one step further and introduce new properties that are not naturally found on it. In this work, we developed a methodology to induce superconductivity in graphene by growing Pb islands on top of it. These islands induce superconductivity by the proximity effect below their critical temperature, 7.2K. Superconductivity, combined with magnetism, give rise to the sought-after Yu-Shiba-Rusinov states. By using an ultra-high-vacuum (UHV) and low-temperature (4K) STM, we observed and probed these Shiba states in graphene grain boundaries, proving for the first time the magnetic nature of these reactive regions, even in the absence of magnetic impurities.

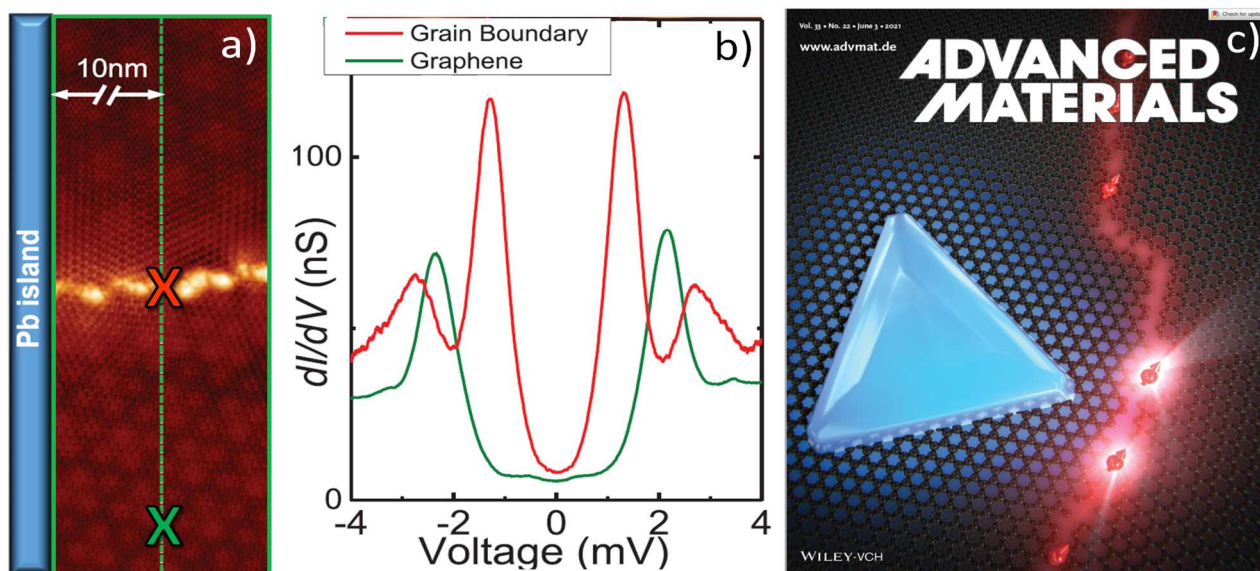


Figure 1. a) STM topography image of a graphene grain boundary. The blue rectangle depicts the position of the Pb island. b)  $dI/dV$  curves acquired on the grain boundary (red) and on graphene (green), corresponding to the X in a). c) Cover of the Advanced Materials magazine featuring this work [1].

[1] E. Cortés-del Río et al., Advanced Materials, **33**, Issue 22, 2008113 (2021).



## Chema Gómez-Rodríguez awards to the best paper

10:40 "Laser Refrigeration by an Ytterbium-Doped NaYF<sub>4</sub> Microspinner"

Elisa Ortiz-Rivero

Física de Materiales

# Laser Refrigeration by an Ytterbium-Doped NaYF<sub>4</sub> Microspinner

E. Ortiz-Rivero<sup>1</sup>, K. Prorok<sup>2</sup>, I. R. Martín<sup>3</sup>, R. Lisiecki<sup>2</sup>, P. Haro-González<sup>1</sup>, A. Bednarkiewicz<sup>2</sup>, D. Jaque<sup>1</sup>

<sup>1</sup>Nanomaterials for Bioimaging Group, Departamento de Física de Materiales & Instituto Nicolás Cabrera, Facultad de Ciencias, Universidad Autónoma de Madrid, Madrid, 28049 Spain

<sup>2</sup>Institute of Low Temperature and Structure Research, Polish Academy of Sciences, Okólna 2, 50-422 Wrocław, Poland

<sup>3</sup>Departamento de Física & Instituto Universitario de Materiales y Nanotecnología (IMN), Universidad de La Laguna, 38200 San Cristóbal de La Laguna, Spain

Email: [elisa.ortiz@uam.es](mailto:elisa.ortiz@uam.es)

Thermal control of liquids with high (micrometric) spatial resolution is required for advanced research such as single molecule/cell studies (where temperature is a key factor) or for the development of advanced microfluidic devices (based on the creation of thermal gradients at the microscale). Local and remote heating of liquids is easily achieved by focusing a laser beam with wavelength adjusted to the absorption bands of the liquid medium or of the embedded colloidal absorbers. The opposite effect, highly localized cooling, is much more difficult to achieve. It requires the use of a refrigerating micro-/nanoparticle which should overcome the intrinsic liquid heating. Remote monitoring of such localized cooling, typically of a few degrees, is even more challenging. In this work, a solution to both problems is provided. Remote cooling in D<sub>2</sub>O is achieved via anti-Stokes emission by using an optically driven ytterbium-doped NaYF<sub>4</sub> microparticle. Simultaneously, the magnitude of cooling is determined by mechanical thermometry based on the analysis of the spinning dynamics of the same NaYF<sub>4</sub> microparticle. The angular deceleration of the NaYF<sub>4</sub> microspinner, caused by the cooling-induced increase of medium viscosity, reveals liquid refrigeration by over  $-6$  K below ambient conditions. [1]

The results presented here open a new way of simultaneous controlling and monitoring temperature (and viscosity) at the microscale in biocompatible fluids by a simple experimental approach. Therefore, they can be of critical importance, for instance, in the control of cellular activity by simultaneous thermal and mechanical stimulus.

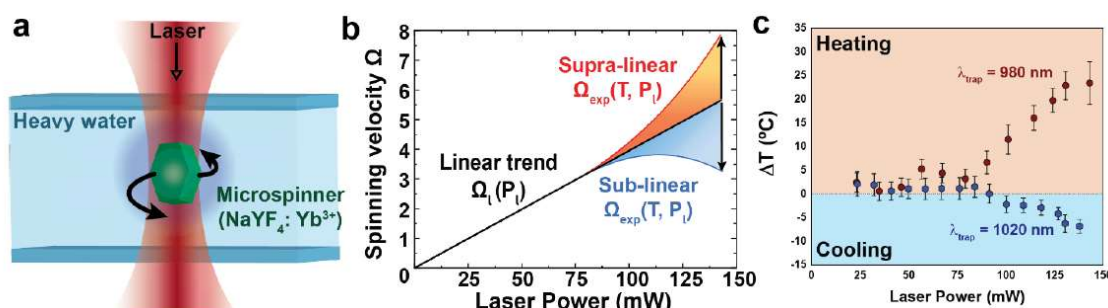


**Figure 1.** a) Schematic representation of an optically trapped and rotated NaYF<sub>4</sub>:Yb<sup>3+</sup> microspinner. b) Graphic representation of the spinning velocity as a function of laser power for a constant temperature (black line), in presence of laser-induced heating (red line) and in presence of laser-induced cooling (blue line). c) Power-dependent temperature increment of the spinning particle under 980 nm and 1020 nm laser manipulation, respectively, evidencing the presence of cooling.

[1] E. Ortiz-Rivero, et al., Small 15, 1904154 (2019)

## Session II - Chair of the session: A. Gutiérrez

INC & Programa de Doctorado en Materiales Avanzados y Nanotecnología:

11:30 "BCN coatings on TiO<sub>2</sub>/TiS<sub>3</sub> heterostructures for electrolytic water splitting"

Nuria Jiménez Arévalo

Física de Materiales

### BCN coatings on TiO<sub>2</sub> /TiS<sub>3</sub> heterostructures for electrolytic water splitting

Nuria Jiménez-Arévalo <sup>1</sup>, Eduardo Flores <sup>2</sup>, Alessio Giampietri <sup>3</sup>, Marco Sbroscia <sup>3</sup>, Maria Grazia Betti <sup>3</sup>, Carlo Mariani <sup>3</sup>, José R. Ares <sup>1</sup>, Fabrice Leardini <sup>1,4</sup>, Isabel J. Ferrer <sup>1,4</sup>.

<sup>1</sup> Departamento de Física de Materiales, Universidad Autónoma de Madrid, Campus de Cantoblanco, E-28049 Madrid, Spain.

<sup>2</sup> Centro de Nanociencias y Nanotecnología (CNyN), Universidad Nacional Autónoma de México (UNAM), Ensenada, Baja California C.P. 22860, Mexico

<sup>3</sup> Dipartimento di Fisica, Università di Roma 'La Sapienza', I-00185, Italy.

<sup>4</sup> Instituto Nicolás Cabrera, Universidad Autónoma de Madrid, Campus de Cantoblanco, E-28049 Madrid, Spain.

\* Correspondence: [nuria.jimenez@uam.es](mailto:nuria.jimenez@uam.es)

Titanium trisulfide (TiS<sub>3</sub>) has been previously used as an anode for photoelectrolytic hydrogen production in the presence of a sacrificial agent. In this work TiS<sub>3</sub> was protected with a shell of titanium dioxide (TiO<sub>2</sub>) to carry out water electrolysis in KOH electrolyte. The TiS<sub>3</sub>/TiO<sub>2</sub> heterostructures were formed using a thermal annealing treatment that permitted us to modify the thickness and structure of the TiO<sub>2</sub> shell with the oxidation time and the atmosphere used. Ultrathin borocarbonitride (BCN) layers were then grown on top of the TiS<sub>3</sub>/TiO<sub>2</sub> heterostructures to act as electrocatalysts. TiS<sub>3</sub>/TiO<sub>2</sub> and TiS<sub>3</sub>/TiO<sub>2</sub>/BCN heterostructures have been characterised by several morphological, structural and compositional techniques. Moreover, preliminary photoelectrochemical experiments have been done, demonstrating the adequacy of protecting TiS<sub>3</sub> from corrosion with a layer of TiO<sub>2</sub>.

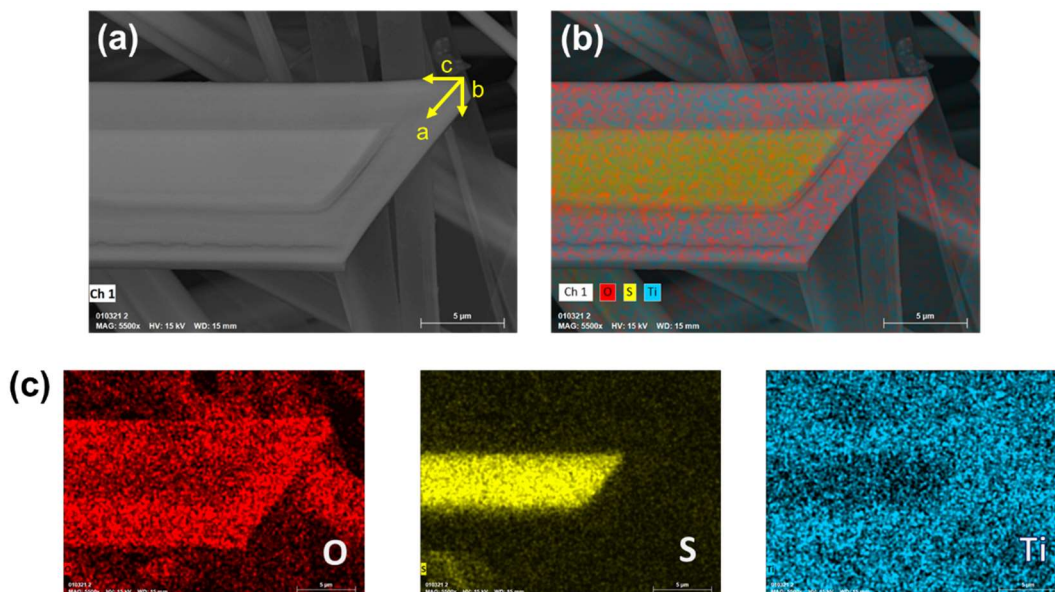


Figure 1. (a) SEM image for a TiS<sub>3</sub> sample oxidised in air (b) EDX mapping analysis superposed with image in (a). (c) EDX mapping results for oxygen (red), sulfur (yellow) and titanium (blue).

## Deep learning for disordered topological insulators through entanglement spectrum

Alejandro José Uría Álvarez<sup>1</sup>, Daniel Molpeceres Mingo<sup>1</sup>, Juan José Palacios Burgos<sup>1</sup>

<sup>1</sup>Department of Condensed Matter Physics, Universidad Autónoma de Madrid, Madrid, Spain

Email: alejandro.uria@uam.es

Calculation of topological invariants for crystalline systems is well understood in terms of the Wilson loop [1] in reciprocal space, allowing for algorithmic evaluation of the invariants for a wide spectrum of materials. While this same approach may still be valid for disordered or complex materials, where the supercell must be big enough to capture the physics of the material, it becomes a limiting factor as the calculation is expensive, disabling high-throughput computations. On top of that, the Wilson loop technique is only well-defined in insulating materials, i.e., systems whose bands are fully occupied. There are several methods to try to overcome these difficulties, such as the local Chern marker or the Bott index [2], which are defined in real space but not for time-reversal invariant insulators.

In our work, we present a new technique based on the entanglement spectrum of a system, which has been shown to contain information on the topological behaviour of a system [4, 5]. We show that it is possible to train a neural network to distinguish between trivial and topological phases with the entanglement spectrum from crystalline phases and use it to predict the topological phase diagram of disordered systems, or fractal lattices such as the Bethe lattice. This approach is shown to be robust, as it does not depend on boundary conditions and can be computed without need of a gap, also providing a speed-up compared with the Wilson loop technique.

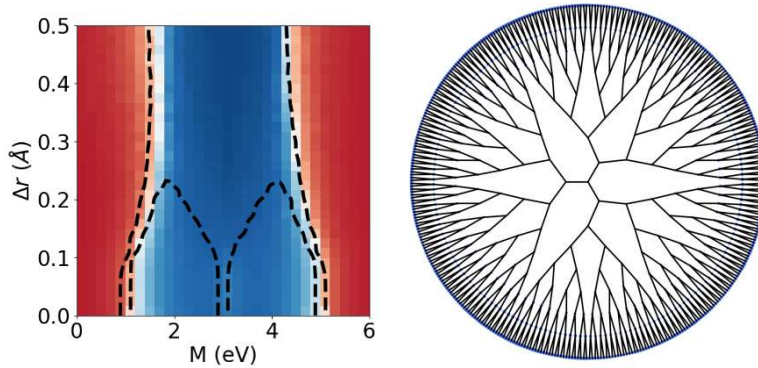


Figure 1. (Left) Topological phase diagram as predicted by the neural network. Dashed lines correspond to gap closings. (Right) Edge states in the Bethe lattice using a Wilson-fermion model.

- [1] A. Alexandradinata, Xi Dai and B. Andrei Bernevig, Phys. Rev. B., **89**, 155114 (2014)
- [2] R. Bianco, R. Resta, Phys. Rev. B., **84**, 241106 (2011)
- [3] A. Author et al., Phys. Rev. Lett., **99**, 11111 (2013)
- [4] Hui Li and F. D. M. Haldane, Phys. Rev. Lett. **101**, 010504 (2008)
- [5] L. Fidkowski, Phys. Rev. Lett. **104**, 130502 (2010)

# Light and Thermally Induced Charge Transfer and Ejection of Micro/Nanoparticles from Ferroelectric Crystal Surfaces

C. Sebastián-Vicente<sup>1</sup>, A. García-Cabañes<sup>1,2</sup>, F. Agulló-López<sup>1,2</sup> and M. Carrascosa<sup>1,2</sup>

<sup>1</sup>Departamento de Física de Materiales, Universidad Autónoma de Madrid, 28049 Madrid, Spain

<sup>2</sup>Instituto Nicolás Cabrera, Universidad Autónoma de Madrid, 28049 Madrid, Spain

Email: carlos.sebastian@uam.es

During real-time operation of photovoltaic (PV) optoelectronic tweezers, a novel intriguing phenomenon has been recently observed, namely, Ag nanoparticles previously deposited on ferroelectric  $\text{LiNbO}_3\text{:Fe}$  surfaces are ejected from them by illumination [1]. Here, it is shown that this phenomenon results from the electrical charging of the micro/nanoparticles previously trapped on the  $\text{LiNbO}_3\text{:Fe}$  surfaces and the subsequent Coulomb repulsion [2]. Specific experiments are performed to determine the sign of the transferred charges, which is negative/positive for the  $+c/-c$  sample face, i.e., it coincides with that of the stored PV charges on each surface. The charging/ejection process is proved to occur regardless of the illuminated crystal surface ( $z$ -cut and  $x$ -cut crystals), the dielectric or metallic nature of the particles and in different surrounding media (nonpolar liquids and air). Besides, multiple excitation wavelengths from 395 nm up to 633 nm are tested to trigger the effect, and the role of light intensity is explored. Next, to assess the generality of the ejection phenomenon, similar experiments based on the pyroelectric effect are performed, i.e., generating the electric fields by changing the crystal temperature. Thereby, thermally-driven particle ejection is demonstrated using different ferroelectric crystals. The similarities found for the two approaches throw light on the charge transfer and ejection mechanism and remark the universality of the phenomenon for ferroelectrics, which should be fairly relevant for a variety of applications.

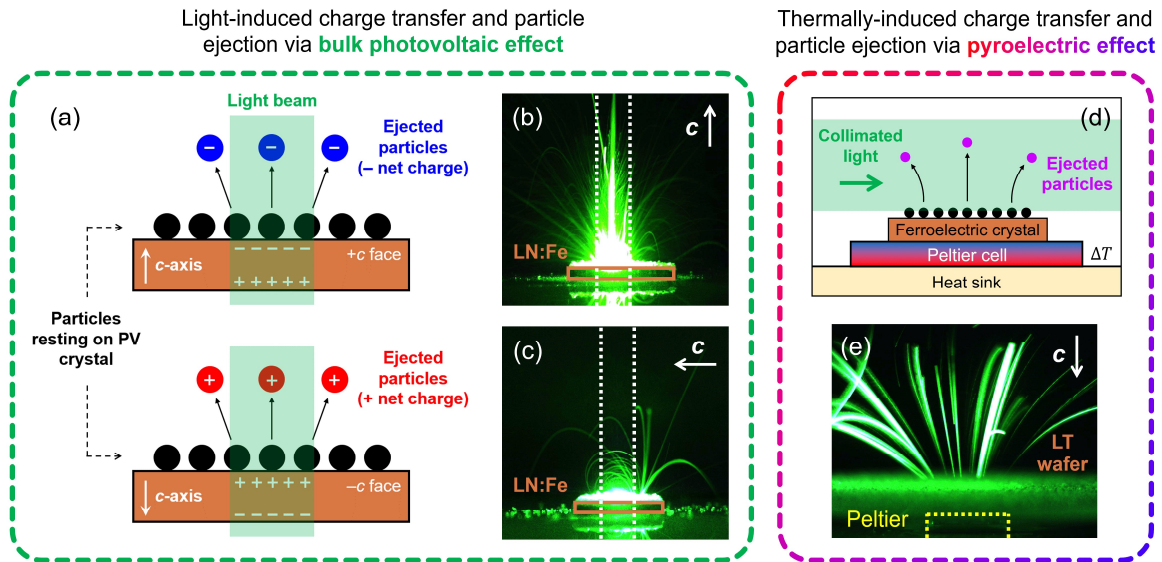


Figure 1. a) Illustration of the charge transfer and subsequent ejection of particles from  $z$ -cut ferroelectric PV crystals triggered by optical excitation. Images b) and c) show the ejection of  $\text{Al}_2\text{O}_3$  microparticles from  $z$ -cut  $\text{LiNbO}_3\text{:Fe}$  and  $\text{CaCO}_3$  microparticles from  $x$ -cut  $\text{LiNbO}_3\text{:Fe}$ , respectively. The white dotted lines indicate the position and diameter (3 mm) of the light beam. d) Experimental configuration for the observation of thermally-driven ejection of particles from ferroelectric surfaces. e) Ejection of  $\text{CaCO}_3$  microparticles from  $z$ -cut  $\text{LiTaO}_3$  upon local cooling (Peltier area:  $9 \times 9 \text{ mm}^2$ ).

[1] C. Sebastián-Vicente et al., Part. Part. Syst. Charact., **36**, 1900233 (2019)

[2] C. Sebastián-Vicente et al., Adv. Electron. Mater., 2100761 (2021)



12:30 "On-Surface Dehydrogenation and Cyclisation of n-Octane (C<sub>8</sub>H<sub>18</sub>) on Pt(111)"

Daniel Arribas

Física Aplicada

## On-Surface Dehydrogenation and Cyclisation of n-Octane (C<sub>8</sub>H<sub>18</sub>) on Pt(111)

D. Arribas<sup>1</sup>, P. Merino<sup>1</sup>, V. Villalobos<sup>1</sup>, E. Tosi<sup>2</sup>, P. Lacovig<sup>2</sup>, A. Baraldi<sup>2,3</sup>, L. Bignardi<sup>3</sup>, S. Lizzit<sup>2</sup>, J. I. Martínez<sup>1</sup>, A. Gutiérrez<sup>4,5</sup> and J.A. Martín-Gago<sup>1</sup>

<sup>1</sup>Instituto de Ciencia de Materiales de Madrid (ICMM-CSIC), Madrid, Spain

<sup>2</sup>Elettra-Sincrotrone Trieste, Trieste, Italy

<sup>3</sup>University of Trieste, Trieste, Italy

<sup>4</sup>Universidad Autónoma de Madrid (UAM), Madrid, Spain

<sup>5</sup>Instituto Nicolás Cabrera (INC), Madrid, Spain

Email: (daniel.arribas.mercado@csic.es)

Formed by a single sp<sup>3</sup>-bonded carbon chain fully saturated with hydrogen atoms, n-alkanes stand as one of the simplest organic molecules in the nature. As one of the main components of the most used fuels and being crucial in a wide range of chemical industry processes [1], alkanes are ubiquitous in modern economy. Alkane dehydrogenation, giving as result from unsaturated chains –alkenes and alkynes– to poly-aromatic species, allows not only to increase the strategic value of these molecules, but could also be key to explain the complex interstellar organic chemistry observed by infrared spectroscopy [2,3].

In this work, we focus our attention on the dehydrogenation and cyclisation reactions that n-octane, C<sub>8</sub>H<sub>18</sub>, undergoes upon thermal treatment on a Pt(111) surface. We have deposited C<sub>8</sub>H<sub>18</sub> by evaporation on a Pt single-crystal and characterised the samples by synchrotron X-ray photoelectron spectroscopy (XPS), thermal programmed desorption (TPD), and scanning tunneling microscopy (STM) after annealing at different temperatures. Our XPS experiments show that molecules undergo a complex temperature-dependent chemistry as it is confirmed from the variety of features resolved by STM. These results are in good agreement with a scheme of four stages, in which molecules present different degrees of dehydrogenation, from simple physisorption/chemisorption to full dehydrogenation forming graphene patches.

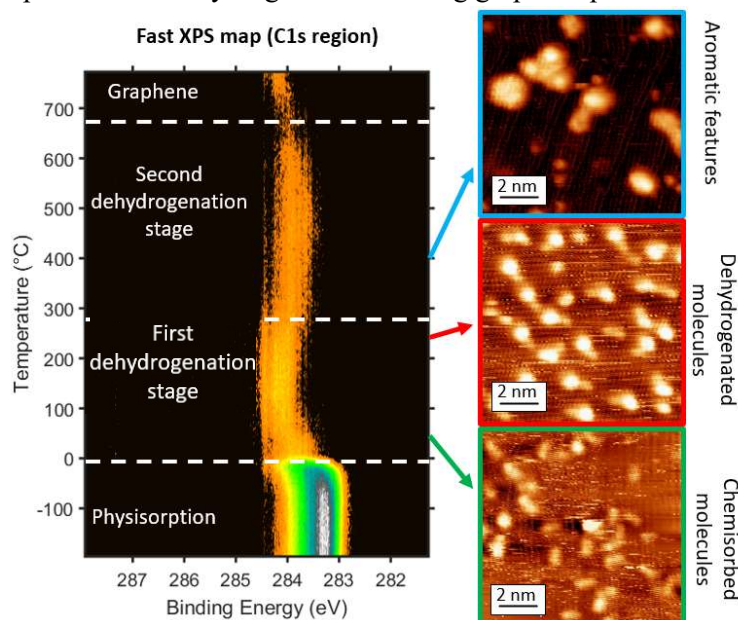


Figure 1. **Left:** Fast XPS plot of the C1s region. A temperature ramp (2°C per second) was performed on a sample of Pt(111) dosed with 0.1 Langmuir of octane at liquid nitrogen temperature. Four main stages can be distinguished.

**Right:** STM images taken at different temperatures (V=0.5-1V, I=0.2-0.3nA)

[1] M.C. Haibach *et al.*, Accounts of Chemical Research, Vol. 45, No. 6, 947-958 (2012)

[2] P. Merino *et al.*, Nat. Comms, 5:3054 (2014)

[3] A.G.G.M. Tielens, Annu. Rev. Astron. Astrophys. 46:289-337 (2008)

## Session III - Chair of the session: J. J. de Miguel

INC & Programa de Doctorado Interuniversitario en Física de la Materia Condensada, Nanociencia y Biofísica

15:45 “The two-dimensional Fermi polaron problem”

Antonio Tienne

Física Teórica de la Materia Condensada

### The two-dimensional Fermi polaron problem

A. Tienne<sup>1,4</sup>, J. Levinsen<sup>2</sup>, J. Keeling<sup>3</sup>, M. M. Parish<sup>2</sup>, F. M. Marchetti<sup>1</sup>

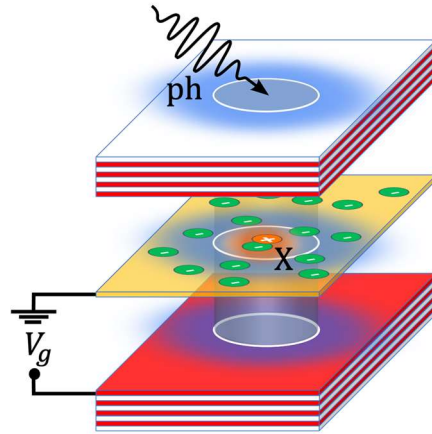
<sup>1</sup>Universidad Autónoma de Madrid, Instituto Nicolás Cabrera, IFIMAC, Madrid 28049, Spain

<sup>2</sup>Monash University, Victoria 3800, Australia

<sup>3</sup>University of St Andrews, St Andrews, KY16 9SS, United Kingdom

<sup>4</sup>Email: antonio.tienne@uam.es

The concept of “impurity problem” in quantum physics, i.e., few particles surrounded by a quantum gas, goes back to 1933, when the Russian physicist Lev Landau described the properties of conduction electrons in a dielectric medium. Here, polarons are quasi-particles resulting from the dressing of electrons by collective excitations of the dielectric medium. Despite nearly a century of work, the polaron problem continues to attract significant interest. In particular, recent ground-breaking experiments in ultracold atomic gases and semiconductor TMD monolayers have renewed interest in this topic. This seminar focuses on the properties of Fermi polarons in 2D semiconductors, the elementary optical excitations of a 2D electron (or hole) gas. These systems have the unique possibility of being embedded into optical cavities to allow strong coupling between matter and light, leading to the formation of polaritonic quasi-particles. After reviewing the literature, I will describe our recent results in this area [1], where we study the optical absorption spectrum of a doped two-dimensional semiconductor in the spin-valley polarized limit. In this configuration, the carriers in the Fermi sea are indistinguishable from one of the two carriers forming the exciton. Most notably, this indistinguishability requires the three-body trion state to have p-wave symmetry. To explore the consequences of this, we evaluate the system’s optical properties within a polaron description, which can interpolate from the low density limit—where the relevant excitations are few-body bound states—to higher density many-body states.



[1] A. Tienne, J. Levinsen, J. Keeling, M. M. Parish and F. M. Marchetti (arXiv:2109.12994 (2021))

## Fine Defect Engineering of Graphene Friction

A. Zambudio<sup>1,2</sup>, E. Gnecco<sup>3</sup>, J. Colchero<sup>1</sup>, R. Pérez<sup>4,5</sup>, J. Gómez-Herrero<sup>2,5</sup> and C. Gómez-Navarro<sup>2,5</sup>

<sup>1</sup>Optics and Nanophysics Research Center, Universidad de Murcia, 30100, Murcia, Spain

<sup>2</sup>Condensed Matter Physics Dept., Universidad Autónoma de Madrid, Madrid, E-28049, Spain

<sup>3</sup>Otto Schott Institute of Materials Research, Friedrich Schiller University of Jena, D-07743, Jena, Germany

<sup>4</sup>Theory Condensed Matter Physics Dept., Universidad Autónoma de Madrid, Madrid, E-28049, Spain

<sup>5</sup>Condensed Matter Physics Center, Universidad Autónoma de Madrid, Madrid, E-28049, Spain

Email: aitor.zambudio@uam.es

Two-dimensional materials, in particular graphene, exhibits a low friction coefficient and good wear properties. However, the presence of atomic defects, inherent to any large-scale production of atomic-layered material, hugely influence the friction and other mechanical properties of graphene. Up to date, tribological studies of defective graphene mix coexistent substitution-like and vacancy defects with several defect size[1], leading to a difficult interpretation and comparison of results, and preventing from a fundamental understanding of the role of defects on graphene friction.

In this work, we quantify the influence of controlled-induced monoatomic vacancies in graphene tribology using Atomic Force Microscopy (AFM). This simplest and very common type of defects is demonstrated to increase the friction of graphene. Furthermore, friction coefficient is as well enhanced by defects in a highly efficient manner. Only 0.1% of defects yields to a five-fold increase of friction coefficient[2]. At the atomic-scale, we resolve monoatomic vacancies in friction images and obtain real-space distribution of their influence in tribology, showing a great correlation with Prandtl-Tomlinson model atomic simulations.

Thorough analysis of friction data reveals two main factors contributing to friction enhancement. One is related to reactivity of dangling bond localized at monovacancy site ( $\sim 1\text{nm}^2$ ) and is responsible of  $\sim 20\%$  of the increase. The other is a more extended one ( $\sim 25\text{nm}^2$ ) and arises from the long-range strain distribution around vacancies, being the main contribution to friction enhancement on defective graphene. These results elucidate the subtle connection between friction, reactivity, and mechanical properties in two-dimensional materials.

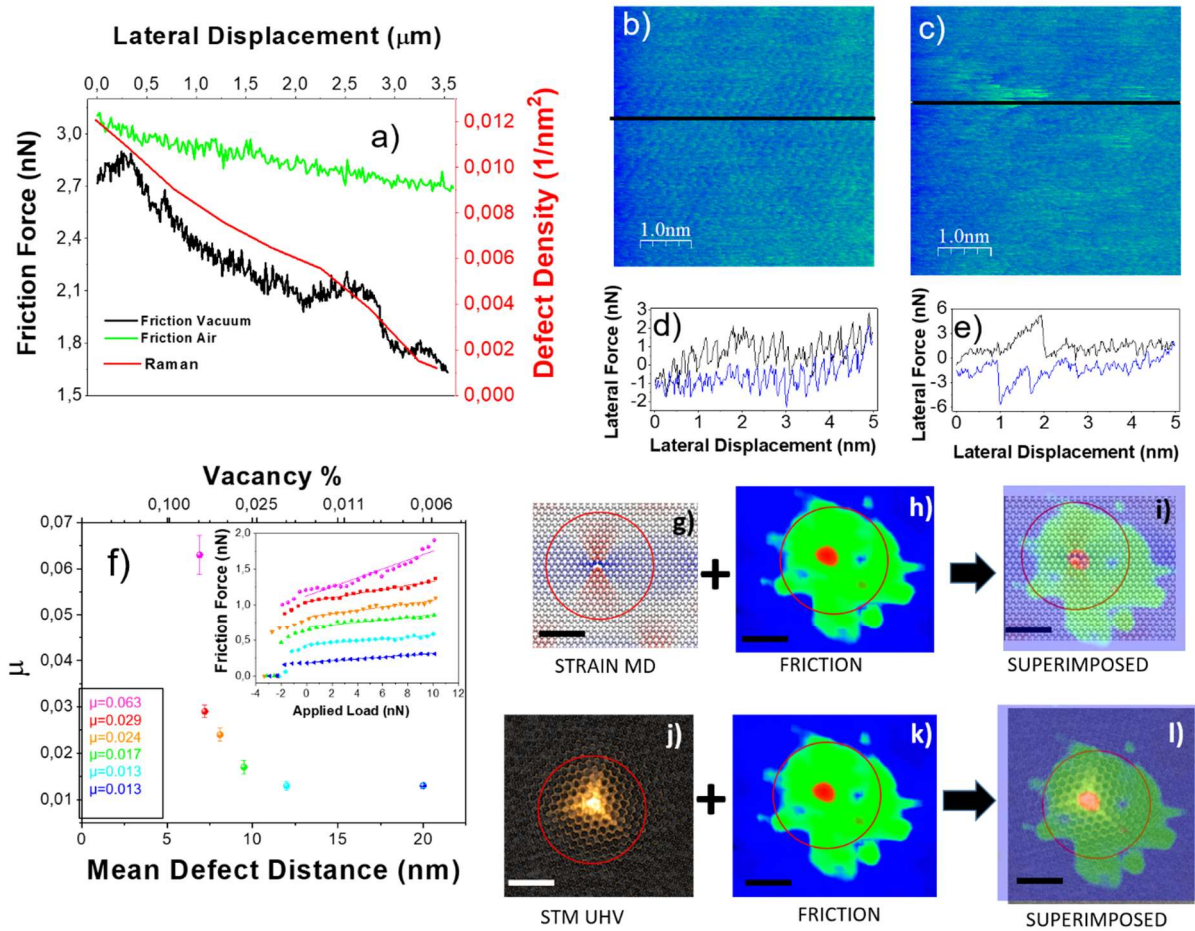


Figure 1. a) Friction force along a region with increasing defect density, acquired in air (green) and vacuum (black). Red line represents defect density along the same region as for the friction force, extracted by Raman microscopy. Friction force exhibits a clear enhancement with defect density. b) and c) Measured lateral force image of a pristine and a defective region of graphene, respectively, showing stick-slip features. d) and e) Profiles extracted along the black line at the respective images above b) and c), acquired in forward scan (from left to right, in black) and backward scan (from right to left, in blue). We can observe the stick-increased feature of the defect, as well as the regular stick-slip behaviour of graphene lattice. f) Friction coefficient at different mean defect distances, obtained from friction  $\nu$ s applied normal force curves depicted at upper inset. Lower inset shows extracted friction coefficient values. g) 2D stress map obtained from Molecular Dynamic simulations[3] in a region surrounding a carbon monovacancy. h) and k) Lateral force images centred on a carbon monovacancy. c) Superposition of panels a) and b). d) Experimental STM image of a carbon monovacancy acquired in UHV conditions. (courtesy of I. Brihuega) f) Superposition of panels d) and e). Both c) and f) panels show a clear spatial correlation between the defect influence area on friction images acquired in the present work and previous theoretical and experimental results on similar graphene monovacancies. Scale bar for g) to l) images is 2 nm.

- [1] S. Kwon et al., Nano Lett., **12**(12), 6043-6048 (2012)
- [2] A. Zambudio et al., Carbon, **182**, 735-741 (2021)
- [3] G. López-Polín et al., Carbon, **116**, 670-677 (2017)



## Refraction and lensing of nano-light in an anisotropic two-dimensional material

G. Álvarez-Pérez<sup>1,2,12</sup>, J. Duan<sup>1,2,12</sup>, A. I. F. Tresguerres-Mata<sup>1</sup>, J. Taboada-Gutiérrez<sup>1,2</sup>, K. V. Voronin<sup>3</sup>, A. Bylinkin<sup>4,5</sup>, B. Chang<sup>6</sup>, S. Xiao<sup>7</sup>, S. Liu<sup>8</sup>, J. H. Edgar<sup>8</sup>, J. I. Martín<sup>1,2</sup>, V. S. Volkov<sup>3,9</sup>, R. Hillenbrand<sup>10,11</sup>, J. Martín-Sánchez<sup>1,2</sup>, A. Y. Nikitin<sup>5,10</sup> and P. Alonso-González<sup>1,2</sup>

<sup>1</sup>Department of Physics, University of Oviedo, Oviedo, Spain. <sup>2</sup>Center of Research on Nanomaterials and Nanotechnology, CINN (CSIC-Universidad de Oviedo), El Entrego, Spain. <sup>3</sup>Center for Photonics and 2D Materials, Moscow Institute of Physics and Technology, Dolgoprudny, Russia. <sup>4</sup>CIC nanoGUNE BRTA, Donostia San Sebastian, Spain. <sup>5</sup>Donostia International Physics Center (DIPC), Donostia/San Sebastián, Spain. <sup>6</sup>National Centre for Nano Fabrication and Characterization, Technical University of Denmark, Lyngby, Denmark. <sup>7</sup>DTU, Fotonik, Department of Photonics Engineering and Center for Nanostructured Graphene, Technical University of Denmark, Lyngby, Denmark. <sup>8</sup>Tim Taylor Department of Chemical Engineering, Kansas State University, Manhattan, KS, USA. <sup>9</sup>GrapheneTek, Skolkovo Innovation Center, Moscow, Russia. <sup>10</sup>IKERBASQUE, Basque Foundation for Science, Bilbao, Spain. <sup>11</sup>CIC nanoGUNE BRTA and Department of Electricity and Electronics, UPV/EHU, Donostia - San Sebastian, Spain. <sup>12</sup>These authors contributed equally: J. Duan, G. Álvarez-Pérez  
Email: [gonzaloalvarez@uniovi.es](mailto:gonzaloalvarez@uniovi.es), [pabloalonso@uniovi.es](mailto:pabloalonso@uniovi.es)

Refraction between isotropic media is characterized by light bending towards the normal to the boundary when passing from a low- to a high-refractive-index medium. However, refraction between anisotropic media is a more exotic phenomenon which remains barely investigated, particularly at the nanoscale. Here [1], we visualize and comprehensively study the general case of refraction of electromagnetic waves between two strongly anisotropic (hyperbolic) media, and we do it with the use of nanoscale-confined polaritons —hybrid light matter waves— in a naturally anisotropic van der Waals material: alpha phase molybdenum trioxide ( $\alpha$ -MoO<sub>3</sub>) [2-4]. The refracted polaritons exhibit non-intuitive directions of propagation as they traverse planar nanoprisms, enabling to unveil an exotic optical effect: anomalous refraction. Furthermore, we develop an in-plane refractive hyperlens, yielding foci as small as  $\lambda_p/6$ , being  $\lambda_p$  the polariton wavelength ( $\lambda_0/50$  compared to the wavelength of free-space light). Our results set the grounds for planar nano-optics in strongly anisotropic media, with potential for effective control of the flow of energy at the nanoscale.

[1] J Duan, G Álvarez-Pérez, et al. Nature Communications 12, 4325 (2021).

[2] W Ma, P Alonso-González, S Li, et al. Nature 562, 557–562 (2018).

[3] G Álvarez-Pérez, et al. Advanced Materials 32, 1908176 (2020).

[4] G Álvarez-Pérez, KV Voronin, et al. Physical Review B 100, 235408 (2019).

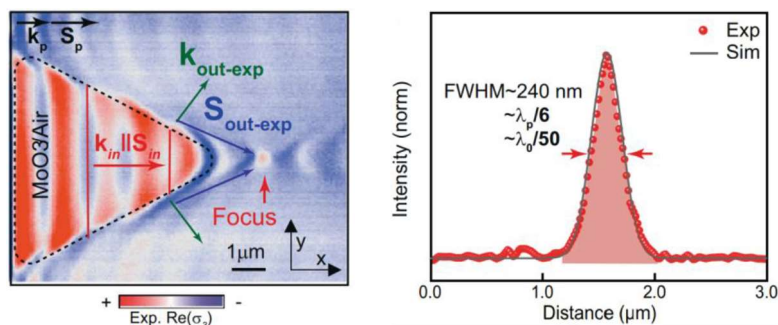


Figure. Sub-diffractive planar lens based on refraction of nano-light.

## In-plane anisotropic optical and mechanical properties of two-dimensional MoO<sub>3</sub>

Sergio Puebla<sup>1</sup>, Roberto D’Agosta<sup>2,3</sup>, Gabriel Sanchez-Santolino<sup>4</sup>, Hao Li<sup>1</sup>, Riccardo Frisenda<sup>1</sup>, Carmen Munuera<sup>1</sup> & Andres Castellanos-Gomez<sup>1</sup>.

1. Materials Science Factory, Instituto de Ciencia de Materiales de Madrid (ICMM-CSIC), Madrid, Spain.

2. Nano-Bio Spectroscopy Group and European Theoretical Spectroscopy Facility (ETSF), Departamento Polimeros y Materiales Avanzados: Física, Química y Tecnología, Universidad del País Vasco UPV/EHU, San Sebastián, Spain.

3. IKERBASQUE, Basque Foundation for Science, Bilbao, Spain.

4. GPMC, Departamento de Física de Materiales & Instituto Pluridisciplinar, Universidad Complutense de Madrid, Madrid, Spain  
Email: sergio.puebla@csic.es

Molybdenum trioxide (MoO<sub>3</sub>) in-plane anisotropy has increasingly attracted the attention of the scientific community in the last few years [1, 2]. Many of the observed in-plane anisotropic properties stem from the anisotropic refractive index and elastic constants of the material [3,4] but a comprehensive analysis of these fundamental properties is still lacking. Here we employ Raman and micro-reflectance measurements, using polarized light, to determine the angular dependence of the refractive index of thin MoO<sub>3</sub> flakes. We study the directional dependence of the MoO<sub>3</sub> Young’s modulus using the buckling metrology method, finding large in-plane anisotropic mechanical properties [5]. Raman shift rates also exhibit distinctive anisotropic strain responses with an intriguing positive shift in wavenumber in polarized Raman micro-reflectance measurements, opposite in sign to almost the rest of the reported materials.

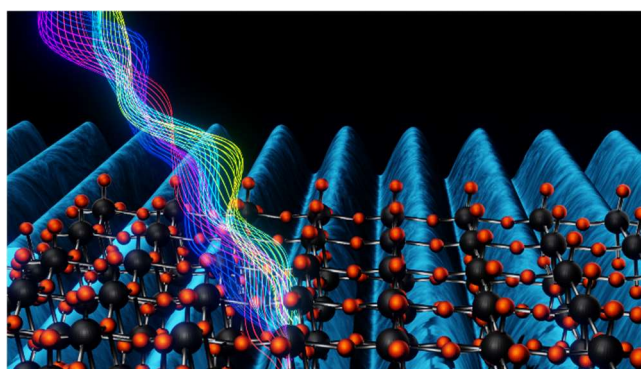


Figure 2. Artistic representation of the mechanical and optical measurements applied to MoO<sub>3</sub>.

- [1] Balendhran, S. et al. *Adv. Mater.* **25**, 109–114 (2013).
- [2] Arash, A. et al. *ACS Appl. Mater. Interfaces*
- [3] Ma, W. et al. *Nature* **562**, 557–562 (2018).
- [4] Zhang, W. B., Qu, Q. & Lai, K. *ACS Appl. Mater. Interfaces* **9**, 1702–1709 (2017).
- [5] Puebla, S., D’Agosta, R., Sanchez-Santolino, G. et al. *npj 2D Mater Appl* **5**, 37 (2021).

# Boosting Room Temperature Tunnel Magnetoresistance in Hybrid Magnetic Tunnel Junctions Under Electric Bias

César González-Ruano<sup>1</sup>, Coriolan Tiusan<sup>2</sup>, Michel Hehn<sup>2</sup> and Farkhad G. Aliev<sup>1</sup>

<sup>1</sup>*Departamento Física de la Materia Condensada C-III, INC and IFIMAC, Universidad Autónoma de Madrid, Madrid, 28049 Spain*

<sup>2</sup>*Institut Jean Lamour, Nancy Université, Vandoeuvre-les-Nancy Cedex, 54506 France*

Email: cesar.gonzalez-ruano@uam.es

Spin-resolved electron symmetry filtering is a key mechanism behind giant tunneling magnetoresistance (TMR) in Fe/MgO/Fe and similar magnetic tunnel junctions (MTJs), providing room temperature functionality in spin electronics. However, the electron symmetry filtering breaks down under applied bias, dramatically reducing the TMR above 0.5 V. This strongly hampers the application range of MTJs. To circumvent the problem, resonant tunneling through quantum well states in thin layers has been used so far. This mechanism, however, is mainly effective at low temperatures.

Here, a fundamentally different approach is demonstrated, providing a strong TMR boost under applied bias in V/MgO/Fe/MgO/Fe/Co hybrid magnetic tunnel junctions (MTJs) where the conductance is mainly provided by spin orbit coupling (SOC) controlled interfacial states with symmetries different from the bulk states in vanadium, which contrary to the bulk states are allowed to tunnel to Fe(001) at low biases. This configuration provides a robust increase of the TMR with bias up to 0.5 V in a wide temperature range and unprecedented high output voltage values in room temperature spintronics. The experimental results are modeled using two nonlinear resistances in series, with the low bias conductance of the first (V/MgO/Fe) element being boosted by the SOC-controlled interfacial states, while the conductance of the second (Fe/MgO/Fe) junction is controlled by the relative alignment of the ferromagnetic layers.

This approach demonstrates the importance of the electron-symmetry-protected surface states in metallic interfaces. The observed results pave a way to unexplored and fundamentally different spintronic device schemes with tunneling magnetoresistance uplifted under applied electric bias, which could push the applicability range of spintronic devices toward higher biases.

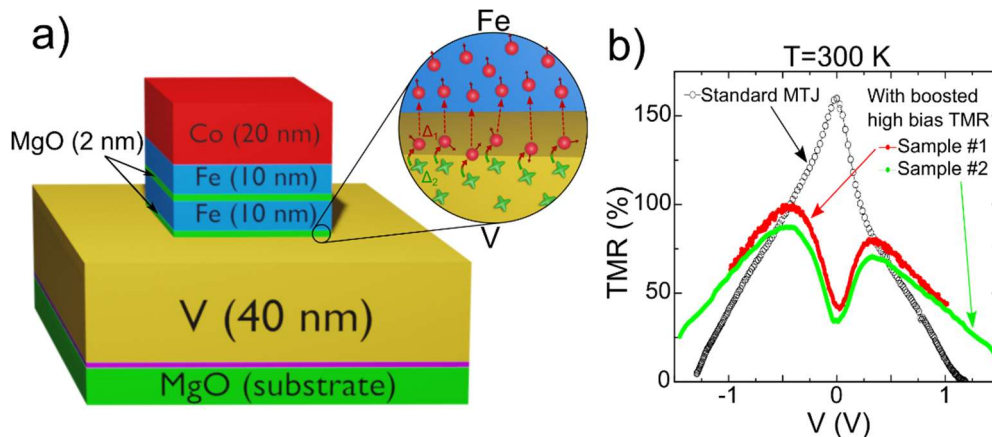


Figure 1. **a)** Sketch of the junctions studied. The zoom depicts the main transport mechanism responsible for the observed results, with electrons in V changing their symmetry at the V/MgO interface due to SOC before tunneling into the Fe electrode. **b)** TMR vs applied bias. An increase in the TMR is observed up to 0.5 V, where it becomes higher than for standard MTJs.

## Poster Session

13:00 – 14:30

---

### List of Posters:

1. **Fernández-Lomana Gómez-Guillamón, Marta:** Tunneling spectroscopy at very high magnetic fields in the iron based superconductor  $\text{KFe}_2\text{As}_2$
2. **Moreno, Jose Antonio:** Scanning AC Josephson Spectroscopy
3. **Ramírez González, Juan Pedro:** Phase behavior of hard circular arcs: purely entropy-driven cluster phases
4. **Balduque Picazo, José:** Interference induced thermoelectric response of ballistic conductors
5. **Al Shuhaib, Jinan Hussein:** Synthesis, crystal structure, band gap energy and Seebeck coefficient of trigonal  $\text{Sr}_{x+1}\text{TiS}_{3-y}$  chalcogenide perovskites
6. **Muñoz Ortiz, Tamara:** Gold nanoshells for molecular imaging of inflammation by Optical Coherence Tomography
7. **Fernández Martínez, Javier:** Manipulating coherence and directionality of rare earth quantum emitters by plasmonic chains
8. **López Nebreda, Rubén:** Simultaneous measurement of conductance and thermopower using STM and multifrequency detection
9. **Martín Pérez, Lucía:** Liquid-phase exfoliation of magnetic van der Waals crystals and its role in the synthesis of 2D-2D covalent heterostructures
10. **Casal, Ignacio:** Implementation of high frequency techniques for measuring hybrid superconductor/semiconductor devices
11. **Exposito, Diego:** Development of a true variable temperature gateable-STM/AFM in LT-UHV conditions to probe 2D materials
12. **García, Pablo:** Reduced size STM in high magnetic fields
13. **Strobl, Klara:** Electromechanical photophysics of individual P22 protein cages loaded with GFP
14. **Cantero, Miguel:** Probing the structural stability of SARS-CoV-2 surrogate TGEV under stringent environmental conditions
15. **Hernández del Valle, Miguel:** A coarse-grained approach to model the dynamics of the actomyosin cortex
16. **Camarero, Pablo:** Laser Irradiation in spheroids MCF-7 and U-87
17. **Ramírez, M<sup>a</sup> Jesús:** Preparation of thin film  $\text{LiCoO}_2$  cathodes by pulsed laser deposition for Li-ion batteries
18. **Díaz Escribano, Samuel:** Proximity effects and topological superconductivity dependency on layer thickness in superconductor/ferromagnetic/semiconductor hybrid devices
19. **Viñals, Silvia:** Characterization of the external pulsed beam at CMAM for proton-therapy studies at the FLASH regime
20. **Rodríguez Espinosa, M<sup>a</sup> Jesús:** Unraveling the structure of RNA-packed within Penicillium Chrysogenum Virus and its influence in the mechanical stability
21. **Campusano, Richard:** Bacillus Subtilis swimming motility in liquid broth and structured media

22. **Gómez, Mario:** The Josephson effect in full-shell Al-InAs nanowires in the Little-Parks regime
23. **Vivas Viaña, Alejandro:** Unconventional mechanism of virtual-state population through dissipation
24. **Lu, Dasheng:** Improving stability and thermal sensitivity of an optically trapped upconversion nanoparticle by coating with a thermo-sensitive polymer
25. **Díaz Sánchez, Jesús:** Electronic characterization of LiCoO<sub>2</sub> thin films in the overlithiation regime by XPS and ARPES
26. **Caso, Diego:** Excitation and propagation of edge spin waves in ferromagnetic triangles
27. **Álamo Vargas, Pablo:** Luminescence of GaP<sub>1-x</sub>N<sub>x</sub> layers grown on nominally (001) oriented Si substrates
28. **Guo, Haojie:** Unraveling the highly complex nature of antimony on Pt(111)
29. **García Esteban, Juan José:** Deep Learning for the Modeling and Inverse Design of Radiative Heat Transfer
30. **Águeda Velasco, Miguel:** Superconducting gap and magnetoresistance of layered AuSn<sub>4</sub>
31. **Hurtado Gallego, Juan:** Quantum Interference in Radical and Neutral Single-Molecule Junctions
32. **Singh, Raghvendra:** Irradiation of Bi-Sb crystals for possible subsurface amorphization
33. **Salazar Beitia, Iñigo:** GaSe and carbon nanotubes for Li-ion batteries
34. **Li, Hao:** Strongly anisotropic strain-tunability of excitons in exfoliated ZrSe<sub>3</sub>
35. **de la Peña Ruiz, Sebastián:** Theory of drift-enabled control in nonlocal magnon transport
36. **Arranz Jiménez, Marcos:** Photovoltaic effects study on hybrid perovskites thin layers
37. **Lasso, Alejandro:** Density Functional Theory and Machine Learning techniques for the study of amorphous materials
38. **Fernández Alonso, Francisco Javier:** Deposition of impedimetric electrodes on steel for the development of embedded sensors
39. **Galante, Clara:** Machine Learning in Nonlinear Dynamic Systems
40. **Lizarraga Lallana, Juan:** Polariton condensation in semiconductor microcavity pillars
41. **Luengo-Márquez, Juan:** Force-dependent mechanical properties of nucleic acids from fluctuations
42. **Mangriya, Paula:** Confined motion of active rotating particles within lipid vesicles
43. **Tinao, Berta:** Artificial Vesicle Fusion: from Fundamentals to Applications
44. **Esteve-Paredes, Juan José:** Light-matter interaction from density functional theory with application to attosecond electron dynamics
45. **Geva, Galor:** Assessing the predictive ability of the effective temperature in a driven colloidal suspension
46. **Manzanares Negro, Yolanda:** Controlling toughness of MoS<sub>2</sub> single layers by introducing atomic vacancies
47. **Salagre, Elena:** Surface Evolution in epitaxial Li<sub>x</sub>CoO<sub>2</sub> films studied by LEEM/PEEM for  $x \leq 1$
48. **García Blázquez, Antonio:** Projective representations from non-symmorphic space groups and spin-orbit coupling: how and why
49. **Ibabe Aviles, Angel:** Transport and heating effects in proximitized InAs nanowire islands

# Tunneling spectroscopy at very high magnetic fields in the iron based superconductor $\text{KFe}_2\text{As}_2$

M.Fernández-Lomana<sup>1</sup>, B.Wu<sup>1</sup>, E. Herrera<sup>1</sup>, A. A. Haghighirad<sup>2</sup>, H.Suderow<sup>1,3</sup>, A.E. Böhmer<sup>2,4</sup> and I.Guillamón<sup>1,3</sup>

<sup>1</sup>*Laboratorio de Bajas Temperaturas, Departamento de Física de la Materia Condensada, Instituto de ciencia de Materiales Nicolás Cabrera, Condensed Matter Physics Center (IFIMAC), Universidad Autónoma de Madrid, E-28049*

<sup>2</sup>*Institute for Quantum Materials and Technologies (IQMT), Karlsruhe Institute of Technology, 76021 Karlsruhe, Germany*

<sup>3</sup>*Unidad Asociada de Bajas Temperaturas y Altos Campos Magnéticos, UAM, CSIC, Cantoblanco, E-28049 Madrid, Spain 3 Segainvex, Universidad Autónoma de Madrid, 28049 Madrid, Spain*

<sup>4</sup>*Institut für Experimentalphysik IV, Ruhr-Universität Bochum, 44801 Bochum, Germany*

\*Presenting author: marta.fernandez-lomana@uam.es

We present scanning tunneling spectroscopy measurements in  $\text{KFe}_2\text{As}_2$ . This system is a superconductor with  $T_c$  which is at the end of the  $\text{Ba}_{1-x}\text{K}_x\text{Fe}_2\text{As}_2$  series. It has been proposed to be a nodal superconductor. The electronic effective mass is strongly enhanced due to the proximity to an orbital-selective Mott transition [1]. Here we make first STM measurements at very low temperatures and high magnetic fields [2]. At zero field, we identify an unprecedented anisotropy of the superconducting gap. In the intermediate state, we observe the vortex lattice to very large values of the magnetic field. We finally present measurements of the bandstructure in superconducting and normal phases, obtained at zero magnetic field and at magnetic fields of 20 T from quasiparticle interference scattering.

[1] F. Hardy et al., Phys. Rev. Lett. **111**, 027002 (2013)

[2] M. Fernández-Lomana et al, Rev. Sci. Instrum. **92**, 093701 (2021)

## Scanning AC Josephson Spectroscopy

**Víctor Barrena<sup>1</sup>, Jose Antonio Moreno<sup>1\*</sup>, Samuel Díaz Escribano<sup>2</sup>, David Perconte<sup>1</sup>, Marta Fernández Lomana<sup>1</sup>, Edwin Herrera<sup>1</sup>, Beilun Wu<sup>1</sup>, Isabel Guillamón<sup>1</sup>, Alfredo Levy Yeyati<sup>2</sup> and Hermann Suderow<sup>1</sup>**

<sup>1</sup> *Laboratorio de Bajas Temperaturas y Altos Campos Magnéticos, Departamento de Física de la Materia Condensada, Instituto Nicolás Cabrera and Condensed Matter Physics Center (IFIMAC), Unidad Asociada UAM-CSIC, Universidad Autónoma de Madrid, E-28049 Madrid, Spain*

<sup>2</sup> *Departamento de Física Teórica de la Materia Condensada, Instituto Nicolás Cabrera and Condensed Matter Physics Center (IFIMAC), Universidad Autónoma de Madrid, Madrid, Spain*

\*Email: (josea.moreno@estudiante.uam.es)

Scanning tunneling microscopy with superconducting tip is a powerful technique capable of enhancing the energy and spatial resolution of conventional STM with superconducting materials. Furthermore, with a superconducting tip we can probe superconductor-superconductor junctions and measure the Josephson effect between tip and sample, which can yield relevant information about correlated states. Here we have performed Josephson tunneling microscopy (JSTM) with a Pb tip on both Pb and 2H-NbSe<sub>2</sub>. We have characterized the recently discovered AC Josephson component using an AC amplification lock-in technique. Our approach leads to an order of magnitude increase in the Josephson signal strength and allows to considerably improve studying the Josephson coupling as a function of the position.

## Phase behavior of hard circular arcs: purely entropy-driven cluster phases

**Juan Pedro Ramírez González<sup>1</sup>, Giorgio Cinacchi<sup>1,2,3</sup>**

*Departamento de Física Teórica de la Materia Condensada<sup>1</sup>,*

*Instituto de Física de la Materia Condensada (IFIMAC)<sup>2</sup>,*

*Instituto de Ciencias de Materiales “Nicolás Cabrera”<sup>3</sup>,*

*Universidad Autónoma de Madrid, Ciudad Universitaria de Cantoblanco, E-28049 Madrid, Spain*

*Email: [juanp.ramirez@uam.es](mailto:juanp.ramirez@uam.es)*

By using Monte Carlo numerical simulations we have investigated the complete phase behavior of systems of hard infinitesimally-thin circular arcs in two dimensions and sketched their phase diagram in the plane subtended angle,  $\theta$ , versus the inverse of the number density,  $1/\rho$  [1]. Despite their simplicity, systems of hard infinitesimally-thin circular arcs manifest a rich auto-assembly phenomenology that is driven by the sole entropy. In particular, these systems form a filamentary phase for arcs denotable as minor ( $\theta < \pi$ ) and a hexagonal cluster phase for arcs denotable as major ( $\theta > \pi$ ). In the former phase minor circular arcs tend to organize on the same semi-circumference and then file to generate filaments. While in the latter phase major circular arcs intertwine and tend to pack on the same parent circumference, forming circular clusters which, in turn, arrange on a triangular lattice [2]. Interestingly, these circular clusters are natural chiral structures while the cluster hexagonal phase is globally non-chiral.

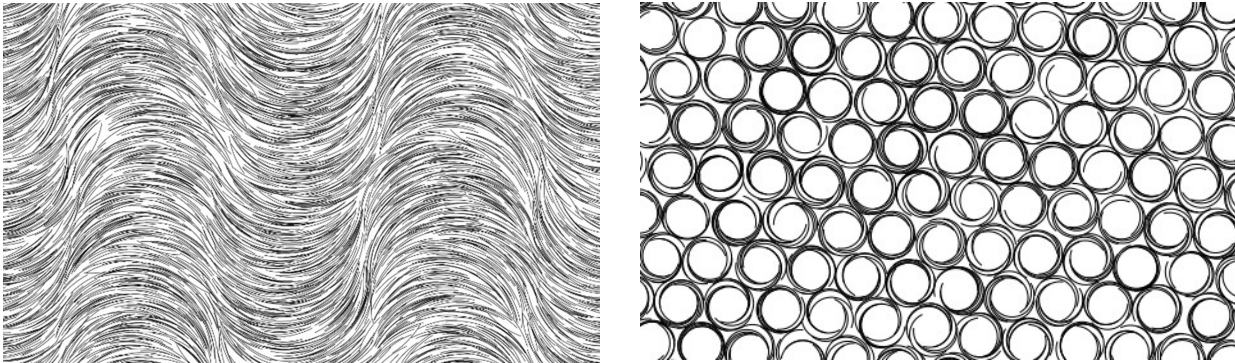


Figure: on the left panel an example of a filamentary phase is shown for minor arcs subtending an angle  $\theta=0.5$ ; on the right panel an example of a cluster hexagonal phase is shown for major arcs subtending an angle  $\theta=1.1\pi$ .



# Interference induced thermoelectric response of ballistic conductors

José Balduque<sup>1</sup> and Rafael Sánchez<sup>1,2</sup>

<sup>1</sup>*Departamento de Física Teórica de la Materia Condensada, Universidad Autónoma de Madrid, Madrid, Spain.*

<sup>2</sup>*Condensed Matter Physics Center (IFIMAC), and Instituto Nicolás Cabrera, Universidad Autónoma de Madrid, Madrid, Spain.*

Email: jose.balduque@uam.es

Quantum conductors have been proposed to work as quantum thermocouples for heat to work conversion at the nanoscale [1]. Three-terminal configurations (quantum analogues of traditional thermocouples) allow to inject heat directly to the nanostructure, this way enhancing the phase coherence effects. We investigate a simple model consisting on a one-dimensional ballistic conductor coupled to the hot tip of a scanning probe (see figure). The interference of trajectories with multiple internal reflections is sufficient to generate a multiterminal thermoelectric effect, even if the conductor does not effectively break electron-hole symmetry [2]. We find a nonlocal thermoelectric response which is modulated by the different parameters of the system, e.g., by the position of the hot probe tip. Different configurations with or without internal resonances are studied in order to improve the efficiency for heat to work conversion.

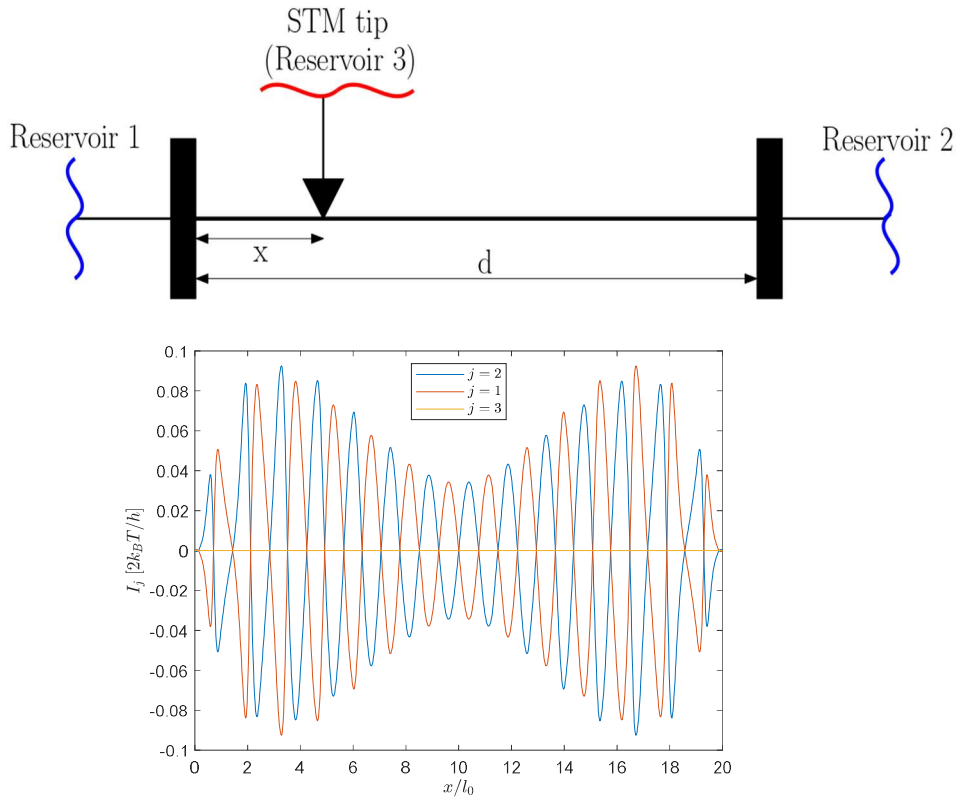


Figure 1. (*Upper panel*) Sketch of the system: a two terminal conductor with two barriers is connected to a scanning probe which injects a heat current in different positions,  $x$ . (*Lower panel*) Particle current  $I_j$  in terminal  $j$  when the tip is hot.

[1] G. Benenti, G. Casati, K. Saito, R.S. Whitney. Phys. Rep., **694**, 1 (2017)

[2] R. Sánchez, C. Gorini, and Geneviève Fleury. Phys. Rev. B., **104**, 115430 (2021)

## Synthesis, crystal structure, band gap energy and Seebeck coefficient of trigonal $\text{Sr}_{x+1}\text{TiS}_{3-y}$ chalcogenide perovskites

Jinan Hussein Al shuhaib<sup>1</sup>, Jose Francisco Fernández<sup>1,2</sup>, Julio Bodega<sup>1</sup>, José R. Ares<sup>1</sup>, Isabel J. Ferrer<sup>1,2</sup>, Fabrice Leardini<sup>1,2</sup>

jinan.awadh@estudiante.uam.es

<sup>1</sup> Departamento de Física de Materiales, Universidad Autónoma de Madrid, Campus de Cantoblanco, E-28049 Madrid, Spain.

<sup>2</sup> Instituto Nicolás Cabrera, Universidad Autónoma de Madrid, Campus de Cantoblanco, E-28049 Madrid, Spain.

We present original results on the synthesis and characterization of inorganic chalcogenide perovskites with chemical formula  $\text{Sr}_{x+1}\text{TiS}_{3-y}$  in a powder form. Samples have been obtained by solid-gas reaction of  $\text{SrTiO}_3$  with  $\text{CS}_2$  in closed quartz ampoules at different temperatures ranging from 900 °C up to 1050 °C. The crystal structure was determined by x ray diffraction measurements (XRD), which showed that  $\text{Sr}_{x+1}\text{TiS}_{3-y}$  has a single phase for all samples, belonging to the trigonal R-3c space group (S.G. 167). Lattice parameters have been obtained by Rietveld refinement of XRD patterns. Raman spectra confirmed that the compounds have a single and homogenous phase. The chemical composition has been obtained by energy dispersive x-ray analysis (EDX). Termogravimetric analyses revealed that samples have a good thermal stability until 685°C in air and till 1200°C in Argon atmosphere. The band gaps of the samples have been obtained from diffuse optical reflectance measurements (see Figure 1). Transport properties have been also investigated based on thermoelectric and electrical conductivity measurements. This work will show that  $\text{Sr}_{x+1}\text{TiS}_{3-y}$  perovskites can have potential interest in thermoelectric, photovoltaic and photoelectrochemical applications.

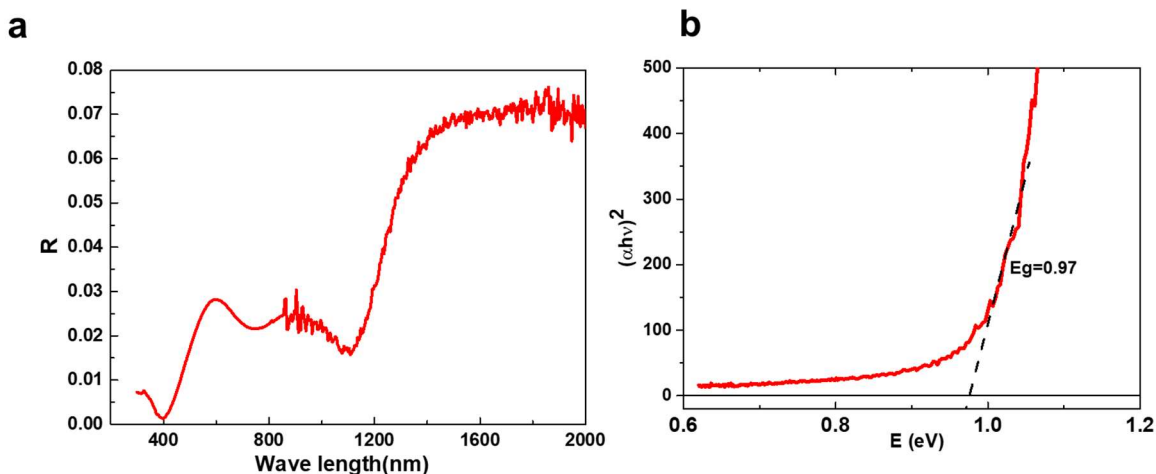


Figure 1. Typical diffuse reflectance spectra of  $\text{Sr}_{x+1}\text{TiS}_{3-y}$  sample (a) and Tauc plot of the Kubelka-Munk function showing the estimated band gap (b) considering a direct allowed transition.

## Gold nanoshells for molecular imaging of inflammation by Optical Coherence Tomography

T Muñoz-Ortiz<sup>1</sup>, J Hu<sup>2</sup>, F Sanz-Rodríguez<sup>1</sup>, F Rivero<sup>3</sup>, D H Ortgies<sup>1,4</sup>, R Aguilar Torres<sup>3</sup>, F Alfonso<sup>3</sup>, D Jaque<sup>1,4</sup>, E Martín Rodríguez<sup>1,4</sup> and J García-Solé<sup>1</sup>

<sup>1</sup>Nanomaterials for Bioimaging Group, Universidad Autónoma de Madrid, Madrid, Spain.

<sup>2</sup>Xiamen Institute of Rare-earth Materials, Haixi Institutes Chinese Academy of Sciences, Fujian, China.

<sup>3</sup>Cardiology Department, Hospital Universitario de la Princesa, Universidad Autónoma de Madrid, Madrid, Spain.

<sup>4</sup>Nanobiology Group Instituto Ramón y Cajal de Investigación Sanitaria IRYCIS, Madrid, Spain.  
Email: tamara.munoz@uam.es

There is an urgent need for contrast agents to detect the first stage of atherosclerosis, which is characterized by the inflammation of endothelial cells and the subsequent overexpression of several cell adhesion molecules [1]. Cardiovascular Optical Coherence Tomography (CV-OCT) is the imaging technique with the highest spatial resolution and sensitivity of those used for the diagnosis of atherosclerosis. Among the available commercial nanoparticles, core/shell gold nanoparticles (gold nanoshells, GNSs) provide the strongest signal by CV-OCT [2].

In this work, GNSs are functionalized with the cLABEL peptide that binds specifically to the ICAM-1 molecules upregulated after endothelial inflammation (figure 1 (a)). Dark field microscopy and CV-OCT are used to evaluate the specific adhesion of the functionalized GNSs to inflamed cells. This adhesion is investigated under static and dynamic conditions, for flow rates comparable to those of physiological conditions (figure 1(b)). An increase in the scattering signal given by the functionalized GNSs attached to inflamed cells is observed compared to non-inflamed ones. Thanks to the molecular interaction of the peptide with the ICAM-1 molecules, cLABEL functionalized GNSs combined with clinical CV-OCT, have shown to be a highly sensitive approach to detect endothelial inflammation. Thus, these nanoparticles behave as excellent contrast agents for CV-OCT and promise a novel strategy for clinical molecular imaging of atherosclerosis.

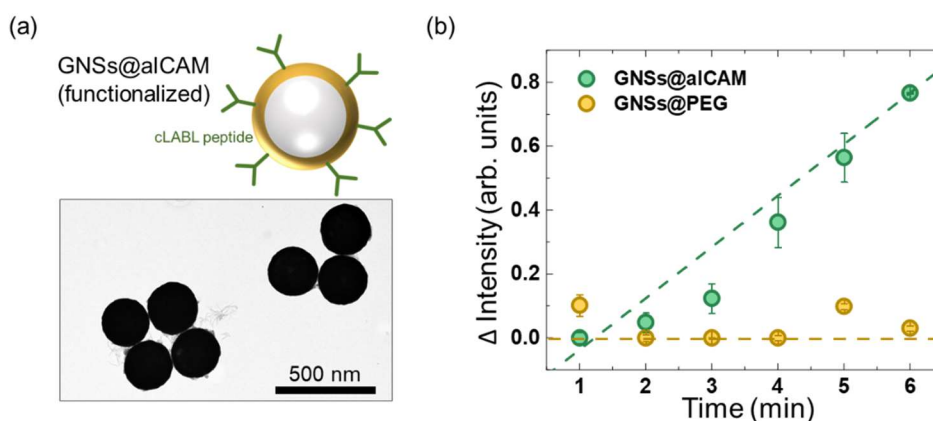


Figure 1. (a) Schematic representation of the cLABEL-functionalized GNSs (top) and their TEM image (bottom). (b) Functionalized GNSs (GNSs@αICAM) adhesion efficiency to inflamed endothelial cells as a function of circulation time. Non-functionalized GNSs (GNS@PEG) have been used as a control.

[1] J. Sanz et al., Nature, **451**, 953 (2008)

[2] J. Hu et al., Journal of Biophotonics, **5**, 674 (2017)

# Manipulating coherence and directionality of rare earth quantum emitters by plasmonic chains

**Javier Fernández-Martínez<sup>1\*</sup>, Sol Carretero-Palacios<sup>1</sup>, Laura Sánchez-García<sup>1</sup>, Jorge Bravo-Abad<sup>2</sup>, Pablo Molina<sup>1</sup>, Niels Van Hoof<sup>3</sup>, Mariola O. Ramírez<sup>1</sup>, Jaime Gómez Rivas<sup>3</sup> and Luisa E. Bausá<sup>1</sup>**

<sup>1</sup> Dept. Física de Materiales, Instituto de Materiales Nicolás Cabrera (INC) and Condensed Matter Physics Center (IFIMAC), Universidad Autónoma de Madrid, 28049-Madrid, Spain

<sup>2</sup> Dept. Física Teórica de la Materia Condensada and Condensed Matter Physics Center (IFIMAC), Universidad Autónoma de Madrid, 28049-Madrid, Spain

<sup>3</sup> Dutch Institute for Fundamental Energy Research, DIFFER, and Eindhoven University of Technology, Groene Loper 5, 5612 AE Eindhoven, The Netherlands

\*Email: [javier.fernandezm@uam.es](mailto:javier.fernandezm@uam.es)

Nowadays, Rare Earth (RE) ions are the focus of a great attention due to their applicability in relevant fields such as quantum light-matter interfaces or photonics networks. In this context, controlling the emission features of RE ions is necessary to develop novel devices. For that matter, the association of plasmonic structures with RE doped crystals has proven useful giving rise, for instance, to solid-state nanolasers with improved and novel characteristics [1,2].

Here, we are going a step forward towards the manipulation of coherence and angular distribution of the RE emission in the absence of photonic cavity. By means of Fourier microscopy experiments, we show the presence of an interference pattern in the emission of Nd<sup>3+</sup> ions located in the vicinities of a single plasmonic chain formed by closely-spaced Ag nanoparticles (NPs). The results are interpreted by numerical simulations, which support the presence of a near-field coherent coupling of the Nd<sup>3+</sup> emitters with the plasmonic mode of the NP chain, radiating light to the far field at specific directions [3].

This work provides fundamental insights of the near-field coupling between quantum emitters and plasmonic nanostructures, and offers novel ways of controlling the RE emission, which could be of potential interest for quantum-light interfaces or integrated optical circuits.

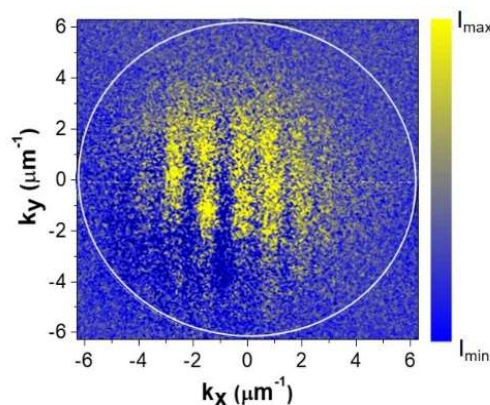


Figure 1. Interference fringe pattern of Nd<sup>3+</sup> emission collected in the vicinity of a plasmonic chain of Ag nanoparticles

- [1] M. O Ramírez et al., *Adv. Mater.* **31**, 1901428 (2019)
- [2] L. Sánchez-García et al. *Light-Sci. Appl.* **8**:14 (2019)
- [3] J. Fernández-Martínez et al., *Opt. Express* **29**, 26244 (2021)

# Simultaneous measurement of conductance and thermopower using STM and multifrequency detection

Rubén López Nebreda,<sup>\*a</sup> Laura Rincón-García<sup>a</sup> and Nicolás Agraït<sup>a,b,c</sup>

<sup>a</sup> Departamento de Física de la Materia Condensada and Condensed Matter Physics Center (IFIMAC), Universidad Autónoma de Madrid, 28049 Madrid, Spain.

<sup>b</sup> Instituto Madrileño de Estudios Avanzados en Nanociencia IMDEA-Nanociencia, E-28049 Madrid, Spain

<sup>c</sup> Instituto Universitario de Ciencia de Materiales "Nicolás Cabrera", Universidad Autónoma de Madrid, E-28049 Madrid, Spain

E-mail: [ruben.lopez@uam.es](mailto:ruben.lopez@uam.es)

The measurement of the thermopower of molecular junctions is a powerful tool for understanding transport phenomena in the nanoscale, in particular in molecular junctions<sup>[1]</sup>. We present a novel multifrequency method that allows for the simultaneous measurement of conductance and thermopower using a scanning tunneling microscope (STM). The STM tip is biased with an AC voltage ( $\sim 2$  kHz) and heated resistively to a constant temperature difference with respect to the sample ( $\Delta T \sim 50$  °C) resulting in an AC tunneling current and a DC thermocurrent which are separated using a multifrequency lockin amplifier. The STM can operate in the conventional imaging mode acquiring simultaneously a topography image and a thermopower image, and in break-junction mode in which the z-voltage is ramped to contact the sample while both conductance and thermopower are recorded.

Figure 1 shows a topography image of C<sub>60</sub> molecules on a gold substrate measured in ambient conditions. We find that the thermopower of a single fullerene in the tunneling regime is around  $-20 \mu\text{V/K}$  in agreement with previously obtained results in contact<sup>[2]</sup>. Unexpectedly, we also found that the magnitude of the thermopower reaches much higher values in C<sub>60</sub> clusters, exceeding  $100 \mu\text{V/K}$ .

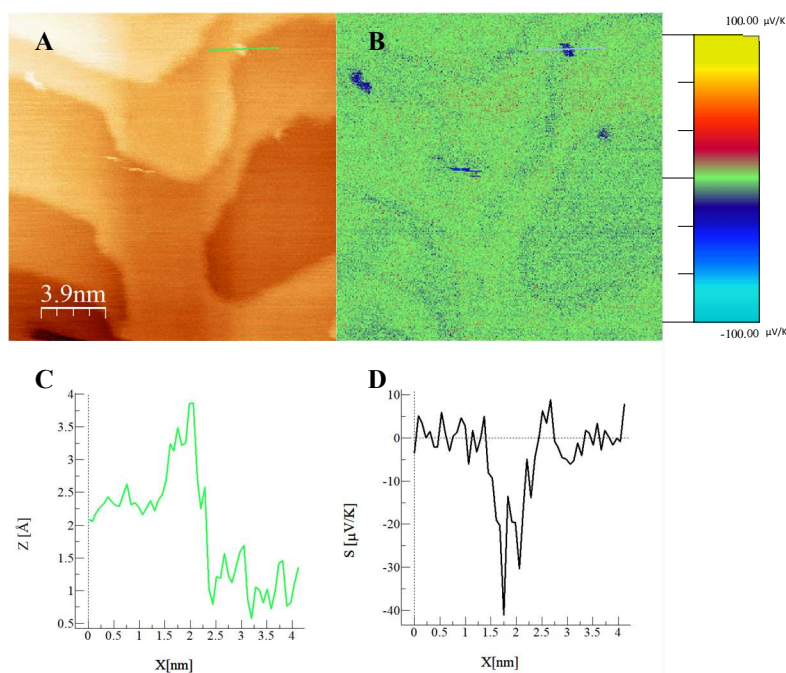


Figure 1: A) Topography image. B) Thermopower image. In C) and D) height profile and thermopower profile, respectively, on a fullerene.

## Notes and References

- 1 Laura Rincón-García, Charalambos Evangelis, Gabino Rubio-Bollinger and Nicolás Agraït. Thermopower measurements in molecular junctions. *Chem. Soc. Rev.*, **2016**, 45, 4285-4306
- 2 Charalambos Evangelis, Katalin Gillemot, Edmund Leary, M. Teresa Gonzalez, Gabino Rubio-Bollinger, Colin J. Lambert, and Nicolas Agraït. Engineering the Thermopower of C<sub>60</sub> Molecular Junctions. *Nano Lett.* **2013**, 13, 2141-2145.



# Liquid-phase exfoliation of magnetic van der Waals crystals and its role in the synthesis of 2D-2D covalent heterostructures

Lucía Martín-Pérez<sup>1</sup>, Manuel Vázquez Sulleiro<sup>1</sup>, Aysegul Develioglul<sup>1</sup>, Mar García-Hernández<sup>2</sup>, Andres Castellanos-Gomez<sup>2</sup>, Emilio M. Pérez<sup>1</sup> and Enrique Burzurí<sup>1,3</sup>

<sup>1</sup>IMDEA Nanociencia, C/Faraday 9, Ciudad Universitaria de Cantoblanco, 28049 Madrid, Spain

<sup>2</sup>Materials Science Factory, Instituto de Ciencia de Materiales de Madrid (ICMM), Consejo Superior de Investigaciones Científicas (CSIC), Sor Juana Inés de la Cruz 3, 28049 Madrid, Spain.

<sup>3</sup>Departamento de Física de la Materia Condensada, Facultad de Ciencias, Universidad Autónoma de Madrid, 28049 Madrid, Spain

Email: lucia.martin@imdea.org

Layered magnetic materials are emerging as the latest acquisition of the van der Waals (vdW) materials family and their heterostructures. An increasingly growing number of reports demonstrate exfoliation of the bulk and persistence of the magnetism down to the monolayer limit. Magnetism is intrinsically linked to the dimensionality of the materials and therefore cleavable magnetic materials are particularly interesting testbeds to study magnetic phenomena that may appear or be quenched at the 2D limit [1,2]. The methods to obtain and characterize the magnetism in the 2D limit remain challenging. The monolayer is typically reached by mechanically breaking the vdW interactions between the layers and the magnetism is indirectly studied by MOKE or Raman [3]. Alternative approaches to produce large amounts of flakes rely on wet methods like liquid-phase exfoliation (LPE) (Figure 1a), where the bulk material is sonicated in a liquid media, leading to the separation of the layers [4,5].

Here we report an optimized route to obtain monolayers of different magnetic vdW crystals by LPE, in particular cylindrite and the FePS<sub>3</sub> trichalcogenide. We show that the fine tuning of sonication and centrifugation times is determinant to produce a statistically significant amount of monolayers with relative big areas ( $\sim 1 \mu\text{m}^2$ ) (Figure 1b). The topological and structural analysis shows that the crystal lattice is preserved after LPE. Importantly, this method has allowed a direct study of the magnetism on frozen solutions of dispersed flakes. We observe that the magnetic transition temperature decreases in both materials. The electron transport properties are studied in field-effect transistors where flakes are deterministically positioned between nanoscale electrodes by dielectrophoresis. AC admittance spectroscopy gives light to the role played by potential barriers between different. Finally, we show how covalent chemistry can be used as an alternative method for the connection of 2D magnetic materials into 2D-2D covalent heterostructures [6].

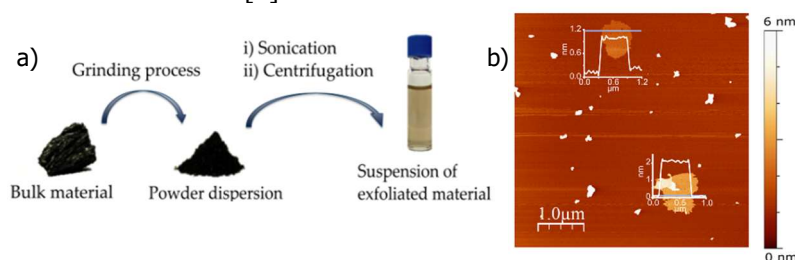


Figure 1. a) Schematic of the two-step liquid-phase exfoliation (LPE) process. b) Atomic force microscopy (AFM) topographic characterization of LPE cylindrite nanoflakes with the corresponding height profile.

## References

- [1] B. Huang et al., *Nature*, **546**, 270–273 (2017)
- [2] C. Gong et al., *Nature*, **546**, 265–269 (2017)
- [3] X. Wang et al., *2D Mater.* **3**, 031009 (2016)
- [4] E. Burzurí et al., *Nanoscale*, **10**, 7966–7970 (2018)
- [5] Y. Niu et al., *2D Mater.* **6**, 035023 (2019)
- [6] M. Vazquez Sulleiro et al., accepted in *Nature Chemistry*, **2021**

# Implementation of high frequency techniques for measuring hybrid superconductor-semiconductor devices

**I. Casal<sup>1</sup>, A. Ibabe<sup>1</sup>, M. Calero<sup>2</sup>, A. Gómez<sup>2</sup>, M. Hocevar<sup>3</sup> and E. J. H. Lee<sup>1</sup>**

<sup>1</sup>*Condensed Matter Physics Department, Universidad Autónoma de Madrid, Madrid, Spain*

<sup>2</sup>*Centro de Astrobiología, CSIC-INTA, Madrid, Spain*

<sup>3</sup>*Univ. Grenoble Alpes, CNRS, Grenoble INP, Institut Néel, Grenoble, France*

Email: ignacio.casal@uam.es

Hybrid semiconductor-superconductor devices are currently at the center of intensive experimental exploration owing to their rich phenomenology and to their potential in quantum technologies [1] [2] [3]. Because of the growing complexity of experiments, high frequency microwave measurements appear as powerful tools for performing faster measurements [4] and for gaining new insights on the physics of the devices which are otherwise not possible with DC transport measurements [5]. In this work, I will present our ongoing efforts to implement high frequency techniques for studying devices based on proximitized nanowires. I will focus particularly on the development of a reflectometry experimental set-up which we have benchmarked by measuring quantum dots (QD) naturally occurring in InAs nanowires. This technique relies on a high frequency resonator that is weakly coupled to the QD. By probing the resonator with a high frequency excitation at the resonant frequency, it is possible to relate changes in its response to capacitive and conductance variations in the QD. Reflectometry has several advantages over DC transport techniques such as higher SNR with measurement times an order of magnitude lower and simpler fabrication at the nanoscale level (when compared to other charge detection techniques). Here, I will compare DC and reflectometry measurements where the latter was carried out up to three times faster than the former. I will also present some other developments that are being currently undertaken for our final objective of demonstrating a gatemon qubit.

[1] Prada, E. et al. From Andreev to Majorana bound states in hybrid superconductor–semiconductor nanowires. *Nature Reviews Physics* 2, 575–594 (2020)

[2] Lee, E. J. H. et al. Spin-resolved Andreev levels and parity crossings in hybrid superconductor–semiconductor nanostructures. *Nature Nanotech* 9, 79–84 (2014)

[3] Hays, M. et al. Coherent manipulation of an Andreev spin qubit. *Science* 373, 430–433 (2021).

[4] Petersson, K. D. et al. Charge and Spin State Readout of a Double Quantum Dot Coupled to a Resonator. *Nano Lett.* 10, 2789–2793 (2010).

[5] Tosi, L. et al. Spin-Orbit Splitting of Andreev States Revealed by Microwave Spectroscopy. *Phys. Rev. X* 9, 011010 (2019).

## Development of a true variable temperature gateable-STM/AFM in LT-UHV conditions to probe 2D materials

D. Exposito<sup>1</sup>, I. Brihuega<sup>2</sup>

<sup>1</sup> Universidad Autónoma de Madrid, IFIMAC and INC, Madrid (Spain)

Email: diego.exposito@uam.es

Since their first isolation, 2D materials have been widely studied, showing very interesting properties, both locally and globally. Techniques such as STM/AFM have proven to be really useful in this task, producing some of the most exciting findings in these unique materials.

In this work we've developed a new scanning tunneling microscope/atomic force microscope (STM-AFM) with transport and gating capabilities in Ultra-High-Vacuum (UHV) conditions, specifically designed to track, with atomic resolution, the same sample region from 4K to 400K, and also to position, with few micrometer precision, in a given sample region. The combination of these capabilities, unique in this kind of microscopes, will enable, on one hand, to measure gateable 2D samples with a much reduced total size and track the evolution of its properties in an exceptionally wide range of temperatures and, on the other, to correlate the global transport response of a device with its local atomic properties.

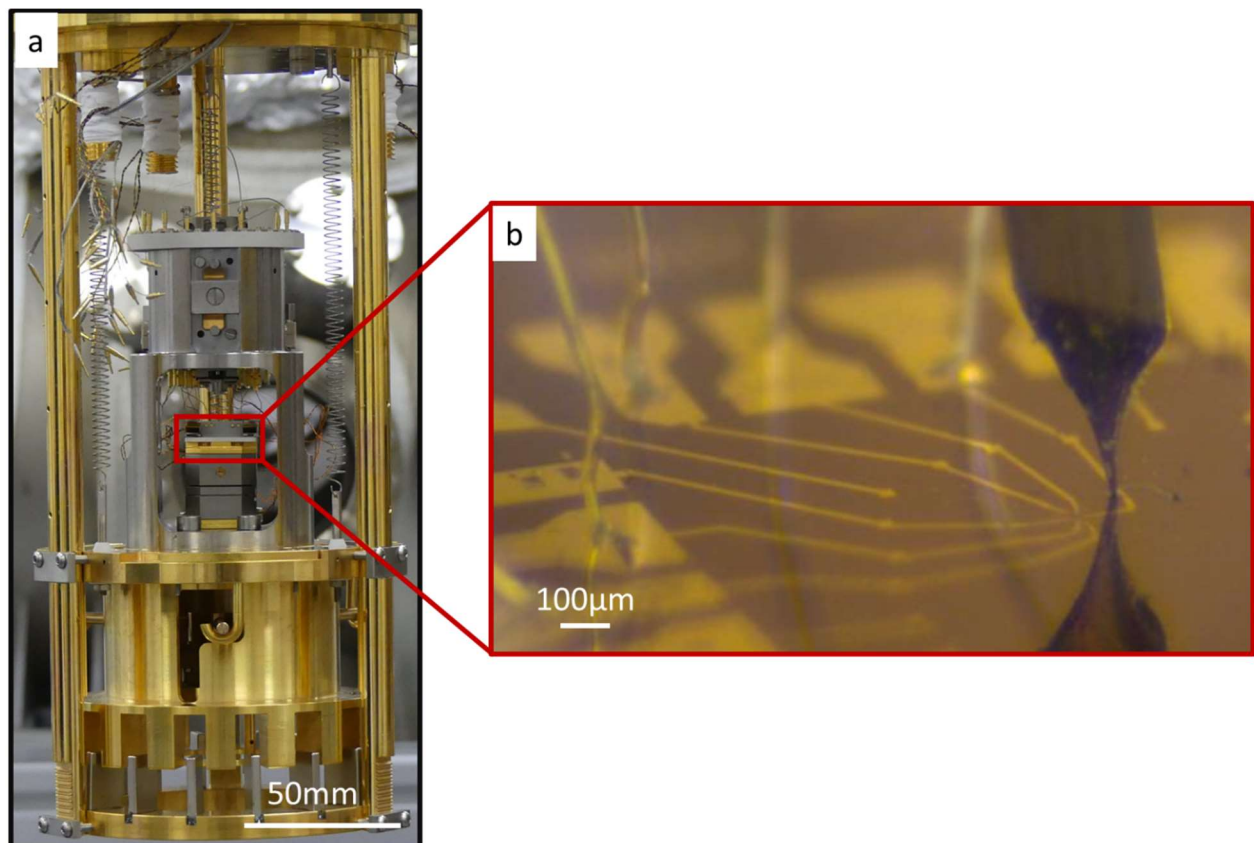


Figure 1. a) Photo of the full microscope. The microscope is mounted on a copper base with springs and magnets acting as an Eddy current break to isolate the system from mechanical vibrations. b) Photo of the tip of the microscope on top of a single flake of 30μm x 30μm.



## Reduced size STM in high magnetic fields

**Pablo García<sup>1</sup>, Rafael Álvarez-Montoya<sup>1</sup>, Raquel Sanchez-Barquilla<sup>1</sup>, Beilun Wu<sup>1</sup>, Edwin Herrera<sup>1,3</sup>, José Navarrete<sup>2</sup>, Juan Ramón Marijuan<sup>2</sup>, Hermann Suderow<sup>1,3</sup> Isabel Guillamón<sup>1,3</sup>**

<sup>1</sup>*Laboratorio de Bajas Temperaturas, Departamento de Física de la Materia Condensada, Instituto de Ciencia de Materiales Nicolás Cabrera, Condensed Matter Physics Center (IFIMAC), Universidad Autónoma de Madrid, E-28049*

<sup>2</sup>*Segainvex, Universidad Autónoma de Madrid, 28049 Madrid, Spain*

<sup>3</sup>*Unidad Asociada de Bajas Temperaturas y Altos Campos Magnéticos, UAM, CSIC, Cantoblanco, E-28049 Madrid, Spain*

Email: pablo.garcia@estudiante.uam.es

Cryogenic Scanning Tunneling Microscopy (STM) has been instrumental in the development of scanning probe microscopies. Actually, the first observation of the work function, which established vacuum tunneling, could only be confirmed after knowing the cryogenic properties of piezos, with measurements performed at ETH and at UAM[1]. The reduction of thermal activation and smearing is unavoidable to obtain surfaces with a spatial and energy resolution that allows sufficiently accurate comparison to calculations[2]. The addition of a magnetic field opens new prospects, such as the observation of vortex lattices in superconductors or of Landau quantization[3,4,5]. For the latter, it is of particular importance to decrease as far as possible the size of the STM. Although efforts made during past years have led to some improvements[6,7,8], the size is still far above the typical sizes available for instruments used in high magnetic fields. Here we discuss efforts to further reduce the size of the STM, with the aim to be able to work at extremely high magnetic fields and to build a system allowing for rotation of the STM in a magnetic field. Both the head and the base of the main body of the STM have been manufactured through 3D printing in grade 3 Titanium, which could turn out to be a good method to optimize the weight without modifying too much the stiffness of the microscope. Finite element calculations of the 3D printed system support the latter aspect. The STM has a diameter of 16 mm and a height of 23 mm. We discuss a new design of the approach motor and the piezotube support system, as well as results of the first tests.

[1] G. Binnig and H. Rohrer, "Scanning Tunneling Microscopy—from Birth to Adolescence", Nobel Lecture, Physics (1986).

[2] I. Guillamón et al, "Superconducting Density of States and Vortex Cores of 2H-NbS<sub>2</sub>", Physical Review Letters 101, 166407 (2008).

[3] H. Suderow, I. Guillamón, J.G. Rodrigo and S. Vieira, "Imaging superconducting vortex core and lattice with the scanning tunneling microscope", Superconductor Science and Technology 27, 063001 (2014).

[4] I. Guillamón et al, "Enhancement of long-range correlations in a 2D vortex lattice by an incommensurate 1D disorder potential", Nature Physics 10, 851–856 (2014).

[5] F. Martín Vega et al, "Tunneling spectroscopy of WTe<sub>2</sub>: bandstructure and high magnetic field Landau quantization", in preparation.

[6] H. Suderow, I. Guillamón, and S. Vieira, "Compact very low temperature scanning tunneling microscope with mechanically driven horizontal linear positioning stage", Review of Scientific Instruments 82, 033711 (2011).

[7] M. Fernández-Lomana et al, "Millikelvin scanning tunneling microscope at 20/22 T with a graphite enabled stick-slip approach and an energy resolution below 8  $\mu$ eV: Application to conductance quantization at 20 T in single atom point contacts of Al and Au and to the charge density wave of 2H-NbSe<sub>2</sub>", Review of Scientific Instruments 92, 093701 (2021).

[8] Y. Jae Song et al, "Invited Review Article: A 10 mK scanning probe microscopy facility", Review of Scientific Instruments 81, 121101 (2010).

## Electromechanical photophysics of individual P22 protein cages loaded with GFP

**Klara Strobl<sup>1</sup>, Ekaterina Selivanovitch<sup>2</sup>, Pablo Ibáñez<sup>1</sup>, Trevor Douglas<sup>2</sup>, Pedro J. de Pablo<sup>1</sup>**

<sup>1</sup>*Universidad Autónoma de Madrid, Madrid, Spain*

<sup>2</sup>*Indiana University, Bloomington, USA*

Email: klara.strobl@uam.es

Viruses are natural nanocompartments optimized for protecting its genome against external physical-chemical agents until delivery to the host organism during infection. The self-assembly of viruses into stable, robust and highly organized structures yields an effective and helpful approach to produce nanoreactors by using the viral capsid as nanocontainer for housing enzymes in its interior. Enzyme activity can be affected by molecular crowding due to the alteration of diffusion rates and the change of protein structure, dynamics and stability. As a result, crowding might enhance or diminish biocatalysis and, thus, it sets the boundaries for producing functional nanoreactors. Green fluorescence protein (GFP), which is extensively used as a biological tag, constitutes an ideal model for scrutinizing its function in densely populated environments such as those happening when confined at the plasma membrane.

In this work we study the behavior of GFP-cargo encapsidated in P22 bacteriophage virus-like particles (VLPs) and use its emission signal to monitor molecular functionality by Total Internal Reflection Fluorescence Microscopy (TIRFM) while probing individual capsids with the stylus of an Atomic Force Microscope (AFM).

With this simultaneous correlative microscopy at single-molecule level, we could identify two phenomena: a) a mechanical quenching of ~10%, b) an additional electronic quenching of ~10% when gold-coated probes were used. In addition, although fluorescence quenches and recovers after the metallic tip releases the capsid no matter its structural integrity, in the insulator tip's case quenching happens only if the capsid keeps the spherical organization of the packed protein. We associate the electronic quenching with the coupling of the protein's fluorescence emission with the tip's surface plasmon resonance and the mechanical quenching with the unfolding of GFP during the mechanical disruption of the capsid. Our results unveil that the mesoscopic local organization of proteins in crowded environments alters their function under mechanical cues but is dispensable under electronic means.

## Probing the structural stability of SARS-CoV-2 surrogate TGEV under stringent environmental conditions

M. Cantero<sup>1</sup>, D. Carlero<sup>2</sup>, F. J. Chichón<sup>2</sup>, J. Martín-Benito<sup>2\*</sup>, P. J. de Pablo<sup>1,3\*</sup>

<sup>1</sup>*Departamento de Física de la Materia Condensada, Universidad Autónoma de Madrid, 28049, Madrid (Spain)*

<sup>2</sup>*Departamento de Estructura de Macromoléculas, Centro Nacional de Biotecnología CSIC, 28049, Madrid (Spain)*

<sup>3</sup>*Instituto de Física de la Materia Condensada IFIMAC, Universidad Autónoma de Madrid, 28049, Madrid (Spain)*

Email: miguel.cantero@uam.es

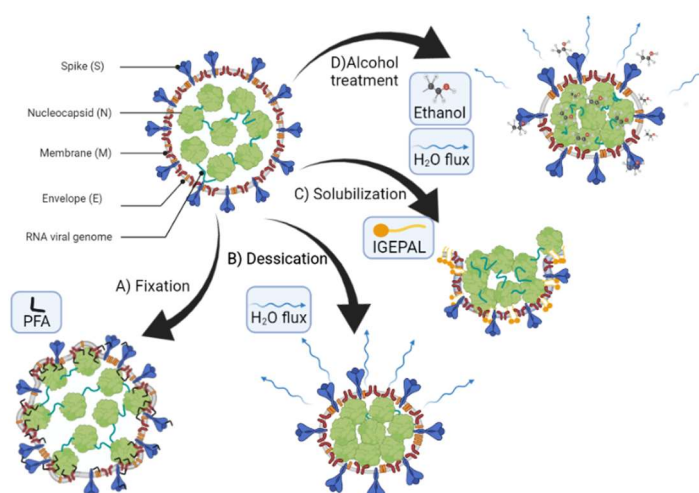


Fig 1. Schematic effect of desiccation, detergent solubilization and ethanol treatment.

Effective airborne transmission of coronaviruses via liquid microdroplets requires a virion structure that must withstand harsh environmental conditions [1]. Due to the demanding biosafety requirements for study of human respiratory viruses, it is important to develop surrogate models to facilitate their investigation. Here we explore the mechanical properties and nanostructure of transmissible gastroenteritis virus (TGEV) virions, an alphacoronavirus, in liquid milieu and their response to different chemical agents commonly used as biocides[2]. Our AFM experiments provide two-fold results on virus stability: First, while particles with larger size and lower packing fraction kept their morphology intact after successive mechanical aggressions, smaller viruses with higher packing fraction showed conspicuous evidence of structural damage and content release. Second, monitoring the structure of single TGEV particles in the presence of detergent and alcohol in real time revealed the stages of gradual degradation of virus structure in situ. These data suggest that detergent is three orders of magnitude more efficient than alcohol in destabilizing TGEV virus particles, paving the way for optimizing hygienic protocols for viruses with similar structure, such as SARS-CoV-2.

[1]. Petersen, E. *et al.* Comparing SARS-CoV-2 with SARS-CoV and influenza pandemics. *Lancet Infect. Dis.* **20**, e238–e244 (2020).

[2]. Kampf, G., Todt, D., Pfaender, S. & Steinmann, E. Persistence of coronaviruses on inanimate surfaces and their inactivation with biocidal agents. *J. Hosp. Infect.* **104**, 246–251 (2020).

# A coarse-grained approach to model the dynamics of the actomyosin cortex

Miguel Hernández-del-Valle <sup>1,2,3,4</sup>, Andrea Valencia-Expósito <sup>6</sup>, Antonio López-Izquierdo <sup>1,2,3,4</sup>, Pau Casanova-Ferrer <sup>1,2,3,4</sup>, Pedro Tarazona <sup>2,3,5</sup>, Maria D. Martín-Bermudo <sup>6</sup>, David G. Míguez <sup>1,2,3,4</sup>

1. Centro de Biología Molecular Severo Ochoa, Universidad Autónoma de Madrid, 28049 Madrid

2. IFIMAC, Fac. de Ciencias, Universidad Autónoma de Madrid, 28049 Madrid.

3. Instituto Nicolás Cabrera, Fac. de Ciencias, Universidad Autónoma de Madrid, 28049 Madrid.

4. Física de la Materia Condensada, Fac. de Ciencias, Universidad Autónoma de Madrid, 28049 Madrid.

5. Física Teórica de la Materia Condensada, Fac. de Ciencias, Universidad Autónoma de Madrid, 28049 Madrid.

6. Centro Andaluz de Biología del Desarrollo, Universidad Pablo de Olavide/CSIC/JA, Carretera de Utrera km 1, Sevilla 41013, Spain

Email: miguel.hernandez@uam.es

The dynamics of the actomyosin machinery is at the core of many important biological processes. Several relevant cellular responses such as the rhythmic compression of the cell cortex are governed, at a mesoscopic level, by the nonlinear interaction between actin monomers, actin crosslinkers and myosin motors. Coarse grained models are an optimal tool to study actomyosin systems, since they can include processes that occur at long time and space scales, while maintaining the most relevant features of the molecular interactions. Here, we present a coarse grained model of a two-dimensional actomyosin cortex, adjacent to a three-dimensional cytoplasm. Our simplified model incorporates only well characterized interactions between actin monomers, actin crosslinkers and myosin, and it is able to reproduce many of the most important aspects of actin filament and actomyosin network formation, such as dynamics of polymerization and depolymerization, treadmilling, network formation and the autonomous oscillatory dynamics of actomyosin. Furthermore, the model can be used to predict the in vivo response of actomyosin networks to changes in key parameters of the system, such as alterations in the anchor of actin filaments to the cell cortex.

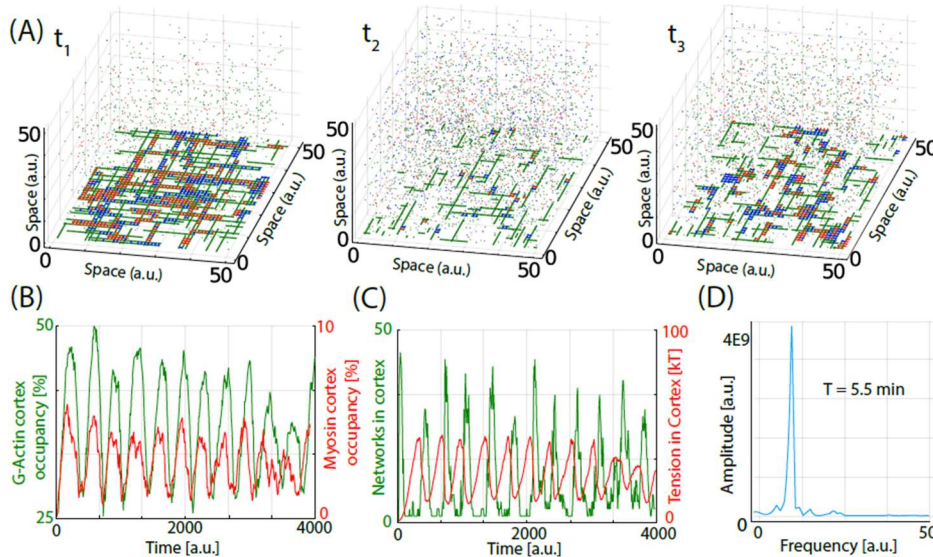


**Figure 1. The model reproduces actomyosin oscillations.** (A) Snapshots of the system for three different time points of a given simulation (green is G-Actin, blue is ACs, red is Myosin). (B) Temporal evolution of total actin and myosin in the cortex. (C) Temporal evolution of tension (red) and number of bundles (green). (D) Fourier transform of the oscillations.

## Laser irradiation in spheroids MCF and U-87

**Pablo Camarero<sup>1</sup>, Francisco Sanz-Rodríguez<sup>2</sup>, Marta Quintanilla<sup>2</sup> and Patricia Haro-González<sup>1</sup>**

<sup>1</sup>Departamento de Física de Materiales e Instituto de materiales Nicolás Cabrera, Facultad de Ciencias, Universidad Autónoma de Madrid, Ciudad Universitaria de Cantoblanco, C. Francisco Tomás y Valiente, 7, 28049 Madrid, España

<sup>2</sup>Departamento de Biología, Facultad de Ciencias, Universidad Autónoma de Madrid, Ciudad Universitaria de Cantoblanco, C. Darwin, 2, 28049 Madrid, España

Email: Pablo.camarero1@estudiante.uam.es

During last decades, many researches are employing 3D cell culture for multicellular spheroids growth [1]. These have multiples numerous applications into the biomedicine field [2] and they are supposed to be an ideal model to use into tissues reconstruction. During this investigation we have growth two different spheroids set up with two epithelial cell lines: MCF-7 (adenocarcinoma) and U-87 (glioblastoma). The main physiological difference between both is how they join among them (Fig. 1). By laser irradiation, we cause a temperature increase at the sample [3], taking the cells to a hyperthermia situation. Afterwards, we have studied the spheroids resizing as a cell death symptom. This event has been analysed depending on three different wavelength (808nm, 980 nm and 1450nm) and the laser power (values below 250 mW) (Fig. 2).

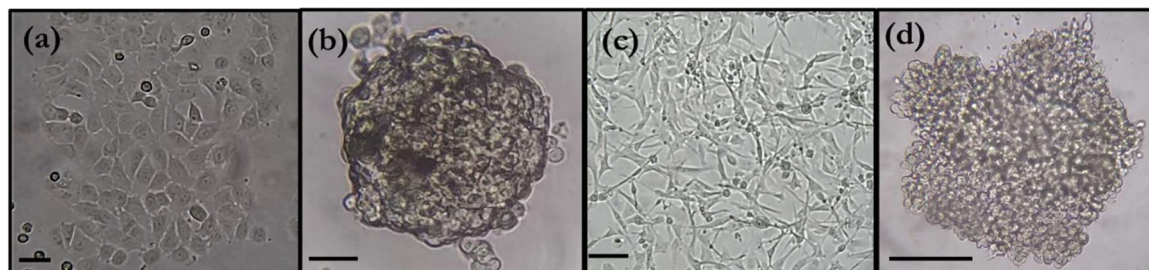


Figura 1: (a) Células MCF-7 (b) Esferoide de células MCF-7 (c) Células U-87 (d) Esferoide de células U-87 Escala: 80μm

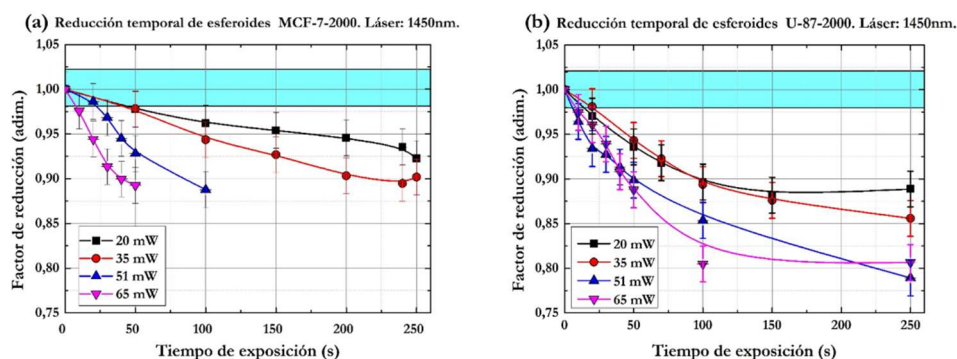


Figura 2: Reducción temporal a diferentes potencias láser (a) MCF-7-2000 (b) U-87-2000

- [1] J. Meseguer, et al., Eubacteria, **34**, 15 (2015)
- [2] K. Juárez-Moreno et al., Mundonano, **13**, 25 (2020)
- [3] Hanbin Mao et al., Biophys. J, **89**, 1308-1316 (2004)

This research was funded by the Ministerio de Ciencia e Innovación de España (PID2019-106211RB-I00 and PID2019-105195RA-I00) and by Universidad Autónoma de Madrid and Comunidad Autónoma de Madrid (SII/PJI/2019-00052).



## Preparation of thin film LiCoO<sub>2</sub> cathodes by pulsed laser deposition for Li-ion batteries

M. J. Ramírez-Peral<sup>1,2,3</sup>, J. Díaz<sup>1</sup>, A. Galindo<sup>1,2</sup>, H. P. van der Meulen<sup>3,4</sup>, C. Polop<sup>1,3,5</sup> and E. Vasco<sup>2</sup>.

<sup>1</sup> Departamento de Física de la Materia Condensada, Universidad Autónoma de Madrid, Madrid, Spain

<sup>2</sup> Instituto de Ciencia de Materiales de Madrid, CSIC, Sor Juana Inés de la Cruz 3, 28049 Madrid, Spain

<sup>3</sup> INC (Instituto Universitario de Ciencia de Materiales Nicolás Cabrera), Madrid, Spain

<sup>4</sup> Departamento de Física de Materiales, Universidad Autónoma de Madrid, Madrid, Spain.

<sup>5</sup> IFIMAC (Condensed Matter Physics Center), Madrid, Spain

Email: mariajesus.ramirez@uam.es

Li-ion batteries (LIBs) are a key technology for clean, efficient transportation and sustainable development. They play a pivotal role in the transition to a future zero-emission society [1]. The evolution of LIBs will boost an entire economic sector, including power suppliers, grid operators, energy storage integrators, solar developers, and energy-service companies, providing an opportunity to enhance Europe's industrial competitiveness in the energy sector, a major enabler of economic growth and job creation.

Within the framework of the "StressLIC" Consortium [2] granted by M-Era.Net (EU) and AEI (Spain), we have set up a Pulsed Laser Deposition (PLD) - Multibeam Optical Stress Sensor (MOSS) facility to deposit and characterize in-situ thin films of Li-ion components. We present here our results concerning the preparation of LiCoO<sub>2</sub> (LCO) cathodes (CATs) by PLD. LCO, which was the first CAT marketed by Sony in 1991, and later replaced due to its poor thermal stability, has regained prominence in the design of "zero-strain" composite CATs for solid-state LIBs (SSLBs) as it is the only commercial CAT with a negative chemical expansion coefficient [3]. LCO thin films have been deposited on different substrates, and characterized in terms of composition, microstructure and morphology by microRaman spectroscopy, SEM, DRX and AFM. LCO films show a compact columnar structure with faceted surface grains exhibiting 3-fold symmetry. This morphology agrees with the (00*l*) LCO texture measured by  $\theta - 2\theta$  DRX. MicroRaman reveals that two phases coexist in the films: a main stoichiometric LCO phase and a minor Co<sub>3</sub>O<sub>4</sub> phase. The fact that the Co<sub>3</sub>O<sub>4</sub> to LCO ratio decreases with increasing film thickness or with a thermal SiO<sub>2</sub> coating, suggests that Co<sub>3</sub>O<sub>4</sub> is the result of the loss of Li via diffusion towards Si substrate. Li-poor LCO formation is ruled out by impedance spectroscopy (IS). This phenomenon is currently being studied by RBS at CMAM (UAM).

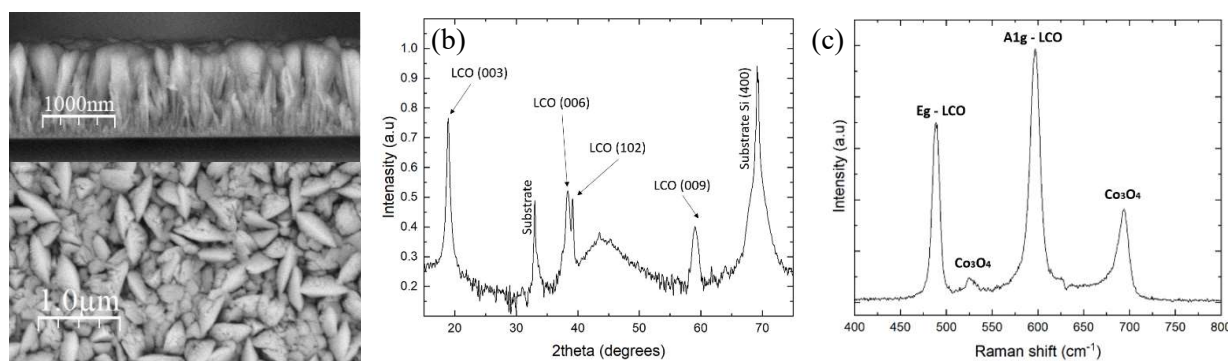


Fig. Structural and chemical analysis of a LCO film: (a) Cross-section and top SEM images, (b) XRD and (c) Raman spectrum.

[1] European Green Deal, [https://ec.europa.eu/info/strategy/priorities-2019-2024/european-green-deal\\_en](https://ec.europa.eu/info/strategy/priorities-2019-2024/european-green-deal_en)

[2] <https://www.era-learn.eu/network-information/networks/m-era-net-2/m-era-net-joint-call-2018/addressing-the-stress-related-functional-limitations-of-thin-film-li-ion-components-for-energy-intensive-applications>

[3] R. Koerver *et al.*, *Energy Environ. Sci.* **11**, 2142–2158 (2018).

# Proximity effects and topological superconductivity dependency on layer thickness in superconductor/ferromagnetic/semiconductor hybrid devices

**Samuel D. Escribano<sup>1</sup>, Andrea Maiani<sup>2</sup>, Rubén Seoane Souto<sup>2</sup>, Martin Lejinse<sup>2</sup>, Yuval Oreg<sup>3</sup>, Alfredo Levy Yeyati<sup>1</sup>, Karsten Flensberg<sup>2</sup> and Elsa Prada<sup>4</sup>**

<sup>1</sup>Departamento de Física Teórica de la Materia Condensada, UAM, Madrid, Spain

<sup>2</sup>University of Copenhagen, Copenhagen, Denmark

<sup>3</sup>Weizmann Institute for Science, Rehovot, Israel

<sup>4</sup>Instituto de Ciencia de los Materiales, CSIC, Madrid, Spain

Email: samuel.diaz@uam.es

We investigate the topological properties of hybrid devices made of a semiconducting wire partially covered by a ferromagnetic layer, which in turn is covered by a superconducting one [see Fig. 1(a)]. We perform numerical calculations of the system including the three materials and the electrostatic environment, and we analyze how its electronic properties change with the ferromagnetic layer width and the gate potentials. We show that both proximity effects into the wire, the induced superconductivity and the induced exchange field, strongly depends on the ferromagnetic layer thickness. We therefore find a suitable thickness range for which the system can support topological phases, and particularly the so-called Majorana bound states. We also perform the same analysis for a semiconducting 2DEG [see Fig. 1(b)] finding similar results, although the topological phases turn out to be more robust in the later.

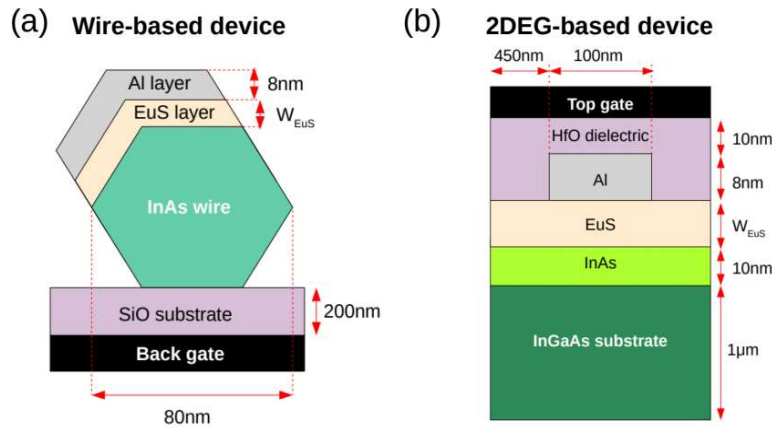


Figure 1. The two devices studied in this work: (a) an InAs nanowire and (b) an InAs 2DEG covered by a ferromagnetic insulating layer made of EuS and a superconducting layer of Al. Notice that the InAs and the Al layer are not directly in contact. We are able to compute the energy spectrum of the whole heterostructure including the interactions with the *realistic* environments shown here.

## Characterization of the external pulsed beam at CMAM for proton-therapy studies at the FLASH regime

S. Viñals<sup>1</sup>, D. Sánchez-Parcerisa<sup>2</sup>, L.M. Fraile<sup>2</sup>, S. España<sup>2</sup>, G. García<sup>1</sup>, M. García-Díaz<sup>2</sup>, V. Sánchez-Tembleque<sup>2</sup>, J.M. Udías<sup>2</sup>, M. Manso<sup>3</sup>

<sup>1</sup>*Centro de Micro-Análisis de Materiales, Madrid, Spain*

<sup>2</sup>*Grupo de Física Nuclear, Universidad Complutense, Madrid, Spain*

<sup>3</sup>*Departamento de Física Aplicada, Universidad Autónoma de Madrid, Spain*

In this contribution, the technicalities performed to obtain a pulsed beam at the CMAM facility will be presented. A pulsed beam is used in many areas such as nuclear physics, material science and, in particular, for proton-therapy medical studies. Proton-therapy is known as the radiotherapy technique for cancer treatment that uses proton beams for producing the damage. The main difference between the conventional radiotherapy treatments with X-Ray or electrons and the treatment with protons relies on how the deposition of energy is produced by each particle. Recent works in radiotherapy have raised interest in studying the outcome of very high dose rates, the so-called FLASH irradiations ( $>40$  Gy/s), which are able to considerably reduce side effects compared to standard dose rates ( $\sim 5$  cGy/s). It is based on delivering ultra-high dose-rates inducing differential biological effects between normal and tumoral tissues and reducing the radiation-induced side effects [1-2].

The Centro de Micro-Análisis de Materiales (CMAM) is one of the two ion accelerators research centers in Spain [3]. It belongs to the Universidad Autónoma de Madrid (UAM) and the building that hosts the laboratory is at the university campus. The equipment of the facility consists of an electrostatic ion accelerator with a maximum terminal voltage of 5 MV and six beam-lines dedicated to various application areas such as the analysis and modification of materials, the study of the nuclear reactions or archaeometry studies. The pulsed beam has been characterized with an 8 MeV proton beam, using an existing equipment at CMAM: two pairs of electrostatic plates (RASTER) that deflect the beam, commonly used for homogeneous irradiation of large areas.

Rectangular and pyramidal functions have been used to generate different pulses and characterize the response of the RASTER. The results point out that the pulses obtained are suitable for preclinical proton-therapy studies in the FLASH regime.

- [1] P. Montay-Gruel et al. "Irradiation in a flash: Unique sparing of memory in mice after whole brain irradiation with dose rates above 100 Gy/s." *Radiotherapy and Oncology* 124.3 (2017) 365–369.
- [2] J. Bourhis et al. "Treatment of a first patient with FLASH-radiotherapy." *Radiotherapy and Oncology* 139 (2019): 18-22.
- [3] A. Redondo-Cubero et al., "Current status and future developments of the ion beam facility at the centre of micro-analysis of materials in Madrid" *Eur. Phys. J. Plus*, 2021, pp. 136-175



# Unraveling the structure of RNA-packed within Penicillium Chrysogenum Virus and its influence in the mechanical stability

**María J. Rodríguez-Espinosa<sup>1,2</sup>, David Gil-Cantero<sup>1</sup>, José R. Castón<sup>1</sup>, Pedro J. de Pablo<sup>2</sup>,**

<sup>1</sup>*Department of Structure of Macromolecules, Nacional Centre for Biotechnology (CNB-CSIC); Cantoblanco, Madrid, Spain.*

<sup>2</sup>*Department of Condensed Matter Physics, Universidad Autónoma de Madrid, Spain.*

Email: mj.rodriguez@cnb.csic.es

Penicillium chrysogenum virus (PcV) is a dsRNA mycovirus. PcV genome consists of four monocistronic segments that code for the capsid protein (CP), the viral polymerase (Pol) and two proteins of unknown functions; each segment is encapsidated separately in a similar particle. PcV has a T=1 capsid and shows a low degree of genome compaction. The 3D structure of the PcV capsid has been determined by single-particle cryo-EM analysis at 2.5 and 2.7 Å resolution for virions and empty viral particles, respectively. The RNA organization was revealed in asymmetric 3D reconstructions as a layer underneath the inner capsid surface formed by RNA filaments that account for ~60% of the total genome. These filaments are located on the positively charged regions of the shell protein and keep the RNA density in close contact with the lumen of the capsid. We also studied with atomic force microscopy (AFM) the mechanical influence of this genome structure by measuring the stiffness and brittleness of RNA-filled and empty capsids.

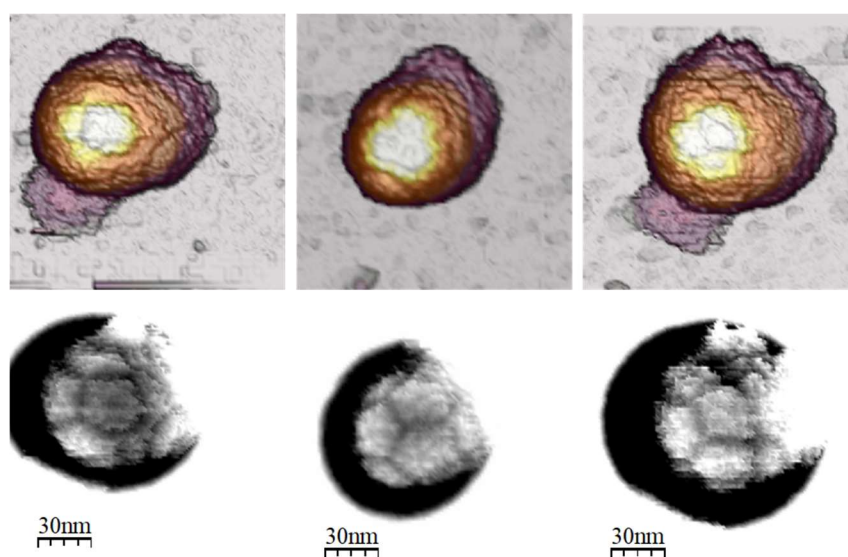


Figure 1. AFM images of PcV. Images of five-fold, three-fold and two-fold symmetry for the PcV capsid by atomic force microscopy.

- [1] CP Mata et al. Adv Virus Res 108 (2020), 213- 247.
- [2] Llauro et al. Nanoscale, 8 (2016), 9328-9336.
- [3] De Pablo et al. Applied Physics Letters, 73(22), 3300-3302 (1998).
- [4] Horcas, I., 2017 Review of Scientific Instruments, 2007, 78 (1), 013705

## ***Bacillus Subtilis* swimming motility in liquid broth and structured media**

Richard A. Campusano<sup>1</sup>, P. Magrinya<sup>1</sup>, P. Llombart<sup>1</sup>, B. Tíno<sup>1</sup>, L.R. Arriaga<sup>1,2</sup> and J.L. Aragones<sup>1,2</sup>

<sup>1</sup> Instituto Nicolás Cabrera and Departamento de Física Teórica de la Materia Condensada, Universidad Autónoma de Madrid, E-28049, Madrid, Spain

<sup>2</sup> Condensed Matter Physics Centre (IFIMAC), Universidad Autónoma de Madrid, E-28049, Madrid, Spain

Email: (richard.campusano@inv.uam.es)

Bacteria have developed a swimming strategy to outrun diffusion, which is required to find food or colonize surfaces. Bacteria species such as *E. coli* or *B. subtilis* exploit a flagellum-mediated swimming motility in liquid broth; however, the dynamics of both bacteria are significantly different. *E. coli* swimming strategy is based on the paradigmatic run and tumbling protocol in which the bacteria alternate periods of swimming in straight lines at constant speed with sudden tumblings that randomizes its swimming direction [1], while *B. subtilis* swimming strategy exhibit a characteristic wiggling motion with a continuous change of the swimming direction [2-5]. We analyze the swimming motility of *B. subtilis* in liquid broth and study the effect of microstructured environments on its dynamics [6]. We consider the effect of the phases of the bacterial growth and the presence of static and dynamic obstacles on the single bacterium dynamics.

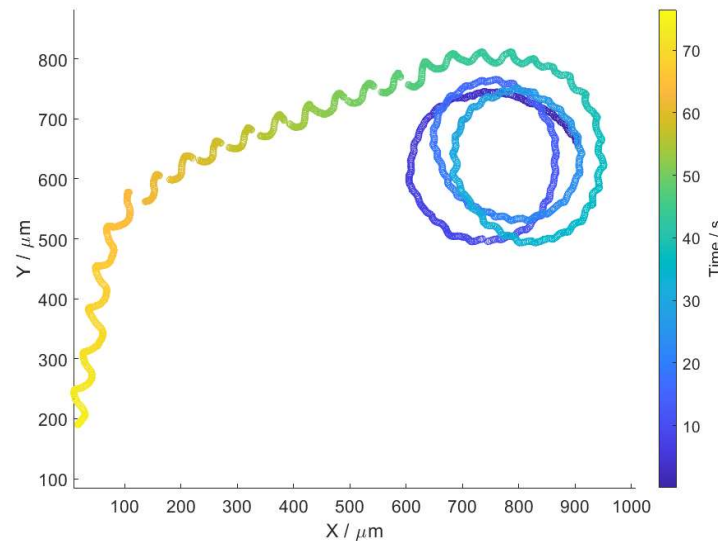


Figure 1. Typical trajectory of *B. subtilis*

- [1] H. C. Berg. Springer-Verlag: New York, Inc., 175 Fifth Avenue, USA (2004)
- [2] L. Turner, L. Ping, M. Neubauer and H. C. Berg, Biophys. J., 111, 630–639 (2016)
- [3] J. Najafi, M. R. Shaeabani, T. John, F. Altegoer, G. Bange and C. Wagner, Sci. Adv., 2018, 4, eaar6425
- [4] J. Najafi, F. Altegoer, G. Benge and C. Wagner, Soft Matter, **15**, 10029-10034 (2019)
- [5] N. Chenouard *et al.*, Nature Methods, (**11**) **3**, 281 (2014)
- [6] S. Makarchuk, V.C. Braz, N.A.M. Araujo, L. Ciric and G. Volpe, Nature Comm., **10**, 4110 (2019)

# The Josephson effect in full-shell Al-InAs nanowires in the Little-Parks regime

M. Gómez<sup>1</sup>, A. Ibabe<sup>1</sup>, J. Nygard<sup>2</sup> and E. J. H. Lee<sup>1</sup>

<sup>1</sup> Condensed Matter Physics Department, Universidad Autónoma de Madrid, Spain

<sup>2</sup> Center for Quantum Devices & Nano-science Center, Niels Bohr Institute, University of Copenhagen, Denmark

Email: mario.gomezg@uam.es

The experimental realization of a topological superconductor and Majorana zero modes (MZMs) has been a hot topic in Condensed Matter Physics during the last decade. One of the most promising proposed routes towards this goal is based on semiconducting nanowires with strong spin-orbit coupling, induced superconductivity, and an external magnetic field [1, 2]. Despite the remarkable improvements in the experiments over the past years, a fully conclusive demonstration of such an exotic phase is however still lacking.

More recently, a proposal to realize the elusive Majorana quasiparticles using lower magnetic fields has been put forward. In this case, the topological phase transition results from the application of an odd number of magnetic fluxes in full-shell proximitized nanowires [3]. This system has been studied in the tunnel regime, whereby zero-bias peaks were interpreted in favor of a topological origin [4]. A detailed study of the Josephson effect in this type of hybrid nanowires is however still missing.

In this work, we present our first measurements of the Little-Parks effect in Josephson Junctions based on InAs nanowires with a full epitaxial Al shell. We observe the characteristic oscillations of the superconducting gap, which is minimum at half-integer values of the magnetic flux and maximum at integer values. We observed a similar oscillatory behaviour in the excess and critical currents of our junctions. The Josephson effect can be used to shed further light onto the physics of full-shell superconductor-semiconductor nanowires.

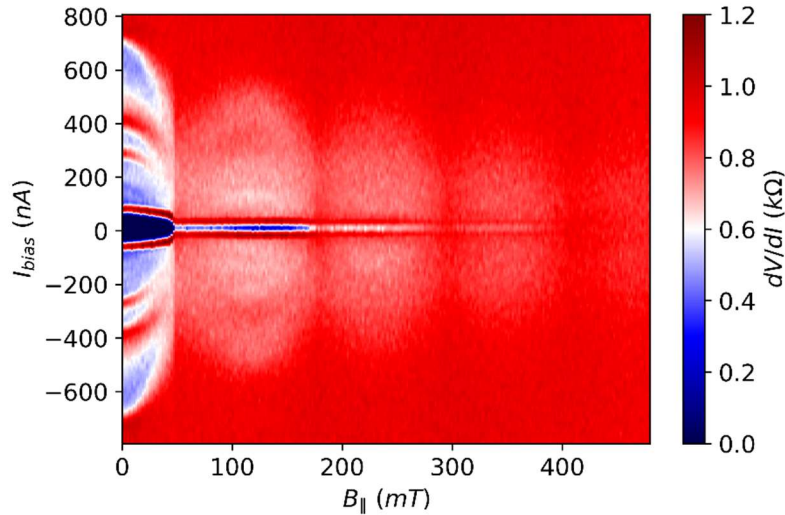


Figure 1. Differential resistance as a function of bias current and magnetic field in a Josephson Junction based on Al full-shell InAs nanowire. The Little-Parks effect is reflected in the lobe-shape modulation of the superconducting gap and critical current.

- [1] R. M. Lutchyn et al., Phys. Rev. Lett., **105**, 077001 (2010)
- [2] Y. Oreg et al., Phys. Rev. Lett., **105**, 177002 (2010)
- [3] R. M. Lutchyn et al., arXiv:1809.05512 (2018)
- [4] S. Vaitiekėnas et al., Science, **367**, eaav3392 (2020)

# Unconventional mechanism of virtual-state population through dissipation

Alejandro Vivas-Viaña<sup>1</sup>, Carlos Sánchez Muñoz<sup>1</sup>,

<sup>1</sup>*Departamento de Física Teórica de la Materia Condensada and Condensed Matter Physics Center (IFIMAC), Universidad Autónoma de Madrid, Madrid, Spain*

Email: alejandro.vivas@uam.es

Virtual states are a concept of paramount importance in quantum mechanics. At its core, the concept of a virtual state requires that the probability of finding the system in such state should be vanishingly small, since time-energy uncertainty only allows it to exist for an extremely short time. Arguably, the simplest scenario described in terms of virtual states consists of two quasi-resonant “real” quantum states, whose interaction is mediated by a third, strongly off-resonant “virtual” state. In this work, we study such a system in a dissipative context with spontaneous decay between the real states, and show that the situation where the virtual state is unpopulated is, in fact, metastable. In stark contrast to common intuition, there is a steady-state reached in the long-time limit where the virtual state has a sizable population. We analyze this phenomenon from the perspective of quantum trajectories, and show that this unconventional population mechanism stems from the non-Hermitian evolution taking place between quantum jumps. Introducing a novel hierarchical scheme of adiabatic elimination, we have obtained analytical expressions for the dynamics and the timescale of metastability that describes for how long the virtual state remains virtual. These results are relevant for the design of interacting quantum systems via artificial environments and their possible application for quantum technologies, such as entanglement generation mediated by photonic structures.

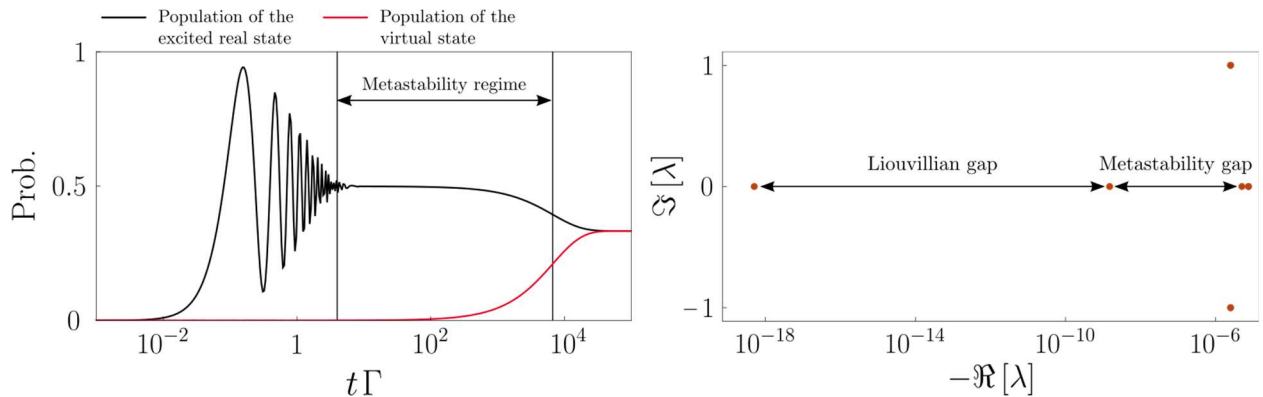


Figure 1. Left panel: Time evolution of the populations of the excited real state and virtual state. Right panel: Diagram of the eigenvalues of the Liouvillian.

- [1] C. Cohen-Tannoudji, J. Dupont-Roc, and G. Grynberg, *Atom-Photon Interactions* (Wiley, 1998).
- [2] K. Macieszczak, D. C. Rose, I. Lesanovsky, and J. P. Garrahan, *Phys. Rev. Research* 3, 33047 (2021).
- [3] A. Gonzalez-Tudela, D. Martin-Cano, E. Moreno, L. Martin-Moreno, C. Tejedor, and F. J. Garcia-Vidal. *Phys. Rev. Lett.* 106, 020501 (2011).

## Improving stability and thermal sensitivity of an optically trapped upconversion nanoparticle by coating with a thermo-sensitive polymer

Dasheng Lu<sup>1, 2</sup>, Jorge Rubio Retama<sup>3, 4</sup>, Ricardo Marín, <sup>1, 3</sup> Manuel I. Marqués<sup>2, 5</sup>, Patricia Haro-González<sup>1, 3</sup>, Daniel Jaque<sup>1, 3</sup>.

<sup>1</sup>Fluorescence Imaging Group, Departamento de Física de Materiales, Facultad de Ciencias, Universidad Autónoma de Madrid, Madrid, 28049 Spain

<sup>2</sup>Instituto Universitario de Ciencia de Materiales Nicolás Cabrera, Facultad de Ciencias, Universidad Autónoma de Madrid, Madrid, 28049 Spain

<sup>3</sup>Nanobiology Group, Instituto Ramón y Cajal de Investigación Sanitaria, IRYCIS, Ctra. Colmenar km. 9.100, Madrid 28034, Spain

<sup>4</sup>Departamento de Química en Ciencias Farmacéuticas, Facultad de Farmacia, Plaza de Ramón y Cajal, s/n, Universidad Complutense de Madrid, Madrid 28040, Spain

<sup>5</sup>Departamento de Física de Materiales and IFIMAC, Universidad Autónoma de Madrid, Madrid, 28049 Spain Region, Country

Email: (dasheng.lu@estudiante.uam.es)

Lanthanide-based upconverting nanoparticles (UCNPs) are trust-worthy workhorses in luminescent nanothermometry [1, 2]. Indeed, using UCNPs-based nanothermometers we have been able to determine the thermal properties of cell membranes and monitor in vivo thermal therapies in real time [3, 4]. However, UCNPs are far from being the ideal nanothermometers, even less so at the single particle level [5], due to their low sensitivity and brightness and the difficulty of controlling individual UCNPs remotely. In this work we show how both problems can be solved simultaneously using a thermoresponsive polymeric coating. Upon coating a NaYF<sub>4</sub>:Er,Yb UCNP with poly(N-isopropylacrylamide) (PNIPAM), a >10-fold enhancement in optical forces is observed, allowing stable trapping and manipulation of a single UCNP in the whole physiological temperature range (25-50 °C). This optical force improvement is accompanied by a significant enhancement of the thermal sensitivity - reaching a maximum value of 9 % °C<sup>-1</sup> caused by the temperature-induced collapse of PNIPAM. Numerical simulations reveal that enhancement in both optical forces and thermal sensitivities is attributable to the interaction of trapping and reemitted radiations with the high-refractive-index coating. The results included in this work demonstrates how UCNP nanothermometers can be further improved by an adequate surface decoration and open a new avenue towards highly sensitive single-particle nanothermometers.

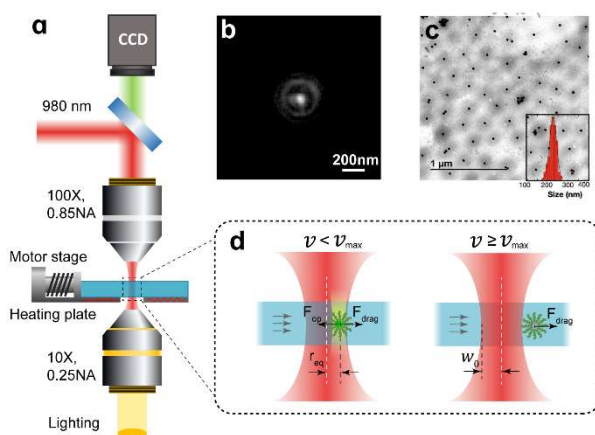


Figure 1. (a) Experimental setup used for single particle optical trapping experiments. (b) Fluorescence image of a single optically trapped UCNP@PNIPAM. (c) TEM image of UCNP@PNIPAM. Inset shows the corresponding histogram of size distribution. (d) Schematic drawings of drag method used to measure optical force.

- [1] Zhou B. et al. Nature nanotechnology, 2015, 10 (11), 924-936.
- [2] Hemmer E. et al. Journal of Materials Chemistry B, 2017, 5(23), 4365-4392.
- [3] Jaque, D. et al. Nanomedicine 2014, 9 (7), 1047-1062.
- [4] Rodríguez-Sevilla P. et al. Advanced Materials, 2016, 28 (12), 2421-2426.
- [5] Wang X. et al. Rsc Advances, 2015, 5 (105), 86219-86236.



## Electronic characterization of LiCoO<sub>2</sub> thin films in the overlithiation regime by XPS and ARPES

J. Díaz<sup>1</sup>, E. Salagre<sup>1</sup>, P. Segovia<sup>1,2,3</sup>, M.A. González-Barrio<sup>4</sup>, J. Pearson<sup>5</sup>, I. Takeuchi<sup>5</sup>, E.J. Fuller<sup>6</sup>, A.A. Talin<sup>6</sup>, M. Jugovac<sup>7</sup>, P. Moras<sup>7</sup>, A. Mascaraque<sup>4</sup>, C. Polop<sup>1,2,3</sup> and E. G. Michel<sup>1,2,3</sup>

<sup>1</sup>Department of Condensed Matter Physics, Universidad Autónoma de Madrid (UAM), Madrid, Spain

<sup>2</sup>Condensed Matter Physics Center (IFIMAC), Madrid, Spain

<sup>3</sup>Instituto Universitario de Ciencia de Materiales Nicolás Cabrera (INC), Madrid, Spain

<sup>4</sup>Dpto. Física de Materiales, Fac. Ciencias Física, Univ. Complutense de Madrid, Spain

<sup>5</sup>Materials Science and Engineering, Univ. of Maryland, College Park (MD), USA

<sup>6</sup>Sandia National Laboratories, Livermore (CA), USA.

<sup>7</sup>Istituto di Struttura della Materia, Consiglio Nazionale delle Ricerche, Trieste, Italy

Email: [jesus.diazs@estudiante.uam.es](mailto:jesus.diazs@estudiante.uam.es)

One of the greatest challenges we face as a society is to fight climate change without negatively affecting the quality of life of the population. In this line, it is essential to improve the efficiency of energy production and storage, as well as the autonomy of devices and machinery powered by electricity. To make progress on the last two points, it is essential to study and understand in greater depth the materials used to build lithium-ion batteries (LIBs) [1]. In this project we study one of the materials most commonly used to build the cathode of a LIB, LiCoO<sub>2</sub> [2]. Specifically, we focus on the study of the changes undergone by the material when it enters its overlithiated state (Li<sub>x</sub>CoO<sub>2</sub> with  $x > 1$ ), which is closely related to the over-discharged state of a battery, using X-ray photoemission spectroscopy (XPS) and angle-resolved photoelectron spectroscopy (ARPES).

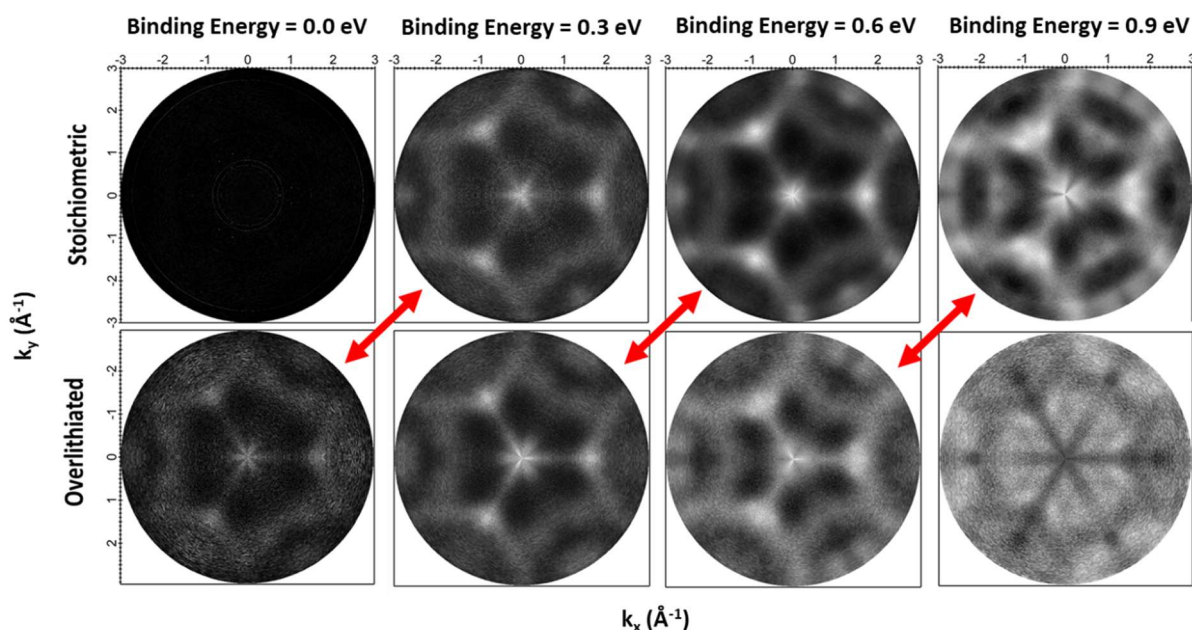


Figure 1. Intensity maps for the Fermi surface ( $h\nu=150$  eV) and constant energy surfaces for different binding energies as a function of reciprocal space momentum ( $k_x$ ,  $k_y$ ) perpendicular to the surface normal for a LiCoO<sub>2</sub> (001) stoichiometric and overlithiated sample.

We report the changes produced in the chemical state of Li and Co atoms and in the electronic structure of a Li<sub>x</sub>CoO<sub>2</sub> (001) epitaxial film when it reaches an overlithiated state. In order to reach the overlithiation, Li was deposited on LiCoO<sub>2</sub> in ultra-high vacuum in vapor phase. The sample was annealed at 500 °C to enhance the incorporation of the deposited Li ions. The study of Li 1s and Co 3p core levels using XPS, shows that the deposited Li is chemisorbed on the surface layer of the sample before annealing, and is incorporated in the same chemical state as the original Li during the annealing. We find no experimental evidence of a valence change of

Co ions upon sample overlithiation. We use the ratio between Li 1s and Co 3p XPS core levels to obtain the value of the new Li molar contents. However, an analysis of the band structure of stoichiometric and overlithiated  $\text{LiCoO}_2$  indicates that this value may be overestimated. Measurements by ARPES show a rigid shift of the valence band of the overlithiated sample with respect to the stoichiometric state of about 0.3 eV towards the Fermi level (Fig 1). This is explained due to the change of occupancy of the 3d levels of a fraction of the  $\text{Co}^{3+}$  atoms [3], which reach an intermediate spin configuration effectively splitting the  $a_{1g}$  band in two, doping the band structure of the  $\text{Li}_x\text{CoO}_2$  with holes.

- [1] A. Manthiram et al., ACS Cent Shi, **3**, 1063 (2017)
- [2] E.Pichita et al., J.Electrochem.Soc, **136**, 1865 (1989)
- [3] S.Levasseur et al., Chem.Mater, **15**, 348-354 (2003)



# Excitation and propagation of edge spin waves in ferromagnetic triangles

Diego Caso<sup>1</sup> and Farkhad G. Aliev<sup>1</sup>

<sup>1</sup>Departamento de Física de la Materia Condensada C-III, IFIMAC and INC, Universidad Autónoma de Madrid 28049, Madrid, Spain.

Email: diego.caso@uam.es

Spin waves, being usually reflected by domain walls, could also be channeled along them. Recent studies allowed observation of spin waves along domain walls in rectangular, circular [1] and triangular dots in the ground or metastable states. Triangular dots could also present edge pinned inhomogeneous magnetic states, depending on the direction of the external magnetic field. These edge domain walls yield the interesting, and potentially applicable to real devices property of broadband spin wave confinement to the edges of the structure [2,3], with capabilities to be redirected at angles exceeding 100 degrees. It has been previously shown how these waves could be generalized for arbitrary shapes and propose few devices (such as edge spin wave interferometers, controllers or splitters) where edge spin waves could be implemented [3].

Here we present simulation results obtained on the YIG based triangles where edge spin waves (ESWs) were propagated over the corner in 2 micron sized triangles with a fixed thickness of 85 nm. The superior vertex angle, studied in the range of 40°-75°, has been optimized in order to obtain a higher transmission coefficient over the vertex of the edge spin waves. Our simulations showed resonance increase of the ESW transmission for the angles close to 50 degrees. A slight excess of the transmission above one could be due to positive interference with SWs propagating directly from the microwave field source to the opposite edge. A generated upper vertex domain wall's topology seems to be key in understanding the efficiency of the ESW propagation. We have also investigated the ESW transmission along the out of plane profile of the triangle and optimized the applied bias field to maximize the effectiveness of the exchange energy channels that behave as a propagation route for the spin wave.

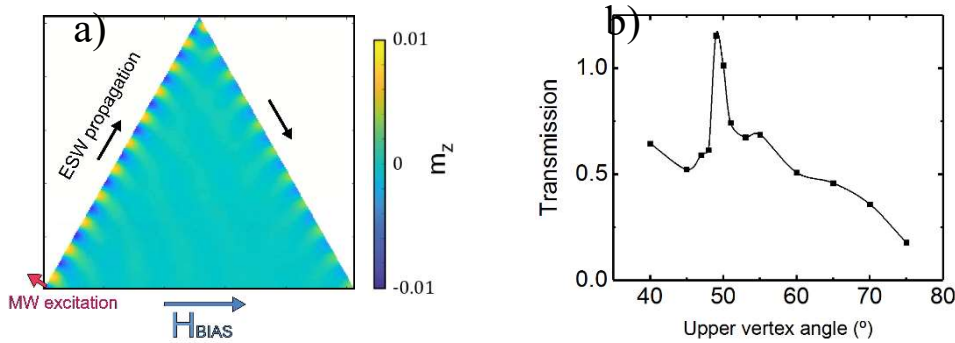


Figure 1. a) Snapshot of an edge spin wave propagated through both sides on a 2 micron side YIG triangle with a local microwave sinusoidal excitation perpendicular to the left side. b) Transmission coefficient of the ESW propagation through the upper vertex topology, showing a distinct increment for upper vertex angles in the 49°-50° range.

- [1] F. G. Aliev, et al., *Phys. Rev. B* **84**, (2011) 144406.
- [2] A. Lara, V. Metlushko, F. G. Aliev, *J. Appl. Phys.* **114** (2013) 213905.
- [3] A. Lara, J. Robledo, K.Y. Guslienko, F. G. Aliev, *Scientific Reports*, **7** (2017) 5597.

## Luminescence of GaP<sub>1-x</sub>N<sub>x</sub> layers grown on nominally (001)-oriented Si substrates

**Pablo Álamo<sup>1\*</sup>, Karim Ben Saddik<sup>1</sup>, Basilio Javier García<sup>1,2</sup> and Sergio Fernández-Garrido<sup>1,2</sup>**

<sup>1</sup>*Electronics and Semiconductors Group, Applied Physics Department, Universidad Autónoma de Madrid, C/ Francisco Tomás y Valiente 7, 28049 Madrid, Spain*

<sup>2</sup>*Instituto Nicolás Cabrera, Universidad Autónoma de Madrid, ES-28049 Madrid, Spain*

\*Email: pablo.alamo@uam.es

The incorporation of small amounts of N into GaP induces an indirect-to-direct band gap transition, as described by the band anticrossing (BAC) model [1]. The ternary compound GaP<sub>1-x</sub>N<sub>x</sub> has the same lattice parameter as Si for a N mole fraction  $x = 0.021$ , which paves the way for the monolithic and pseudomorphic integration of III-V optoelectronic devices with the widespread and highly scalable Si manufacturing technology. However, despite of the potential of this material the optical properties of GaP<sub>1-x</sub>N<sub>x</sub> grown on nominally (001)-oriented Si substrates remain unexplored.

In this work, we analyze the luminescence properties of GaP<sub>1-x</sub>N<sub>x</sub> layers grown on CMOS compatible GaP-on-Si(001) substrates by chemical beam epitaxy (CBE). Specifically, we investigate the photoluminescence (PL) of GaP<sub>1-x</sub>N<sub>x</sub> layers with different N mole fraction at different temperatures [see Fig.1(a) for a sample with  $x = 0.012$ ]. As a general trend, the emission peak energy does not monotonically decrease with increasing temperature [Fig.1(b)]. The overall temperature dependence can thus not be described by Pässler's equation and significantly differs from the BAC prediction when using the previously reported BAC coupling value ( $C_{NM}$ ), a behaviour we attribute to exciton localization effects caused by alloy inhomogeneities. Regarding the temperature dependence of the integrated PL intensity, it can be properly described using the following phenomenological expression including two thermally activated quenching processes:

$$I(T) = \frac{I_0}{1 + \alpha_1 e^{\left(\frac{-E_{a1}}{k_B T}\right)} + \alpha_2 e^{\left(\frac{-E_{a2}}{k_B T}\right)}} \quad (1),$$

where  $I_0$  is the integrated PL intensity at 0 K,  $\alpha_i$  are ratios between the radiative and non-radiative lifetimes, and  $E_{ai}$  are the thermal activation energies. The presence of two quenching processes indicates that there are at least two non-radiative processes limiting the optical quantum efficiency of our samples, as also observed in GaP<sub>1-x</sub>N<sub>x</sub> layers grown by plasma-assisted molecular beam epitaxy [3]. Next, we assessed the mean localization energy, at different temperatures, using the model reported by Almosni et al. in Ref.[2] to describe the PL emission of GaP<sub>1-x</sub>N<sub>x</sub> alloys [an exemplary fit is shown in Fig.2(a)]. Last, we used the obtained localization energies to extract the bandgap values of our samples. The results are summarized in Fig.2(b) where we plotted the bandgap energy as function of the N mole fraction. The fit of the BAC to our experimental data yields to a  $C_{NM}$  value of 2.24 eV, which is lower than those previously reported in the literature [1, 4].

[1] W. Shan et al. Appl. Phys. Lett., **76**, 3251 (2000)

[2] S. Almosni et al., Solar Energy Materials and Solar Cells, **147**, 53 (2016)

[3] M.A.G. Balanta et al., Journal of Alloys and Compounds, **814**, 152233 (2020)

[4] I. Vurgaftman et al. J. Appl. Phys., **94**, 3675 (2003)

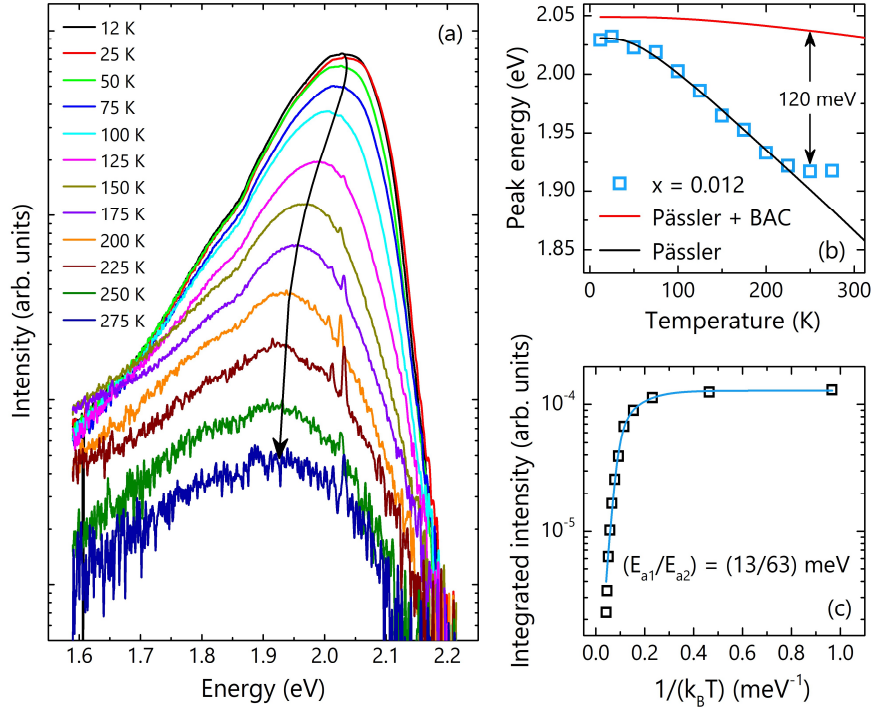


Figure 1. (a) Temperature dependent PL spectrum of a  $\text{GaP}_{1-x}\text{N}_x$  layer with  $x = 0.012$  grown at  $550^\circ\text{C}$ . (b) PL peak energy as a function of temperature. The black line represents a fit to Pässler's equation and the red line the temperature dependent bandgap according to the BAC model taken  $C_{\text{NM}}$  equal to  $3.05\text{ eV}$ . (c) Integrated PL intensity as a function of  $1/k_{\text{B}}T$ . The blue line is a fit of eq.(1) to the experimental data. The fit yields activation energies of  $13$  and  $63\text{ meV}$ .

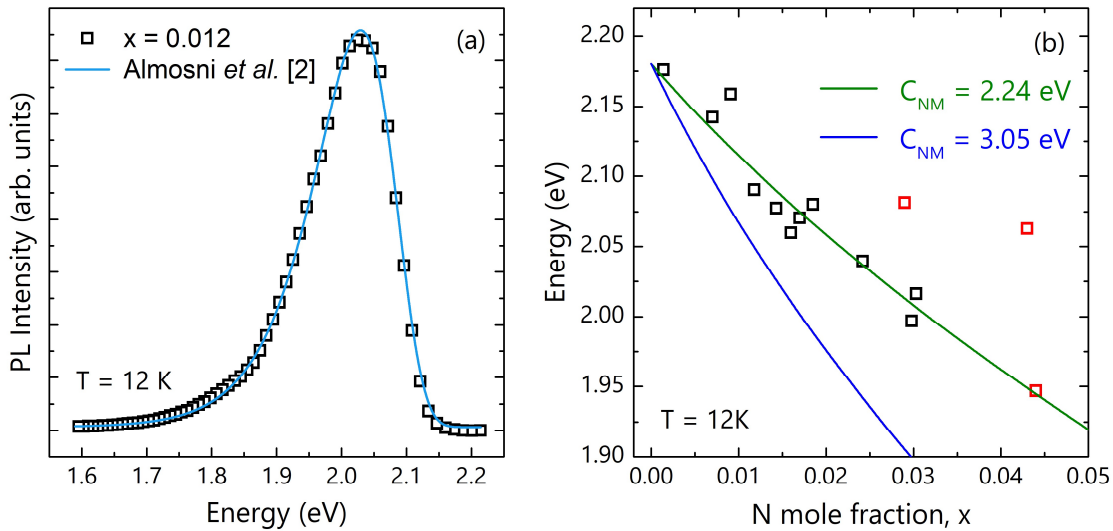


Figure 2. (a) PL spectrum at  $12\text{ K}$  of a  $\text{GaP}_{1-x}\text{N}_x$  layer with  $x = 0.012$  grown at  $550^\circ\text{C}$ . The blue line represents a fit using the model reported by Almosni et al. [2]. (b) Effective bandgap energy as a function of  $x$  for single-phase (black squares) and phase-separated (red squares) samples according to x-ray measurements not shown here. The blue line indicates the bandgap according to the BAC model using the  $C_{\text{NM}}$  value reported in Ref. [1]. The green line shows the best fit of the BAC model to our experimental data for single-phase samples, which yields to a  $C_{\text{NM}}$  value equal to  $2.24\text{ eV}$ .

# Unraveling the highly complex nature of antimony on Pt(111)

**Haojie Guo<sup>1</sup>, Mariano D. Jiménez-Sánchez<sup>1</sup>, Antonio J. Martínez-Galera<sup>1,2,‡</sup> and José M. Gómez-Rodríguez<sup>1,2,3†</sup>**

<sup>1</sup>Departamento de Física de la Materia Condensada, Universidad Autónoma de Madrid, E-28049 Madrid, Spain

<sup>2</sup>Instituto Nicolás Cabrera, Universidad Autónoma de Madrid, E-28049 Madrid, Spain

<sup>3</sup>Condensed Matter Physics Center (IFIMAC), Universidad Autónoma de Madrid, E-28049 Madrid, Spain

<sup>‡</sup>Present address: Departamento de Física de Materiales, Universidad Autónoma de Madrid, E-28049 Madrid, Spain

<sup>†</sup>Deceased

Email: (haojie.guo@uam.es)

Understanding the growth behavior of group-V elements on metal surfaces provides valuable information that can shed light on the feasibility of tailoring atomically thin monoelemental 2D polymorphs composed of pnictogens on these metallic substrates. This poster summarizes our recent study, carried out by a combination of scanning tunneling microscopy (STM), low energy electron diffraction and Auger electron spectroscopy measurements under ultra-high vacuum conditions, of the wide variety of Sb reconstructions on single-crystal Pt(111) [1]. At Sb coverage of  $\approx 0.2$  ML, STM data are compatible with a scenario in which Sb atoms are randomly embedded into the topmost layer of Pt, in a substitutional configuration and without establishing a periodic structure. This disorder is robust against thermal annealing and quenching. Increasing the surface coverage and whether or not the sample is annealed, different well-ordered Sb phases are formed. The Sb structures synthesized at room temperature without any heating process are best interpreted as surface alloys that involve only the first atomic layer. In contrast, experimental evidence points towards the development of multilayer alloy phases for the annealed samples.

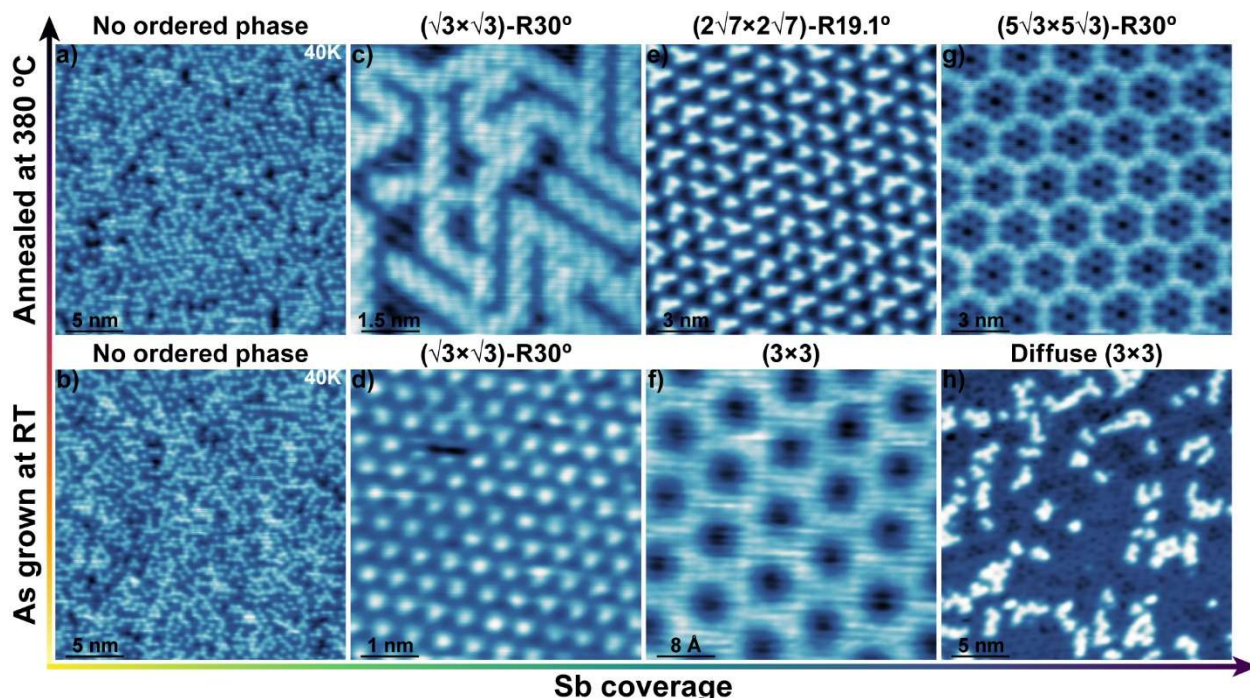


Figure 1. Overview of Sb phases on Pt(111), as proved by STM imaging, versus the annealing temperature and Sb coverage. All images were acquired at RT, except (a) and (b) which were measured at 40 K.

[1] H. Guo et al., Adv. Mater. Interfaces, **Accepted** (In press)

# Deep Learning for the Modeling and Inverse Design of Radiative Heat Transfer

J.J. García-Esteban<sup>1</sup>, J. Bravo-Abad<sup>1</sup> and J.C. Cuevas<sup>1</sup>

<sup>1</sup>*Departamento de Física Teórica de la Materia Condensada and Condensed Matter Physics Center (IFIMAC), Universidad Autónoma de Madrid, Madrid E-29049, Spain*

Email: juanjose.garciae@uam.es

Deep learning is having a tremendous impact in many areas of computer science and engineering. Motivated by this success, deep neural networks are attracting increasing attention in many other disciplines, including the physical sciences. In this work, we show that artificial neural networks can be successfully used in the theoretical modeling and analysis of a variety of radiative-heat-transfer phenomena and devices. By using a set of custom-designed numerical methods able to efficiently generate the required training data sets, we demonstrate this approach in the context of near-field radiative heat transfer between multilayer systems that form hyperbolic metamaterials. We show that simple neural network architectures trained with data sets of moderate size can be used as fast and accurate surrogates for doing numerical simulations, as well as engines for solving inverse design and optimization in the context of radiative heat transfer. Overall, our work shows that deep learning and artificial neural networks provide a valuable and versatile toolkit for advancing the field of thermal radiation. [1]

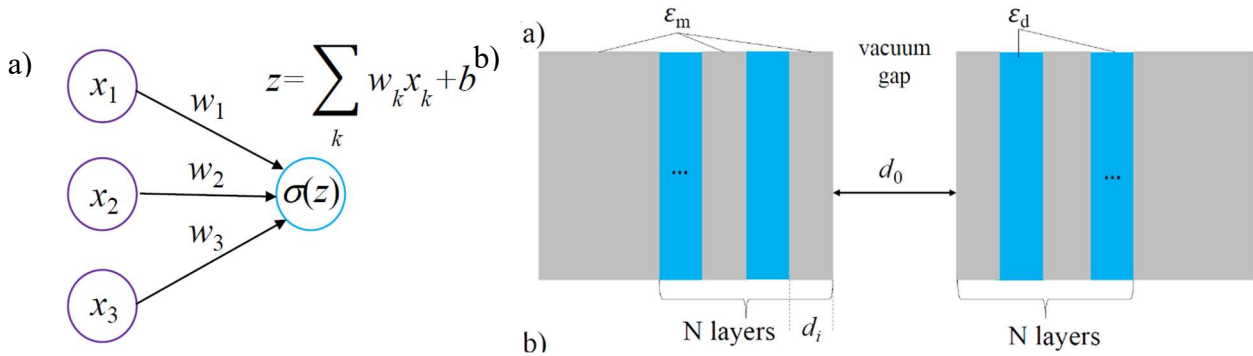


Figure 1. a) Schematic representation of a neuron, the fundamental unit of a Neural Network, the basis of Deep Learning. b) Sketch of the two identical multilayered systems studied in this work. Based on the studies from [2].

[1] J.J. García-Esteban et al., to appear in Phys. Rev. Appl. (2021) (arXiv:2109.03114)

[2] H. Iizuka et al., Phys. Rev. Lett., **120**, 063901 (2018)



# Superconducting gap and magnetoresistance of layered AuSn<sub>4</sub>

Miguel Águeda<sup>1</sup>, Pablo García Talavera<sup>1</sup>, Edwin Herrera<sup>1</sup>, Beilun Wu<sup>1</sup>, Alberto Montoya<sup>2</sup>, Víctor Barrena<sup>1</sup>, Jon Azpeitia<sup>3</sup>, Carmen Munuera<sup>3</sup>, Mar García-Hernández<sup>3</sup>, Paul C. Canfield<sup>4</sup>, José J. Baldoví<sup>2</sup>, I. Guillamón<sup>1</sup>, and H Suderow<sup>1</sup>

<sup>1</sup>Laboratorio de Bajas Temperaturas y Altos Campos Magnéticos,  
Departamento de Física de la Materia Condensada,  
Instituto Nicolás Cabrera and Condensed Matter Physics Center (IFIMAC),  
Unidad Asociada UAM-CSIC, Universidad Autónoma de Madrid, E-28049 Madrid, Spain

<sup>2</sup>Instituto de Ciencia Molecular (ICMol), Universidad de Valencia,  
Catedrático José Beltrán 2, 46980 Paterna, Spain

<sup>3</sup>Instituto de Ciencia de Materiales de Madrid, Consejo Superior de Investigaciones Científicas (ICMM-CSIC),  
Sor Juana Inés de la Cruz 3, 28049 Madrid, Spain

<sup>4</sup>Ames Laboratory, Ames and Department of Physics & Astronomy, Iowa State University, Ames, IA 50011

Email: miguel.agueda@estudiante.uam.es

PtSn<sub>4</sub> and PdSn<sub>4</sub> are semimetals with huge linear magnetoresistance, possibly related to topological bandstructures [1,2]. AuSn<sub>4</sub> is isostructural to these materials while presenting a superconducting phase. Here we report on the synthesis and characterization of single crystals of AuSn<sub>4</sub>. We present the Au-Sn binary phase diagram and discuss the possible single crystalline systems that can be obtained from it. We discuss solution growth [3] as a good method to obtain high quality single crystals of AuSn<sub>4</sub>. We grow AuSn<sub>4</sub> and find platelet crystals oriented along the b-axis of the orthorhombic crystal structure (Nr 68). The crystal size is crucible limited. Samples can be very easily exfoliated into layers. We characterize these crystals via resistivity, finding a residual resistance ratio above 120, sizeably above previous reports in literature [4]. This indicates and excellent crystal quality and a low number of residual impurities and defects. The critical temperature is of T<sub>C</sub>=2.35 K. We also discuss STM measurements of the density of states, where we find a superconducting gap which has an extremely large distribution of values over the Fermi surface. Furthermore, we observe the superconducting gap significantly above the bulk superconducting transition temperature (up to 1.1T<sub>C</sub>). We associate this finding with superconducting fluctuations or strain in detached layers [4,5,6,7]. We also discuss magnetoresistance and bandstructure calculations.

- [1] N. H. Jo et al., Phys. Rev. B, **96**, 165145 (2017)
- [2] E. Mun et al., Phys. Rev. B, **85**, 035135 (2012)
- [3] Paul C Canfield 2020 *Rep. Prog. Phys.*, **83**, 016501 (2020)
- [4] D. Shen et al., Commun Mater **1**, 56 (2020)
- [5] J.A.Galvis et al., Phys. Rev. B, **89**, 224512 (2014)
- [6] J.A.Galvis et al., Phys. Rev. B, **87**, 094502 (2013)
- [7] J.A.Galvis et al., Phys. Rev. B **87**, 214504 (2013)



# Quantum Interference in Radical and Neutral Single-Molecule Junctions

Juan Hurtado-Gallego<sup>1</sup>, Laura Rincón-García<sup>1</sup>, Nicolás Agraït<sup>1,2,3</sup>

<sup>1</sup>Departamento de Física de la Materia Condensada, Universidad Autónoma de Madrid, E-28049 Madrid, Spain.

<sup>2</sup>Condensed Matter Physics Center (IFIMAC) and Instituto Universitatario de Ciencia de Materiales 'Nicolás Cabrera' (INC), Universidad Autónoma de Madrid, E-28049 Madrid, Spain

<sup>3</sup>Instituto Madrileño de Estudios Avanzados en Nanociencia IMDEA-Nanociencia, E-28049 Madrid, Spain

Email: [juan.hurtado@uam.es](mailto:juan.hurtado@uam.es)

## Abstract:

Quantum interference (QI) in single-molecule junctions creates an anti-resonance in the transmission function near the Fermi energy which usually translates in a decrease of the conductance ( $G$ ) and in an increase of the Seebeck coefficient ( $S$ ) (1). In particular, this phenomenon appears in molecules with *meta* connections (2). Here we present an experimental study of the  $G$  and  $S$  in single molecules by comparing *para*- and *meta*-connected fluorene derivatives (2) and Blatter radicals (3) using a scanning tunneling microscope (STM) at room temperature and ambient conditions. Our results reveal the importance of the intrinsic spin state of radicals for a simultaneous enhancement of  $G$  and  $S$  and the influence of QI in these transport properties.

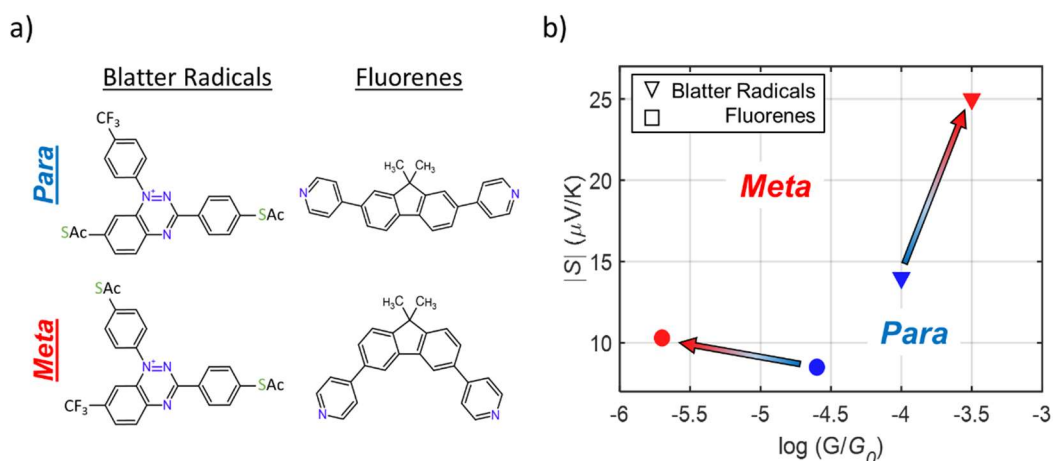


**Figure 1:** *a)* Scheme of the compounds investigated, para- and meta- connected Blatter radicals (left) and fluorenes (right). *b)* Seebeck coefficient ( $S$ ) vs conductance ( $G$ ) values for para- (blue) and meta-connected (red) Blatter radicals (triangles) and fluorenes (circles). The arrows highlight the effect of QI on the transport properties when the connection changes from para to meta.

## References:

- 1- C. J. Lambert, *Chem. Soc. Rev.*, 2015, **44**, 875.
- 2- I. M. Grace, G. Olsen, J. Hurtado-Gallego, L. Rincón-García, G. Rubio-Bollinger, M. R. Bryce, N. Agraït and C. J. Lambert, *Nanoscale*, 2020, **12**, 14682-14688.
- 3- J. Hurtado-Gallego, S. Sangtarash, R. Davidson, L. Rincón-García, A. Daaoub, G. Rubio-Bollinger, C. J. Lambert, V. S. Oganessian, M. R. Bryce, N. Agraït and H. Sadeghi (submitted).

## Irradiation of Bi-Sb crystals for possible subsurface amorphization

R. Singh<sup>1,2,\*</sup>, E. Xenios<sup>2</sup>, A. Redondo-Cubero<sup>1,2,3</sup>, J. L. Pau<sup>1</sup>, G. García<sup>2</sup>, M. A. Ramos<sup>2,3,4,5</sup> and N. Gordillo<sup>1,2,3</sup>

<sup>1</sup> Departamento de Física Aplicada, Universidad Autónoma de Madrid, 28049 Madrid, Spain

<sup>2</sup> Centro de Microanálisis de Materiales (CMAM), Universidad Autónoma de Madrid, 28049, Madrid Spain

<sup>3</sup> Instituto Nicolás Cabrera, Universidad Autónoma de Madrid, 28049, Madrid, Spain

<sup>4</sup> Departamento de Física de la Materia Condensada Universidad, Autónoma de Madrid, 28049 Madrid, Spain

<sup>5</sup> Centro de Física de la Materia Condensada (IFIMAC), Universidad Autónoma de Madrid, 28049, Madrid, Spain

\* raghvendra.singh@estudiante.uam.es

In this work, we study the possibility of amorphizing a buried layer of bismuth-antimony (Bi-Sb) alloys by swift heavy ions at CMAM. The goal of these experiments is to fabricate regions of amorphous Bi or Bi-Sb inside the crystalline alloys, which could remain robust enough at room temperature. If the created structures remain amorphous and avoid recrystallization, they should exhibit superconductivity at helium temperatures and would have the potential to behave as exciting Amorphous Topological Superconductors (ATS).

We have performed Monte Carlo simulations (SRIM code [1]) to determine the proper ion range and fluence to create about 10% of vacancies. Afterwards, three samples of pure Bi, Bi-Sb (3% Sb), and Bi-Sb (5% Sb) were irradiated simultaneously with Bi<sup>+</sup> ions at three consecutive energies 30 MeV, 22 MeV, 14 MeV and the same fluence of  $3.5 \times 10^{12}$  ions/cm<sup>2</sup>. Finally, the eventual superconductivity and structural properties of the samples will be characterized through Superconducting Quantum Interference Device (SQUID) and X-ray diffraction (XRD).

These studies will help to define future strategies and methodologies to keep (metastable) amorphous states at ambient conditions in these materials.

[1] J. F. Ziegler, J. P. Biersack, U. Littmark (Eds.), The Stopping and Ranges of Ions in solids, Pergamon Press, New York, 1985. URL <http://www.srim.org/>

## GaSe and carbon nanotubes for Li-ion batteries

Autor: Iñigo Salazar Beitia\*<sup>1</sup>

Dirección: Carmen Morant Zacarés \*<sup>2</sup>, Mario Aparicio \*<sup>3</sup>

\*<sup>1</sup>innigo.salazar@estudiante.uam.es

\*<sup>2</sup>Departamento de Física Aplicada, Universidad Autónoma de Madrid

\*<sup>3</sup>Instituto de Cerámica y Vidrio, CSIC

### Resumen

Las baterías son una de las tecnologías más utilizadas como almacenamiento de energía electroquímica (AEE). Entre las baterías recargables, las de litio-ion (BLI) son las comercializadas. En este trabajo se estudia el seleniuro de galio (GaSe) como material bidimensional, en combinación con una red de nanotubos de carbono (CNTs), para el electrodo de una batería Li-ion. El objetivo es mejorar el rendimiento del composite GaSe:CNTs como electrodo en BLI y proponer una nueva configuración *bicapa* haciendo uso de la ingeniería del material. Con este fin, se fabrica el composite del electrodo, se caracteriza mediante técnicas microscópicas (SEM) y espectroscópicas (EDAX) y se lleva a cabo un análisis de conductividad. Posteriormente, se realiza el montaje de la batería para su caracterización electroquímica y para evaluar el rendimiento del material como electrodo. Como resultado, se confirma que la distancia interlamina de GaSe permite una buena movilidad iónica y desarrolla capacidades elevadas. Por otra parte, la presencia de CNTs proporciona mayor flexibilidad, conductividad y estabilidad a lo largo de los ciclos. Finalmente, se puede afirmar que la configuración *bicapa* propuesta proporciona electrodos sin necesidad de colectores de corriente (free-standing electrodes) y con una mejora de la conductividad.

### Abstract

Batteries are one of the most widely used electrochemical energy storage (EES) technologies. Among the rechargeable batteries, lithium-ion batteries (BLI) are the commercialized ones. In this work, gallium selenide (GaSe) is studied as a two-dimensional material, in combination with a carbon nanotubes (CNTs) network, for the electrode of a Li-ion battery. The objective is to improve the performance of the GaSe:CNTs composite as electrode in BLI and to propose a new bilayer configuration by making use of material engineering. To this end, the electrode composite is fabricated, characterized by microscopic (SEM) and spectroscopic (EDAX) techniques and a conductivity analysis is carried out. Subsequently, the battery is assembled for electrochemical characterization and to evaluate the performance of the material as an electrode. As a result, it is confirmed that the interlaminar distance of GaSe allows a good ionic mobility and develops high capacities. On the other hand, the presence of CNTs provides higher flexibility, conductivity and stability over cycling. Finally, it can be stated that the proposed bilayer configuration provides electrodes without the need of current collectors (free-standing electrodes) and with improved conductivity.

## Strongly anisotropic strain-tunability of excitons in exfoliated ZrSe<sub>3</sub>

Hao Li<sup>1</sup>, Gabriel Sanchez-Santolino<sup>2</sup>, Sergio Puebla<sup>1</sup>, Riccardo Frisenda<sup>1</sup>, Abdullah M. Al-Enizi, Ayman Nafady<sup>3</sup>, Roberto D'Agosta<sup>4\*</sup>, Andres Castellanos-Gomez<sup>1\*</sup>

<sup>1</sup> Materials Science Factory. Instituto de Ciencia de Materiales de Madrid (ICMM-CSIC), Madrid, E-28049, Spain.

<sup>2</sup> GFMC, Departamento de Física de Materiales & Instituto Pluridisciplinar, Universidad Complutense de Madrid, 28040 Madrid, Spain

<sup>3</sup> Department of Chemistry, College of Science, King Saud University, Riyadh 11451, Saudi Arabia

<sup>4</sup> Nano-Bio Spectroscopy Group and European Theoretical Spectroscopy Facility (ETSF), Departamento de Polímeros y Materiales Avanzados: Física, Química y Tecnología, Universidad del País Vasco UPV/EHU, Avenida Tolosa 72, E-20018 San Sebastián, Spain  
IKERBASQUE, Basque Foundation for Science, Plaza Euskadi 5, E-48009 Bilbao, Spain

Email: (lihao-zzu@outlook.com)

Applying mechanical deformations has become a powerful approach to modify the vibrational, optical, and electronic properties of two-dimensional (2D) materials.[1] Among the different strategies to strain engineer 2D materials, the application of uniaxial strain through bending flexible substrates with a bending jig apparatus is one of the most popular approaches.[2] This method presents some issues when applied to 2D materials with in-plane anisotropic properties. Indeed, the effect of uniaxial strain along different crystal orientations is expected to modify the properties of these anisotropic 2Ds differently. Despite the recent interest on these families of anisotropic 2D materials [3,4], the number of reported research works focused on studying the effect of strain along different crystal directions is still very scarce and primarily focused on the investigation of strain tunable Raman modes in black phosphorus, PdSe<sub>2</sub> or tellurium [5-9].

Here we study the effect of uniaxial strain on the band structure of ZrSe<sub>3</sub>, a semiconducting material with a marked in-plane structural anisotropy. By using a modified 3-point bending test apparatus, thin ZrSe<sub>3</sub> flakes were subjected to uniaxial strain along different crystalline orientations monitoring the effect of strain on their optical properties through micro-reflectance spectroscopy. The obtained spectra showed excitonic features that blueshift upon uniaxial tension, which is strongly dependent on the direction along which the strain is being applied. When the flakes are strained along the b-axis, the exciton peak shifts at ~ 60-95 meV/%, while along the a-axis, the shift only reaches ~ 0-15 meV/%. Ab initio calculations were conducted to study the influence of uniaxial strain, applied along different crystal directions, on the band structure and reflectance spectra of ZrSe<sub>3</sub>, exhibiting a remarkable agreement with the experimental results.

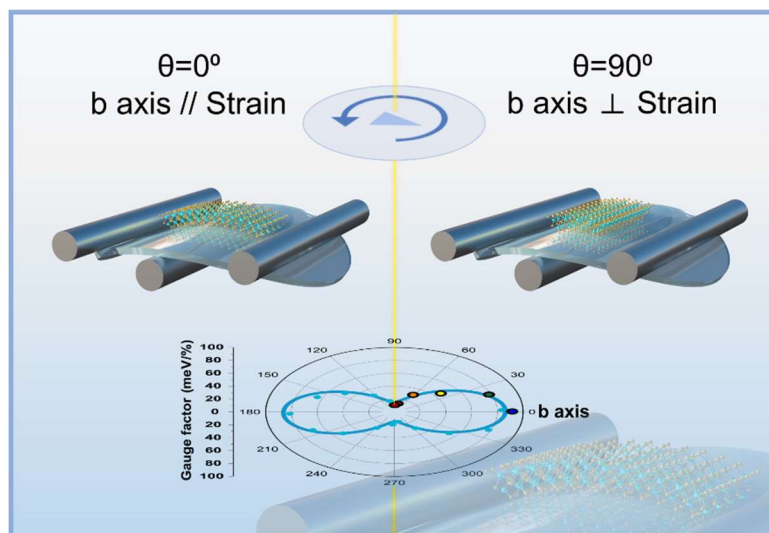


Figure 1. The illustration of the angle-resolved exciton tunability of  $\text{ZrSe}_3$  under uniaxial strain.

- [1] R. Roldán, A. Castellanos-Gomez, E. Cappelluti, F. Guinea, J. Phys. Condens. Matter 2015, 27, 313201.
- [2] K. He, C. Poole, K. F. Mak, J. Shan, Nano Lett. 2013, 13, 2931.
- [3] L. Kou, C. Chen, S. C. Smith, J. Phys. Chem. Lett. 2015, 6, 2794.
- [4] H. Liu, A. T. Neal, Z. Zhu, Z. Luo, X. Xu, D. Tománek, P. D. Ye, ACS Nano 2014, 8, 4033.
- [5] W. Zhu, L. Liang, R. H. Roberts, J.-F. Lin, D. Akinwande, ACS Nano 2018, 12, 12512.
- [6] Y. Li, Z. Hu, S. Lin, S. K. Lai, W. Ji, S. P. Lau, Adv. Funct. Mater. 2017, 27, 1600986.
- [7] G. Zhang, S. Huang, A. Chaves, C. Song, V. O. Özçelik, T. Low, H. Yan, Nat. Commun. 2017, 8, 14071.
- [8] W. Luo, A. D. Oyedele, Y. Gu, T. Li, X. Wang, A. V. Haglund, D. Mandrus, A. A. Puretzky, K. Xiao, L. Liang, X. Ling, Adv. Funct. Mater. 2020, 30, 2003215.
- [9] Y. Wang, S. Yao, P. Liao, S. Jin, Q. Wang, M. J. Kim, G. J. Cheng, W. Wu, Adv. Mater. 2020, 32, 2002342.

# INC Research awards for Physics students 2021

de la Peña Ruiz, Sebastián

Física Teórica de la Materia Condensada

## Theory of drift-enabled control in nonlocal magnon transport

Sebastián de la Peña<sup>1</sup>, Richard Schlitz<sup>2</sup>, Saül Vélez<sup>3</sup>, Juan Carlos Cuevas<sup>1</sup>, and Akashdeep Kamra<sup>1</sup><sup>1</sup> Condensed Matter Physics Center (IFIMAC) and Departamento de Física Teórica de la Materia Condensada, Universidad Autónoma de Madrid, E-28049 Madrid, Spain<sup>2</sup> Department of Materials, ETH Zürich, 8093 Zürich, Switzerland<sup>3</sup> Condensed Matter Physics Center (IFIMAC) and Departamento de Física de la Materia Condensada, Universidad Autónoma de Madrid, E-28049 Madrid, Spain

Email: sebastian.delapenna@estudiante.uam.es

Electrically injected and detected nonlocal magnon transport has emerged as a versatile method for transporting spin as well as probing the spin excitations in a magnetic insulator. We examine the role of drift currents in this phenomenon as a method for controlling the magnon propagation length. Formulating a phenomenological description, we identify the essential requirements for existence of magnon drift. Guided by this insight, we examine magnetic field gradient, asymmetric contribution to dispersion, and temperature gradient as three representative mechanisms underlying a finite magnon drift velocity, finding temperature gradient to be particularly effective

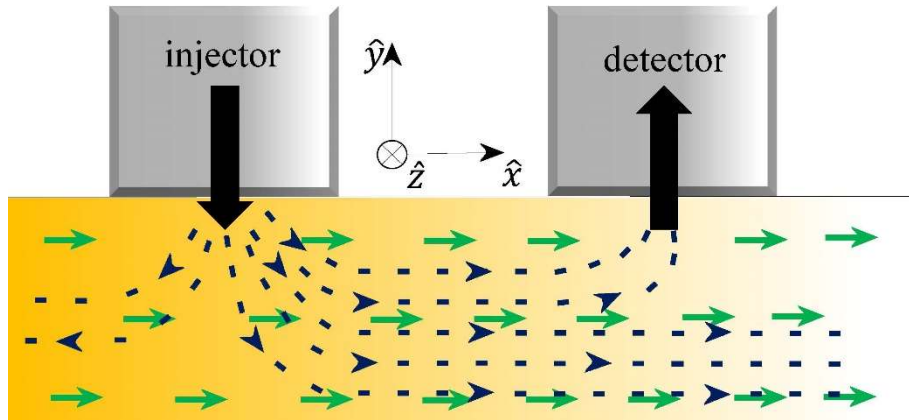


Figure 1. General model for magnonic spin transport observed via electrical injection and detection of spin in a ferromagnetic insulator. Nonequilibrium magnons are injected into a ferromagnetic insulator (yellow) by electronic spin accumulation generated in a heavy metal electrode (gray). This transport through the magnet is detected by a separate heavy metal electrode.



# INC Research awards for Physics students 2021

Arranz Jiménez, Marcos

Física de la Materia Condensada

## Photovoltaic effects study on hybrid perovskites thin layers

Marcos Arranz<sup>1</sup> and Jesús Álvarez<sup>1</sup><sup>1</sup>Departamento de Física de la Materia Condensada, Universidad Autónoma de Madrid, Madrid, Spain

Email: marcos.arranzj@estudiante.uam.es

Perovskites are claimed to be a revolutionary material in solar industry due to their electronic and transport properties. In this project we aim to explore and comprehend these properties, by a structural and electronic characterization (using both XRD and XPS techniques). A thin film of a hybrid chiral perovskite has been deposited on top of a gold single crystal. In photoemission experiments it can be appreciated a rather big peak displacement when the perovskite receives visible light evidencing the apparition of a Surface Photo Voltage. This is a relevant effect that implies the electron-hole separation, being this the most critical step of solar panel functioning as it avoids an electron-hole recombination.

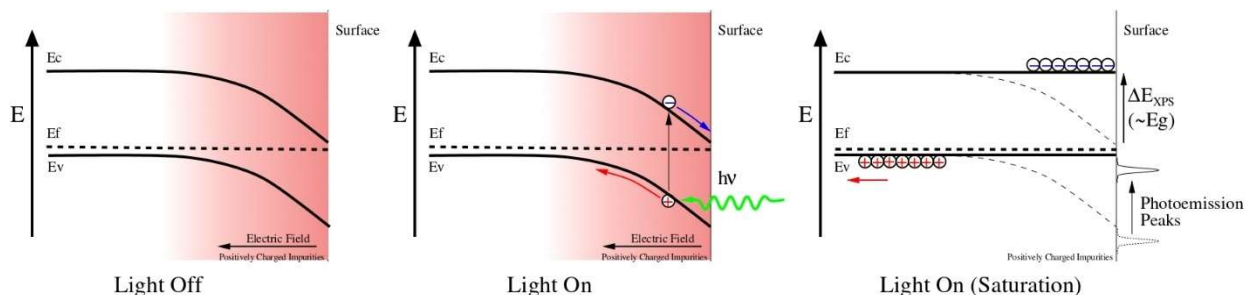


Figure 1. Explanatory figure of peaks displacement by the Surface Photo Voltage effect, which results in the electron-hole separation

# INC Research awards for Physics students 2021

Lasso, Alejandro

Física de la Materia Condensada

## Density Functional Theory and Machine Learning techniques for the study of amorphous materials

**Alejandro Lasso Castillo**

Tutors: Juan José Palacios<sup>1</sup>, Eduardo R. Hernández<sup>2</sup>

<sup>1</sup>Departamento de Física de la Materia Condensada, Universidad Autónoma de Madrid, 28049, Madrid, Spain

<sup>2</sup>Instituto de Ciencia de Materiales de Madrid (ICMM-CSIC), 28049, Madrid, Spain  
Email: (alejandro.lasso@estudiante.uam.es)

A common problem when doing DFT simulations is that it requires a lot of computational resources and it is difficult to deal with more than a few hundreds of atoms in the calculations. Recently, Machine Learning has been presented as a complementary method that could overcome this problem. This type of algorithms are fed with DFT results calculated for a landscape of relevant systems, which are then extrapolated or interpolated to other configurations with the same or even different number of atoms. In this work we have first created a dataset of different configurations simulating amorphous silicon using DFT methods. With this samples our objective is to use a Convolutional Neural Network and train it in order to calculate the total energy from arbitrary configurations.

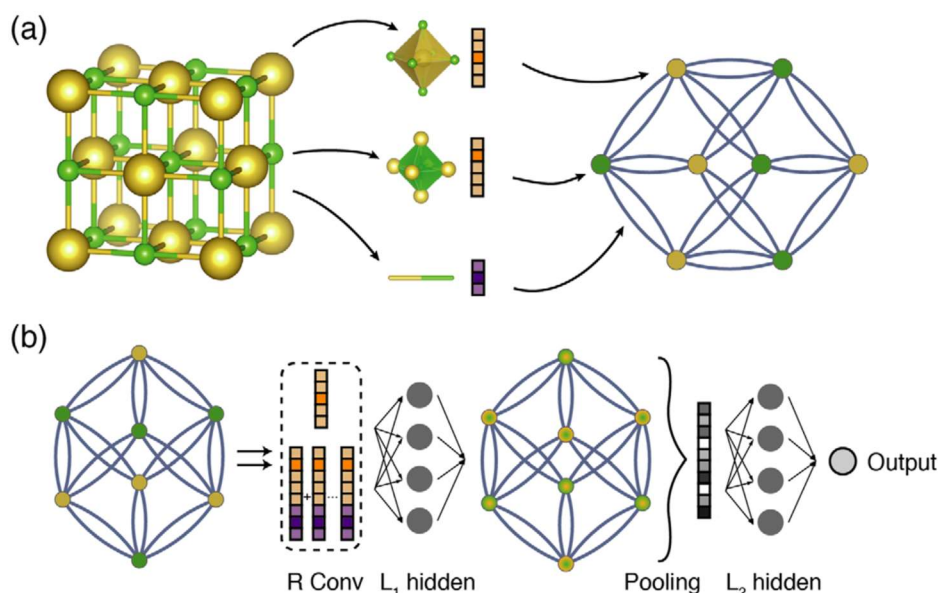


**Figure 1. Schematic view of a crystal graph convolutional neural network. [1]**

**(a) Construction of the crystal graph. (b) Structure of the convolutional neural network.**

[1] T. Xie, and J.C. Grossman, Phys. Rev. Lett., **120**, 145301 (2018)

[2] T. Xie, and J.C. Grossman, J. Chem. Phys. **149**, 174111 (2018)

# INC Research awards for Physics students 2021

Fernández Alonso, Francisco Javier

Física Aplicada

## Deposition of impedimetric electrodes on steel for the development of embedded sensors

**F.J. Fernández-Alonso, L. García-Pelayo, V. Torres-Costa and M. Manso-Silván**

*Department of Applied Physics, Universidad Autónoma de Madrid, 28049 Madrid, Spain*

Email: [franciscoj.fernandez05@estudiante.uam.es](mailto:franciscoj.fernandez05@estudiante.uam.es)

Electrical impedance spectroscopy (EIS) is a technique that has multiple applications, ranging from biological tissue analysis and cancer detection to quality control in the food industry [1,2]. In the present study, stainless-steel needles have been provided with sensing capabilities through the implementation of impedimetric electrodes. To achieve this, first, a thin insulating layer of polylactic acid (PLA) was deposited by dip coating on oxalic acid-activated stainless-steel needles, and the mechanical properties of the layer were improved by mild thermal annealing. Subsequently, Au electrodes were deposited by DC magnetron sputtering along both sides of the needle. Finally, an outer cellulose acetate insulating film was deposited by dip coating leaving part of the electrodes next to the bevelled tip exposed, allowing electrical measurements to be performed at the probe's tip.

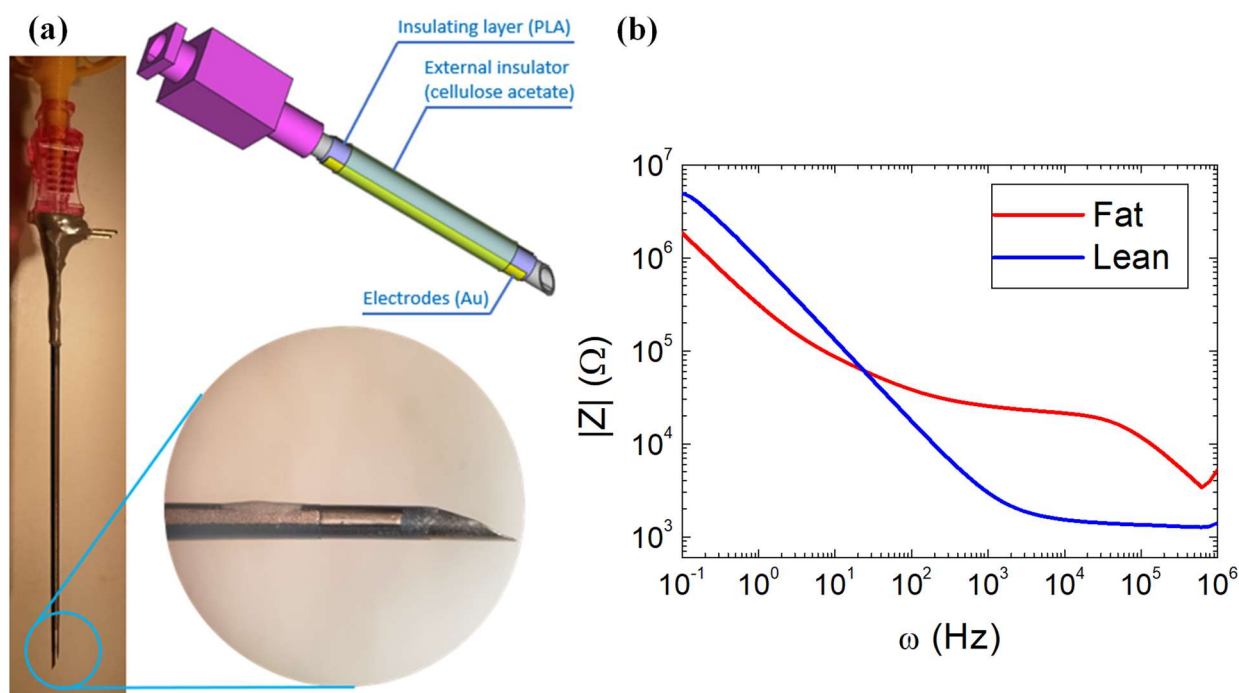


Figure 1. (a) Scheme of the implemented device, and a photograph of it. (b) Impedance spectrum measured for fatty meat and lean meat using the implemented system. The type of meat can be clearly identified at frequencies  $10^3 - 10^5$  Hz.

The performance of the system was tested by measuring the impedance spectra of different biological tissues between 0.1 Hz and 1 MHz. A clear difference in impedance was observed for various types of meat in the 10 kHz range, allowing their identification. Results show that the developed impedimetric probes can be used to probe and identify different types of biological tissues.

[1] B. Chang and S. Park., Annual Review of Analytical Chemistry, **3** (1), 207-229 (2010).

[2] R. Arshad et al., Trends in Food Science & Technology, **104**, 1-13 (2020).

# INC Research awards for Physics students 2021

Galante, Clara

Física Teórica de la Materia Condensada

---

## Machine Learning in Nonlinear Dynamical Systems

**Clara Galante Agero, Jorge Bravo Abad**

*Universidad Autónoma de Madrid*

Clara.galante@estudiante.uam.es

In the world of today, since huge amounts of data are being generated, Machine Learning is quickly providing new powerful tools for scientists to extract essential information from large data, either from experimental or simulations. In this way, some of Machine Learning uses include event predictions and simulations, recognition and classification, data processing and modeling, etc.

As an example of the benefits of using this tool, in this project we use Sparse Identification of Nonlinear Dynamics technique, which combines sparsity-promoting techniques and Machine Learning. By using this algorithm, it is possible to extract governing equations from data with the assumption that only few terms are important in a govern dynamic.

In addition, we implement a neuronal network with a simple architecture, for cleaning noise from raw data. Although there already exist other methods for doing this, Machine Learning proves to be an efficient alternative to approach this problem.

[1] Steven L. Brunton, PNAS April 12, 2016,113(15) 3932-3937

# INC Research awards for Physics students 2021

Lizarraga Lallana, Juan

Física de Materiales

## Polariton condensation in semiconductor microcavity pillars

**J. Lizarraga<sup>1</sup>, M.D. Martín<sup>1,2</sup> and L. Viña<sup>1,2,3</sup>**

<sup>1</sup>*Departamento de Física de Materiales, Universidad Autónoma de Madrid, 28049 Madrid, Spain.*

<sup>2</sup>*Instituto de Ciencia de Materiales Nicolás Cabrera, Universidad Autónoma de Madrid, 28049 Madrid, Spain.*

<sup>3</sup>*Departamento de Física de la Materia Condensada, Universidad Autónoma de Madrid, 28049 Madrid, Spain.*

Email: [juan.lizarraga@estudiante.uam.es](mailto:juan.lizarraga@estudiante.uam.es)

Polaritonics is a very active scientific research field, due to both its many potential applications and the fascinating physics that governs polariton dynamics.

In this work, we have studied the optical properties of semiconductor microcavity pillars of different diameters at cryogenic temperature. Using a non-resonant laser beam we can optically excite these structures, creating exciton-polaritons. With our experimental setup we can collect the photoluminescence emitted by these polaritons in their decay and resolve it both in real and reciprocal space. We have studied the emission regimes of these pillars as a function of the pump power, identifying the polariton condensation thresholds for each diameter. We have also measured the polariton dispersion relation, which allows us to understand the complex mode structure exhibited by these pillars, obtaining Bose-Einstein condensation at some specific modes when the power surpasses the condensation threshold.

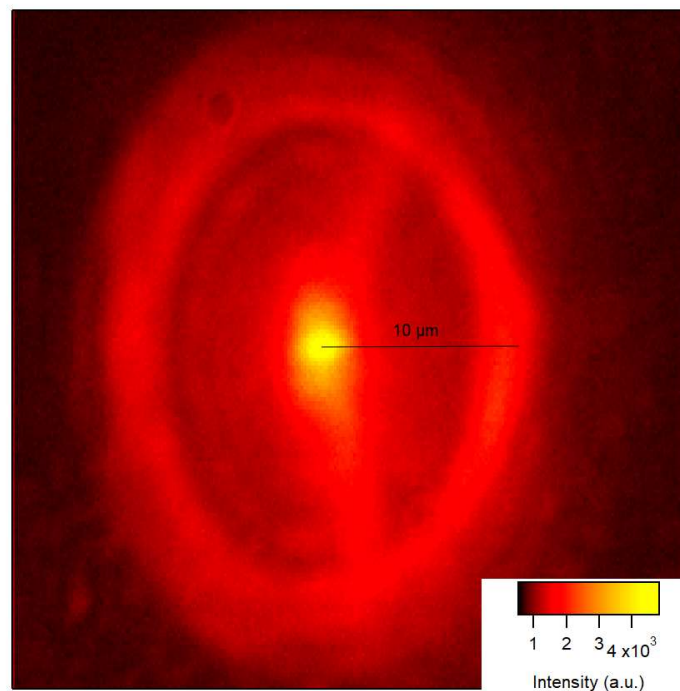


Figure 1. Optical image of the photoluminescence emitted by the decay of polaritons in a semiconductor microcavity pillar, collected from above and resolved in real space.

## Force-dependent mechanical properties of nucleic acids from fluctuations

Juan Luengo-Márquez<sup>1,2</sup> and Salvatore Assenza<sup>1,2,3</sup>

<sup>1</sup>Department of Theoretical Condensed Matter Physics

<sup>2</sup>Instituto Nicolás Cabrera

<sup>3</sup>IFIMAC – Condensed Matter Physics Center

Universidad Autónoma de Madrid, Spain

juan.luengo@uam.es

Double-stranded nucleic acids (dsDNA and dsRNA) are complex macromolecules with important biological functions inside the cell. The packaging conditions in which these molecules are found *in vivo*, such as the bending of dsDNA around histones, suggest that the role of the genetic code is largely determined by the mechanical properties of nucleic acids [1].

The so-called “mechanical code” has been characterized through a broad range of experimental and simulation techniques [2]. However, the methodological approaches aimed at the exploitation of the most common elastic models entail several limitations. Remarkably, they are not adequate for the study of the change of the elastic parameters upon the application of mechanical stresses [3], like a stretching force or a torque. This is important, because some biological processes involve the deformation of the double helix with a force exerted at the base step level, *e. g.* the interaction of dsDNA with enzymes.

In this talk, we present a novel method to compute these elastic parameters from the fluctuations of the deformation modes of double stranded nucleic acids. In contrast with precedent methods involving fluctuations of the double helix [4], our approach is suitable to address the elastic properties of a perturbed chain, *i. e.* a stretched, twisted or bent chain.

Furthermore, employing data of configurations of nucleic acid chains from atomistic MD simulations, we exploit the previously introduced method by inspecting the evolution of the aforementioned elastic parameters with a stretching force. We find that not only the mechanical features of double helices depend on the specific sequence of base pairs – as it has been realized by earlier studies – but also the evolution with the force of such properties displays a clear dependence on the sequence.



Figure 1. Schematic representation of dsDNA

[1] Smith, Steven B., Yujia Cui, and Carlos Bustamante, *Science*. **271**, pp. 795–799 (1996)

[2] Marin-Gonzalez, Alberto, et al., *Quarterly Reviews of Biophysics*, **54** (2021)

[3] Marin-Gonzalez, Alberto, et al. *Proceedings of the National Academy of Sciences*, **114.27**, 7049-7054 (2017)



## Confined motion of active rotating particles within lipid vesicles

P. Magrinya<sup>1</sup>, J. M. Ordoñez<sup>1</sup>, P. Llombart<sup>1</sup>, L. R. Arriaga<sup>1,2</sup>, J. L. Aragoes<sup>1,2</sup>

<sup>1</sup>*Departamento de Física Teórica de la Materia Condensada, Instituto Nicolás Cabrera (INC), Universidad Autónoma de Madrid, Madrid, Spain*

<sup>2</sup>*Condensed Matter Physics Center (IFIMAC), Universidad Autónoma de Madrid, Madrid, Spain*

Email: paula.magrinya@uam.es

In the Stokes limit, a rotating sphere suspended in an unbounded viscous fluid generates a symmetric rotational flow that forces the particle to rotate in place. Importantly, the symmetry of such rotational flow breaks in the presence of a limiting solid surface, which results in translation of rotating particles close to the limiting surface. Further control on the translation of rotating particles on limiting surfaces may be achieved upon confinement [1]. However, this strategy remains widely unexplored, mainly due to the difficulties associated with the controlled encapsulation of rotating particles within capsules with controlled properties. Here, we controllably encapsulate ferromagnetic microparticles within lipid vesicles using microfluidic technologies [2] and force the microparticles to rotate upon application of an external rotating magnetic field. Our results show that the fluid flows generated by the confined particles produces the rotation of the confining vesicles. Optical microscopy is then used to track the trajectory of both the rotating particles and the vesicles as a function of the rotational frequency and degree of confinement. These results represent a first step towards creating motile vesicles that translate on substrates exploiting self-confined rotational flows.

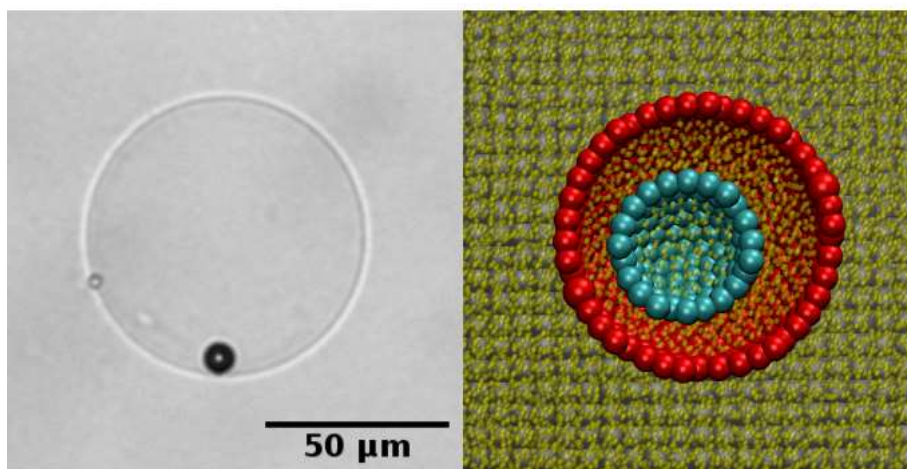


Figure 1. Our synthetic cell-free model to study cell friction: experimental system (left) and computational model (right)

[1] A. Mateos-Maroto, et al., *ACS Applied Materials & Interfaces*, **10** (35), 29367-29377 (2018)

[2] Arriaga, L. R. et al., *Small*, **10** (5), 950–956 (2014)

## Artificial Vesicle Fusion: from Fundamentals to Applications

**B. Tinao<sup>1</sup>, M. A. Tahir<sup>2</sup>, Z. P. Guven<sup>3</sup>, F. Stellacci<sup>3</sup> and A. Alexander-Katz<sup>2</sup>, L. R. Arriaga<sup>1</sup>**

<sup>1</sup>*Department of Theoretical Condensed Matter Physics, Condensed Matter Physics Center and Instituto Nicolás Cabrera, Universidad Autónoma de Madrid, 28049 Madrid, Spain*

<sup>2</sup>*Department of Materials Science and Engineering, Massachusetts Institute of Technology, Cambridge, MA 02142*

<sup>3</sup>*Institute of Materials, Ecole Polytechnique Federale de Lausanne, 1015 Lausanne, Switzerland*

Vesicle fusion is a critical step in many biological processes, including, for example, neural communication in the synapses of the brain. At each synapse, small vesicles called endosomes must fuse with the next neuron to enable nerve impulse propagation through the release of neurotransmitters. A specialized protein complex called SNARE primes such fusion events, which evolve to complete fusion upon calcium influx. Inspired in this complex, here, we show an experimental realization of a complete fusion process primed by synthetic amphiphilic nanoparticles [1]. In the experiments, we use both large and giant unilamellar lipid vesicles (LUVs and GUVs, respectively) as model membranes and fluorescence-based techniques to visualize the different steps of the fusion process. Amphiphilic nanoparticles spontaneously incorporate into the membrane of LUVs, enabling two membranes to become in close contact, which ultimately results in mixing of their lipid content. This intermediate state is known as hemi-fusion and evolves to complete fusion upon addition of calcium ions to the external medium, as shown in Figure 1. Complementary molecular simulations show that complete fusion can be achieved in this system by condensation of lipids in the external monolayer of the bilayer, which can be correlated to the addition of calcium ions in the experiments. The importance of this work relies on the demonstration of a synthetic fusogenic system, which provides insight into the critical design principles required to develop new strategies to replicate certain aspects of cellular communication, which may be potentially applied in the future to combat synaptic loss.

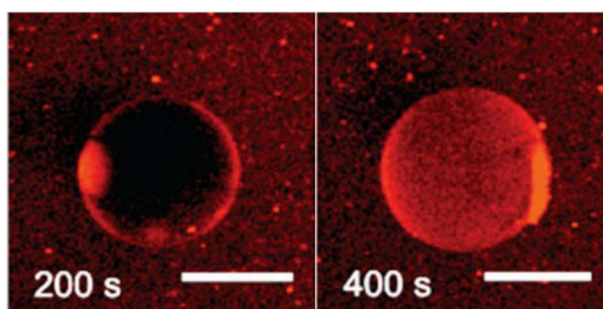


Figure 1. Confocal fluorescence images showing hemi-fusion (left) and fusion (right) of LUVs with GUVs in the presence of amphiphilic nanoparticles

[1] M. A. Tahir, Z. P. Guven, L. R. Arriaga, B. Tinao, Y. S. Yang, A. Bekdemir, J. T. Martin, A. N. Bhanji, D. Irvine, F. Stellacci, A. Alexander-Katz. *Proc. Natl. Acad. Sci. U.S.A.* 117 (31) 18470-18476 (2020)

# Light-matter interaction from density functional theory with application to attosecond electron dynamics

**J.J. Esteve-Paredes<sup>1</sup>, M. Malakhov<sup>2</sup>, G. Cistaro<sup>2</sup>, A. Picón and J.J. Palacios<sup>1,3</sup>**

<sup>1</sup>*Departamento de Física de la Materia Condensada, Universidad Autónoma de Madrid, Madrid, Spain.*

<sup>2</sup>*Departamento de Química, Universidad Autónoma de Madrid, Madrid, Spain.*

<sup>3</sup>*Instituto Nicolás Cabrera (INC) and Condensed Matter Physics Center (IFIMAC).*

Email: [juan.esteve@uam.es](mailto:juan.esteve@uam.es)

We present a methodology to address light-matter interaction with focus on attosecond electron dynamics in 2D materials starting from density functional theory calculations. We combine an accurate DFT-based evaluation of optical matrix elements and Berry connections with the time-resolved Schrödinger equation including several laser pulses, both at the infrared and the x-ray regimes. In the end, carrier dynamics and light absorption can be obtained and readily compared with available experiments without the aid of any phenomenological parameters. Our methodology is particularly suited for DFT calculations based on Gaussian basis sets as those used in codes such as GAUSSIAN or CRYSTAL as a post-selfconsistent procedure. The use of Gaussian basis sets saves computational effort, as all coordinate space integrations become analytical. Our procedure also entails a proper quantification of several approximations for optical matrix elements widely used in the literature and its effect in reproducing experimental curves.

# Assessing the predictive ability of an effective temperature in an optically driven colloidal suspension

Galor Geva<sup>1,3</sup>, Tamir Admon<sup>1</sup> and Yael Roichman<sup>1,2</sup>

<sup>1</sup>*School of Chemistry, Tel Aviv University, Tel Aviv, Israel*

<sup>2</sup>*School of Physics, Tel Aviv University, Tel Aviv, Israel*

<sup>3</sup>*Departamento de Física de la Materia Condensada, Universidad Autonoma de Madrid, Madrid,, Spain*

Email: (galor.geva@uam.es)

One of the current challenges in statistical mechanics is in describing a general non-equilibrium system using a small number of state variables. For example, the temperature of the system is a well-defined state variable in equilibrium, but it is ill-defined for non-equilibrium systems. An effective temperature can be formulated for some non-equilibrium cases through the generalized fluctuation-dissipation theorem, where the effective temperature replaces the role of temperature in relating fluctuations and response [1]. In this work, we test the validity of the effective temperature as a state variable in a system of suspended colloidal particles. We use holographic optical tweezers to induce random athermal fluctuations on the colloidal particles (see Fig.1) [2] and define an effective temperature for the driven particles using the Stokes-Einstein relation [3]. Then, we perform a set of experiments and simulations of two colloidal systems at two different effective temperatures and measured the particle flow between the two systems. Interestingly, we find that the flow of particles is dictated by the mean force exerted on the particles rather than by the effective temperature. Thus, the effective temperature fails to describe the state of the system. These results provide a comprehensive assessment of the dynamics of randomly driven particles and provide insight into the effective temperature and highlight its shortcomings.

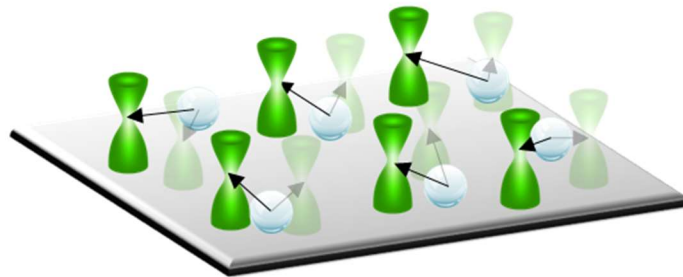


Figure 1. Illustration of the experimental procedure. Randomly placed optical traps, which change positions randomly at a given frequency, drive the colloidal particles. We then define and study the characteristics of the arising effective temperature.

- [1] Cugliandolo, L. F., Kurchan, J., & Peliti, L. (1997). Energy flow, partial equilibration, and effective temperatures in systems with slow dynamics. *Physical Review E*, 55(4), 3898.
- [2] Grier, D. G. (2003). A revolution in optical manipulation. *nature*, 424(6950), 810-816.
- [3] Kubo, R. (1966). The fluctuation-dissipation theorem. *Reports on progress in physics*, 29(1), 255.

# Controlling toughness of MoS<sub>2</sub> single layers by introducing atomic vacancies

Y Manzanares-Negro<sup>1</sup>, G Lopez-Polin<sup>1,2</sup>, K Fujisawa<sup>3,4</sup>, T Zhang<sup>4,5</sup>, F Zhang<sup>4,5</sup>, E Kahn<sup>4,5</sup>, N Perea\_lopez<sup>3,4</sup>, M Terrones<sup>3,4,5,6,7</sup>, J Gómez-Herrero<sup>1,8</sup>, and C Gómez-Navarro<sup>1,8</sup>

<sup>1</sup>Departamento de Física de la Materia Condensada, Universidad Autónoma de Madrid, Madrid E-28049, Spain

<sup>2</sup>ICMM, Campus Cantoblanco Madrid E 28049, Spain

<sup>3</sup>Department of Physics, The Pennsylvania State University, University Park, PA 16802, USA

<sup>4</sup>Center for 2-Dimensional and Layered Materials, The Pennsylvania State University, University Park, PA 16802, USA

<sup>5</sup>Department of Materials Science and Engineering, The Pennsylvania State University, University Park, PA 16802, USA

<sup>6</sup>Department of Chemistry, The Pennsylvania State University, University Park, PA 16802, USA

<sup>7</sup>Institute of Carbon Science and Technology, Shinshu University, 4-17-1 Wakasato, Nagano-city 380-8553, Japan

<sup>8</sup>IFIMAC Condensed Matter Physics Center (IFIMAC). Universidad Autónoma de Madrid, Madrid E-28049, Spain

Email: yolanda.manzanares@uam.es

Two-dimensional crystals are very brittle, i.e. fractures propagate easily. Therefore their mechanical reliability is very restricted, limiting possible applications. In this work, we demonstrate that controlled defect creation constitutes an effective approach to avoid catastrophic failure in MoS<sub>2</sub> monolayers. Here we report a systematic study of fracture mechanics in MoS<sub>2</sub> monolayers as a function of the density of atomic vacancies, created by ion irradiation. The crystalline quality and defect density of pristine and irradiated materials were studied by high-resolution scanning transmission electron microscopy and Raman spectroscopy.

By AFM nanoindentations in MoS<sub>2</sub> microdrumheads, we determine the strength needed to produce fractures, and we determine the length of the propagated cracks within MoS<sub>2</sub> atom-thick membranes from SEM images.

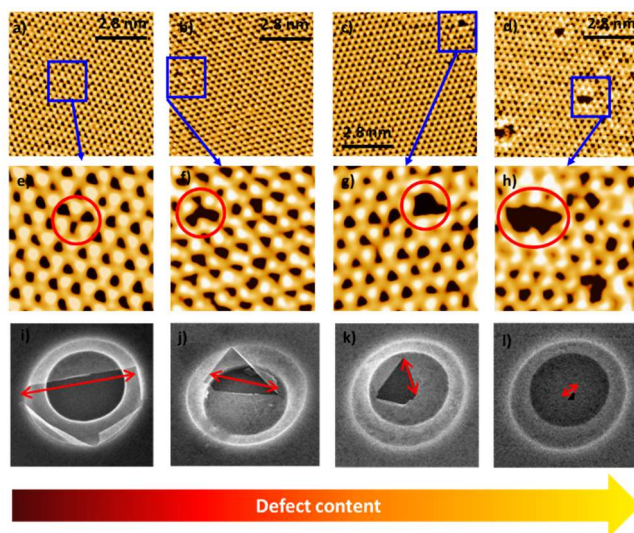


Figure 1. a), b), c), d) Representative HR-STEM images of ion irradiated MoS<sub>2</sub> single layers. e) HR-STEM view of a single S vacancy. f) HR-STEM view of a S<sub>2</sub> vacancy. g) view of a Mo vacancy and the surrounding deformation of the crystalline structure. h) view of a defect created by several missing atoms. i), j), k), l) representative images of the broken samples with increasing defect content.

We find that a 0.15% atomic vacancy induces a decrease of 40% in strength with respect to that of pristine samples. In contrast, while tear holes in pristine 2D membranes span several microns, they are restricted to a few nanometers in the presence of atomic and nanometer-sized vacancies, thus increasing the material's

fracture toughness [1]. This trend has been experimentally observed in other materials such as graphene, whose high brittleness is highly restricted by the inclusion of atomic vacancies [2], and our stress intensity factor ( $K_{\text{c}}$ ) values and observed tendencies are in striking agreement with those calculated by the molecular dynamics simulations reported in [3]. This technique allows tuning the optimal strength/toughness relation needed for different applications.

[1] Y. Manzanares-Negro et al., ACS nano, **15(1)**, 1210-1216 (2021)

[2] G. López-Polín et al., Nano Lett., **15(3)**, 2050-2054 (2015)

[3] S. Wang et al., ACS nano, **10(11)**, 9831-9839 (2016)



# Surface Evolution in epitaxial $\text{Li}_x\text{CoO}_2$ films studied by LEEM/PEEM for $x \leq 1$

**E. Salagre<sup>1</sup>, M.A. González-Barrio<sup>3</sup>, E. Fuller<sup>2</sup>**

**A. Mascaraque<sup>3</sup>, T.O. Mendes<sup>4</sup>, A. Locatelli<sup>4</sup>, A.A. Talin<sup>2</sup>, P. Segovia<sup>1,5</sup> and E.G. Michel<sup>1,5</sup>**

1. Dto Física Materia Condensada, Univ. Autónoma de Madrid, Spain

2. Dto. Física de Materiales, Fac. Ciencias Física, Univ. Complutense de Madrid, Spain

3. Sandia National Laboratories, Livermore (CA), USA.

4. Elettra-Sincrotrone Trieste S.C.p.A., Basovizza, 34149 Trieste, Italy.

5. IFIMAC (Condensed Matter Physics Center), Univ. Autónoma de Madrid, Spain

$\text{Li}_x\text{CoO}_2$  (LCO) and similar intercalation oxides are typically used as cathode materials for Li-ion batteries<sup>1</sup>. The interest on these systems has recently increased due to their potential use in neuromorphic computing devices. The properties making LCO such a relevant material rely on its ability to change its Li molar contents from  $x=1$  (corresponding to the stoichiometric compound) to  $x \approx 0.5$  in a reversible way. Along the Li deintercalation process LCO changes its structure and presents a metal-insulator transition in the electronic structure<sup>2,3</sup>.

We used high-quality Epitaxial thin films of LCO grown on  $\text{SrTiO}_3$  (STO). Different types of films have been studied, from small isolated islands on a wetting layer, to a completely covered surface with outstanding Fermi Surface quality, highlighting the crystalline quality of the surface. We report Photoemission Electron Microscopy (PEEM) and Low Energy Electron Microscopy (LEEM) results obtained at Nanospectroscopy beamline, at Elettra Synchrotron<sup>4</sup>. We characterize the sample with submicrometer resolution using XPS, XAS and ARPES. We identify the LCO islands, wetting layers and different regions regarding their Li content and level of metallization. The delithiation process (Li deintercalation) was performed using Ne sputtering and annealing in oxygen atmosphere. For  $x < 0.95$  the sample metallizes. For  $0.75 < x < 0.95$  we observe coexistence of two phases that coexist and present a different Li contents. We characterize the spectroscopic features of each type of region (electronic structure, Co L and O K absorption edges) and identify them with hex-I and hex-II phases. The fact that the phase separation takes place over regions of approx. 100-200 nm size is analysed is relevant to understand the kinetic processed taking place in the LCO cathode during the deintercalation process. The behaviour of isolated islands vs well prepared epitaxial surfaces is also investigated and provides clues to understand the size dependence of the deintercalation process.

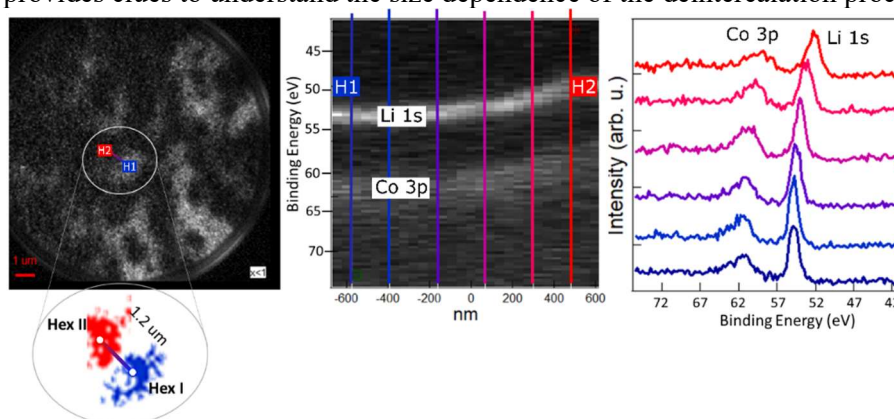


Fig. 1. Correlation between Li content, charge, morphology and phase dominance during delithiation process.

1. Nitta, N., Wu, F., Lee, J. T. & Yushin, G. Li-ion battery materials: Present and future. *Materials Today* vol. 18 252–264 (2015).
2. Marianetti, C. A., Kotliar, G. & Ceder, G. A first-order Mott transition in  $\text{Li}_x\text{CoO}_2$ . *Nature Materials* **3**, 627–631 (2004).
3. Milewska, A. *et al.* The nature of the nonmetal-metal transition in  $\text{Li}_x\text{CoO}_2$  oxide. in *Solid State Ionics* vol. 263 110–118 (Elsevier, 2014).
4. Locatelli, A., Aballe, L., Mendes, T. O., Kiskinova, M. & Bauer, E. Photoemission electron microscopy with chemical sensitivity: SPELEEM methods and applications. in *Surface and Interface Analysis* vol. 38 1554–1557 (John Wiley & Sons, Ltd, 2006).

# Projective representations from non-symmorphic space groups and spin-orbit coupling: how and why

Antonio García Blázquez<sup>1</sup>

<sup>1</sup>*Departamento de Física de la Materia Condensada, Universidad Autónoma de Madrid, Madrid, Spain*

Email: manuelantonio.garcia@estudiante.uam.es

According to group theory, the eigenstates of any quantum system can be classified by the representations of the symmetry group of the Hamiltonian. In particular, the elementary particles (or quasiparticles) in a crystalline solid, such as electrons, phonons or excitons; transform according to representations of the space group containing all the geometrical symmetries of the crystal [1]. These transformation laws ultimately allow to determine all qualitative features of the physical system that are not sample-dependent, as long as the crystal symmetry is mostly preserved; such as band degeneracy, selection rules for transitions, the form of  $\mathbf{k}\mathbf{p}$  Hamiltonians and material tensors, or the response under perturbations [2-4].

While the use of standard representation theory in condensed matter physics is mostly widespread, only the 73 symmorphic space groups (out of the total 230 in three dimensions) can be successfully treated with it. Indeed, quasiparticles in a non-symmorphic crystal generally transform according to projective representations of the corresponding point group, whose use requires an enlarged theoretical framework [4-5]. This construction becomes relevant again when relativistic effects are considered for electrons, allowing to treat on an equal footing the effect of two seemingly unrelated features: non-primitive translations in the crystal and spin-orbit coupling. This way, using the projective representations of the 32 crystallographic point groups one can extend the qualitative study of the electronic eigenstates to the 230 space groups with, or without spin-orbit coupling; which is currently an important tool in the search for topological materials [6-9].

In this presentation I will explain how projective representations naturally arise when applying the Bloch theorem to a non-symmorphic crystal, and when including the relativistic spin-orbit coupling term for the electrons in any crystal. I will also show examples of real materials where the necessity to use projective instead of standard representations is evidenced, based on first-principles calculations.

[1] Bouckaert, L. P., Smoluchowski, R., & Wigner, E. (1936). Theory of Brillouin zones and symmetry properties of wave functions in crystals. *Physical Review*, 50(1), 58.

[2] Dresselhaus, M. S., Dresselhaus, G., & Jorio, A. (2007). *Group theory: application to the physics of condensed matter*. Springer Science & Business Media.

[3] Nye, J. F. (1985). *Physical properties of crystals: their representation by tensors and matrices*. Oxford university press.

[4] Bir, G. L., & Pikus, G. E. (1974). *Symmetry and strain-induced effects in semiconductors* (Vol. 484). New York: Wiley.

[5] Bradley, C., & Cracknell, A. (2010). *The mathematical theory of symmetry in solids: representation theory for point groups and space groups*. Oxford University Press.

[6] Bradlyn, B., Cano, J., Wang, Z., Vergniory, M. G., Felser, C., Cava, R. J., & Bernevig, B. A. (2016). Beyond Dirac and Weyl fermions: Unconventional quasiparticles in conventional crystals. *Science*, 353(6299).

[7] Muechler, L., Alexandradinata, A., Neupert, T., & Car, R. (2016). Topological nonsymmorphic metals from band inversion. *Physical Review X*, 6(4), 041069.

[8] Fang, Y., & Cano, J. (2021). When do Dirac points have higher order Fermi arcs?. *arXiv preprint arXiv:2109.01670*.

[9] Po, H. C., Vishwanath, A., & Watanabe, H. (2017). Symmetry-based indicators of band topology in the 230 space groups. *Nature communications*, 8(1), 1-9.

# Transport and heating effects in proximitized InAs nanowire islands

A. Ibabe<sup>1</sup>, J. Nygard<sup>2</sup>, A. L. Yeyati<sup>1</sup>, Gornm Steffensen<sup>1</sup>, E. J. H. Lee<sup>1</sup>

<sup>1</sup> Department of Condensed Matter Physics, Universidad Autónoma de Madrid, Spain, Ciudad Universitaria de Cantoblanco, Spain.

<sup>2</sup> Center for Quantum Devices and Station Q Copenhagen, Niels Bohr Institute, Univ of Copenhagen, Copenhagen, Denmark.

Email: (angel.ibabe@uam.es)

Mesoscopic islands based on semiconductor nanowires proximitized by a superconductor have been widely studied in recent years in the context of topological superconductivity. On the one hand, the Coulomb blockade in such systems can be employed as a high-resolution spectroscopical tool for studying zero-energy states and their splitting [1]. Superconducting islands also appear as elements in proposals for the manipulation and readout of Majorana zero modes [2]. In this work, we study transport through islands based on InAs nanowires proximitized by an epitaxial Al shell with superconducting leads. Our study focuses on Joule heating effects [3] that can drive the epitaxial superconducting layer to the normal state at moderate currents (down to tens of nA). This transition manifests as dips in the differential conductance, signaling a strong suppression of the Andreev excess current. We investigate this effect as a function of the gate voltages applied to the nanowire junctions, the external magnetic field and temperature. We also study a dynamical Coulomb blockade effect that we observe in the normal state of the devices.

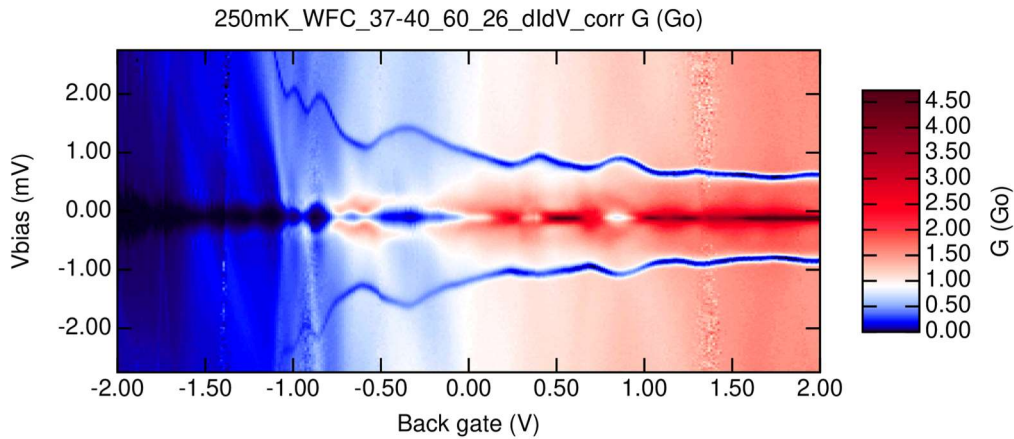


Figure 1. Conductance measurement at base temperature (10mK) as a function of gate voltage, for one of the devices.

[1] S. M. Albrecht, A. P. Higginbotham, M. Madsen, F. Kuemmeth, T. S. Jerspersen, J. Nygard, P. Krogstrup, C. M. Marcus, Nature, 531 (2016) 206-209.

[2] D. Aasen, M. Hell, R. V. Mishmash, A. Higginbotham, J. Danon, M. Leijnse, T. S. Jespersen, J. A. Folk, C. M. Marcus, K. Flensberg, J. Alicea, Phys. Rev. X, 6 (2016) 031016.

[3] M. Tomi, M. R. Samatov, A. S. Vasenko, A. Laitinen, P. Hakonen, D. S. Golubev, arXiv:2106.07503 (2021).



## Organizing committee:

**Enrique Velasco, M<sup>a</sup> Dolores Martín, Carmen Morant and Iván Brihuega**

### **Dirección del INC:**

**Director:** Miguel Angel Ramos.

**Deputy Director:** Isabel Jimenez Ferrer.

**Secretary:** Juan L. Aragonés.

**Admin. assistant:** Rocío Gómez-Argüello.

**Board:** Iván Brihuega, M<sup>a</sup> Dolores Martín, Carmen Morant and Enrique Velasco.

Facultad de Ciencias - Módulo 08, 4ª Planta  
Calle Francisco Tomás y Valiente 7, 28049 Madrid  
Universidad Autónoma de Madrid  
Secretaría: Tel.: 91.497.4689. Fax: 91.497.8734. Email: [inc@uam.es](mailto:inc@uam.es)  
web: [www.inc.uam.es](http://www.inc.uam.es)

